UNIVERSITY OF CALIFORNIA
RIVERSIDE

Role of Light, Humidity, and Nutrition in Sporulation of *Phytophthora* species

A Dissertation submitted in partial satisfaction
of the requirements for the degree of

Doctor of Philosophy

in

Plant Pathology

by

Andrea Linh Vu

March 2020

Dissertation Committee:
Dr. Howard S. Judelson, Chairperson
Dr. Patricia Manosalva
Dr. Jason Stajich

The Dissertation of Andrea Linh Vu is approved:

Committee Chairperson

University of California, Riverside

ABSTRACT OF THE DISSERTATION

Role of Light, Humidity, and Nutrition in Sporulation of *Phytophthora* species

by

Andrea Linh Vu

Doctor of Philosophy, Graduate Program in Plant Pathology
University of California, Riverside, March 2020
Dr. Howard S. Judelson, Chairperson

Oomycetes, a class in the kingdom Stramenopila, are filamentous eukaryotic microorganisms that are known informally as water molds, but have adapted to many environmental niches. *Phytophthora*, an oomycete genus of approximately 100 plant-pathogenic species, has specifically adapted to several environmental niches. Environmental conditions play an influential role in the development of *Phytophthora*, particularly in sporangium formation. Sporangia, the main driver of *Phytophthora* epidemics, are especially susceptible to damage by environmental conditions, such as light-induced DNA lesions or desiccation by drying. Variable by species, light can stimulate (e.g. *P. infestans*) or repress (e.g. *P. capsici*) the production of sporangia. Light may have two developmental roles: an early pre-sporangiophore induction signal, and a later post-sporangiophore repression signal. In this work, I found that although many types of photoreceptors are described in eukaryotes, *Phytophthora* genomes encode only

cryptochrome photoreceptors. The foliar-adapted species *P. infestans* encodes three cryptochromes, while the soilborne species *P. capsici* encodes two cryptochromes. Silencing of the *P. infestans* gene encoding cryptochrome PITG_01718, which lacks an ortholog in *P. capsici*, inhibits sporulation. While cryptochromes have traditionally been described in other organisms as blue light receptors, each red and blue light represses *P. infestans* sporulation. In contrast, *P. capsici* sporulation responds to blue light but not red light. This work also describes the use of RNA-seq to study the genetic control of sporulation by light and humidity. Constant light was found to repress the expression of genes induced in the post-sporangiophore stage by *P. infestans*, while constant darkness repressed the expression of genes in the pre-sporangiophore stage in *P. capsici*. Humidity also had a strong effect on repressing gene expression in the pre-sporangiophore stage of sporulation in *P. infestans*. This work also describes that specific types of nitrogen starvation induce sporulation. In addition to advancing our knowledge of sporulation control in oomycetes, this work also provides a better understanding of the homology-based gene silencing method. While this technique is an effective method for functional genomics in *Phytophthora*, work in this dissertation shows that the technique must be used with prudence due to the frequency of off-target effects.

Acknowledgements

This work was supported by grant 1753749 from the National Science Foundation to Howard S. Judelson.

Part of this work has been published in:

Kagda, M., Vu, A.L., Ah-Fong, A.M.V., Judelson, H.S., 2018. Phosphagen kinase function in flagellated spores of the oomycete *Phytophthora infestans* integrates transcriptional regulation, metabolic dynamics, and protein retargeting. Molecular Microbiology 110, 296–308.

Leesutthiphonchai, W., Vu, A.L., Ah-Fong, A.M.V., Judelson, H.S., 2018. How does *Phytophthora infestans* evade control efforts? Modern insight into the late blight disease. Phytopathology 108, 916–924.

Rodenburg, S.Y.A., Seidl, M.F., Judelson, H.S., Vu, A.L., Govers, F., de Ridder, D., 2019. Metabolic model of the *Phytophthora infestans*-tomato interaction reveals metabolic switches during host colonization. mBio 10, e00454-19.

Vu, A.L., Leesutthiphonchai, W., Ah-Fong, A.M.V., Judelson, H.S., 2019. Defining transgene insertion sites and off-target effects of homology-based gene silencing informs the application of functional genomics tools in *Phytophthora infestans*. MPMI 32, 915–927.

Tables of Contents

List of Figures

List of Tables

Chapter 1: Introduction

Plant pathogens in the genus *Phytophthora* threaten food security and cause billions of dollars of lost revenue every year worldwide. *Phytophthora* species can spread quickly within a field by asexually-produced sporangia. However, little is known about the molecular regulation signals of sporangia production, the specific genes involved in the pathway, or the role of metabolites in sporangia production. We know that light can play a regulatory role in sporangial production, but the specific photoreceptors and proteins involved in this interaction remain unknown. The more that we know about the molecular mechanisms behind sporangial production, the more targeted chemical control strategies can be made to prevent production of sporangia.

Oomycetes

The oomycota is a large class of fungal-like organisms in the Kingdom Stramenopila. This group contains organisms that are important pathogens of plants, animals, and insects, and are commonly found in marine, freshwater, and terrestrial environments (Beakes et al., 2012). Oomycetes are considered to be fungal-like due to convergent evolution, but are more evolutionarily related to other stramenopiles such as brown algae and diatoms based on molecular taxonomies, and physical characteristics such as cell wall composition and the presence of motile cells with tinsel flagella. Oomycetes differ from fungi in

important ways, such as in having cell walls composed largely of cellulose and β-glucans versus chitin as found in fungi, which affects management strategies for the two groups. Also, unlike fungi, oomycetes do not readily exhibit homologous recombination of plasmid DNA with the chromosome during transformation, so distinct strategies for reverse genetics of oomycetes must be employed.

Phytophthora

Phytophthora is a genus within the oomycota that contains approximately 101 described species, most of which are plant pathogens (Kroon et al. 2012). Taken together, *Phytophthora* species cause billions of dollars of crop loss annually in the United States alone, and many times that amount worldwide (Erwin and Ribeiro 1996). *Phytophthora* lifestyles range from soilborne to foliar plant pathogens, and the host range of a species can vary from very narrow (one or two host species) to broad (hundreds of host genera). *Phytophthora infestans* and *Phytophthora capsici* are two significant pathogens that have been studied as model species, and differ in several notable ways.

Phytophthora infestans is perhaps the most notorious plant pathogen, as it caused several devastating epidemics in North America and Europe in the 1840s, including the Irish Potato Famine, which led to the death and emigration of millions of people in Ireland (Bourke 1964, Ristaino 2002). Additionally, this pathogen continues to cause epidemics that threaten crop production and food security worldwide (Fry et al. 2015). The host range of *P. infestans* is limited to

potato, tomato, and several wild *Solanum* spp. relatives of potato and tomato, with few exceptions (Erwin and Ribeiro 1996). *Phytophthora infestans* causes a disease called late blight, and can attack foliage, fruit, stems, and tubers. This pathogen mainly survives without long-term survival structures such as chlamydospores or oospores, and for this reason is not traditionally considered to be a soilborne pathogen.

Phytophthora capsici, however, has a broad host range that includes peppers, cucurbits, solanaceous plants, and lima beans (as reviewed by Lamour et al. 2012b). *Phytophthora capsici* was first described in the southwestern United States in 1918, and has since been reported in locations worldwide (Leonian 1922, Erwin and Ribeiro 1996). *Phytophthora capsici* causes fruit rot, crown and root rot, or a more general disease referred to as Phytophthora blight, and can attack any part of the plant. In contrast to *P. infestans*, *P. capsici* can survive in soil in debris (Schlub 1983, Lamour and Hausbeck 2003).

Life cycle of *Phytophthora* species

The life cycle of *Phytophthora* species includes vegetative hyphae that can develop asexually into sporangia or chlamydospores, or sexually into oospores. Almost all *Phytophthora* species can reproduce both sexually and asexually, though some species, such as *P. infestans*, lack the ability to make chlamydospores. Two mating types for sexual reproduction in Phytophthora exist: A1 and A2. Although some species are heterothallic and require both

mating types for sexual reproduction, other species are homothallic, and thus sexual reproduction can occur within a single strain. Both *Phytophthora capsici* and *Phytophthora infestans* are heterothallic; however, sexual reproduction occurs in nature much more commonly in *P. capsici* than in *P. infestans*. Although there have been reports of sexually-reproducing *P. infestans* populations in North America, *P. infestans* is mainly considered to be clonal, or asexual outside of Mexico and Northern Europe (Danies et al. 2014, Fry 2008, Fry et al. 2015, Niederhauser 1956, Grünwald et al. 2001, Andersson et al. 1998, Yuen and Andersson 2013). Particularly, from the 1840s to the 1980s, only one of the two mating types was found outside of Mexico, so epidemics were caused by asexual lineages due to geographic isolation of mating types (Hohl and Iselin 1984). Even with broader geographic distribution of both mating types, asexual reproductive cycles continue to cause severe epidemics, including in the United States (Fry et al. 2015).

Phytophthora capsici is the only *Phytophthora* species that commonly outcrosses in nature, producing oospores that can survive in soil for years (Hausbeck and Lamour 2004, Lamour and Hausbeck 2003). However, sporangia are crucial in the epidemiology of *P. capsici*, with approximately three billion viable sporangia produced on a single diseased cucurbit fruit, which can be easily dislodged by rain or irrigation water (Lamour et al., 2012). When submerged in water, *P. capsici* sporangia readily cleave and release zoospores, which swim chemotactically towards host tissue. Large-scale epidemics can

occur from just a few diseased plants, particularly in locations with moderate rainfall, and regions that share irrigation water (Schlub 1983, Sujkowski et al 2000, Gevens et al. 2007).

Sporangia

As discussed, sporangia are important infective propagules for *Phytophthora* species. Sporangia are asexually produced, and can cleave into motile zoospores, or directly germinate into hyphae (Fig. 1.1). Sporangium formation starts with a sporangiophore initial, which will extend into a sporangiophore, which is a specialized aerial hypha that bears the sporangium at the end. The tip of the sporangiophore will expand, and then the protoplast from the sporangiophore is pumped into the expanded end, which will become the sporangium. When the sporangium is mature, a specialized septa called a basal plug will form at the base (Fig 1.1).

Relationship of humidity and light to sporulation

It has long been recognized that environmental factors can influence sporangia production in *Phytophthora* species, particularly factors related to light, air, water, and humidity (Waterhouse 1931, Warren and Colhoun 1975, Zentmyer and Ribeiro 1977). Humidity and air speed experiments relative to sporulation in *P. infestans* showed that increased air speed leads to increased sporangial

production, and lower humidity leads to lower sporangial production (Harrison and Lowe 1989).

Light, in particular, has been shown to play a differential role in sporulation in several *Phytophthora* species. In *P. capsici,* sporangial production is starkly affected by light, showing an inhibition in sporangial production in culture on solid media in darkness, as compared to frequent to abundant production in light (Harnish 1965, Alizadeh and Tsao 1985). A similar pattern was shown in *P. cactorum* and *P. palmivora* as well (Harnish 1965, Alizadeh and Tsao 1985). In contrast, blue light will inhibit sporulation of *P. infestans* on potato leaves and on wheat agar media (Cohen et al. 1975). Sporangiophore production by *P. infestans,* however, was not shown to be photosensitive, and in contrast to blue light, green and red wavelengths showed very little effect on sporulation (Cohen et al. 1975).

To investigate the molecular basis of the differential response to light relative to sporulation, a previous study searched the available *Phytophthora* genomes for putative photoreceptor proteins (Xiang and Judelson 2014). Currently, genomes are available for *P. sojae*, *P. ramorum, P. infestans*, *P. capsici*, *P. cinnamomi* and *P. parasitica* (Tyler et al. 2006, Haas et al. 2009, and Lamour et al. 2012a). Domain-level searches revealed that of the six types of photoreceptor proteins (van der Horst et al. 2004), only blue light receptor cryptochrome proteins could be found (Xiang and Judelson 2014). The genome of *P. infestans* is predicted to encode three cryptochrome proteins, which are

produced by genes PITG_01718, PITG_16100, and PITG_16104. *Phytophthora capsici* is predicted to have two cryptochrome genes: Phyca_44729 and Phyca_574436.

Phytophthora infestans asexual life cycle is suited to rapid dissemination

The life cycle of *P. infestans* can involve asexual or sexual reproduction. In the asexual cycle, the vegetative hyphae grow to form sporangiophores that bear sporangia. The mature sporangia are dehiscent to disperse by wind or water (Aylor et al. 2001, Granke et al. 2009). Sporangia can then directly germinate to infect a host, or indirectly germinate through cleavage and release of zoospores. Zoospores are single-nucleate, wall-less, motile spores with two flagella (tinsel and whiplash) and can swim towards host tissue. Upon finding a suitable host, zoospores encyst, attach to the host, and germinate to infect the tissue.

The sexual cycle is important for generating genetic diversity through recombination, while the asexual cycle propels the success of advantageous genotypes through rapid propagation and efficient dissemination. For this reason, the asexually produced sporangia largely drive epidemics of late blight. One example of this is the recent *P. infestans* population dynamics in the Netherlands, and the success of strain A2_13, also known as Blue_13. The aggressive strain Blue_13 had been first characterized in 2005, and quickly became dominant in various parts of Europe and Asia, driving epidemics in areas

where late blight had typically not been severe previously, such as India (Cooke et al. 2007, Cooke et al. 2012, Chowdappa et al. 2013, Li et al. 2012, Li et al. 2013). More recently, Green_33 has displaced Blue_13 as the dominant clonal lineage in fluazinam-sprayed fields in the Netherlands, as Green_33 is resistant to fluazinam while Blue_13 is sensitive (Schepers et al. 2018).

Rapid reproduction

The *P. infestans* asexual reproduction cycle is fast, and produces copious amounts of spores. A single lesion can produce several hundred thousand sporangia. Once sporangiophore initials begin to emerge from stomata, mature, deciduous sporangia will be formed in about 6-7 hours (Maltese et al. 1995). Sporangium production can occur every day from a lesion for several days, allowing for a polycyclic disease cycle. Once sporangium production begins, a plant can reportedly be destroyed in several hours, with whole fields wiped out in 7-9 days (Fry 2008, Fry et al. 2015).

Timing of sporulation is optimized for survival and spread

P. infestans spores can be spread aerially or through water. Wind speeds of 1-2 m/s remove spores from the potato canopy in a field, and sporangia can travel 10-20 km in less than 3 hours (Aylor et al 2001). *P. infestans* sporangia can be sensitive to drying in low humidity, and prone to UV damage from light (Minogue and Fry 1981, Warren and Calhoun 1975). On sunny days, solar

irradiance drastically decreases the viability of *P. infestans* sporangia, and exposure to low humidity significantly decreases the spore germination rate after rehydration (Mitzubuti et al. 2000, Minogue and Fry 1981).

Unlike fungi with colored spores, *P. infestans* spores are not colored and are thus susceptible to damage by light. To avoid damage, *P. infestans* has evolved to sporulate when environmental conditions are optimal, to minimize both damage from light and desiccation. Excessive light can suppress or delay sporulation (Cohen et al. 1975, Xiang and Judelson 2014). *P. infestans* typically sporulates in the dark when the humidity is high, usually early morning in the field, associated with dew (Bashi et al 1982). When humidity drops, *P. infestans* will respond within 60 seconds, with sporangiophores twisting and throwing off mature sporangia in otherwise still cultures (Granke et al. 2009).

Not all of these characteristics are shared by all other *Phytophthora* species. For example, *Phytophthora capsici* sporangia are not spread by wind, and do not detach with a drop in humidity (Granke et al. 2009). Although light cycles can result in cyclic sporangia production in *P. capsici,* and *P. capsici* sporangia production and morphology are highly affected by light, there is not a clear diurnal pattern or time of day for optimal sporangia production in the field (Alizadeh and Tsao 1985, Nielsen et al. 2006, Granke et al. 2009). This may be because *P. capsici* is more adapted for soil dispersal, with faster zoosporogenesis, and a stronger role for oospores and chlamydospores (a survival spore that *P. infestans* does not make) in the disease cycle.

Role of temperature

Temperature affects both the production and germination of sporangia. As temperature rises from 10 to 25°C, the speed of leaf infection on tomato increases and lesion size increases, though sporulation is greatest around 15°C (Mitzubuti and Fry 1998). When sporangia are exposed to wet conditions below 12-15°C, cold shock induces cleavage of the sporangial cytoplasm into single-nucleate zoospores. Zoosporogenesis in *Phytophthora* is considered one of the most rapid developmental processes in any biological system (Walker and van West 2007). The cold temperature is sensed in sporangia through increased rigidity of the membrane, which triggers zoosporogenesis and cold box motif-mediated transcription to control gene expression (Tani and Judelson 2006).

Chemotaxis

When zoospores are released, the spores swim chemotactically towards host tissue (Zentmyer 1961). Zoospores can swim centimeters in soil, or travel meters in water. Chemotaxis allows the spores to quickly and efficiently find suitable host tissue. The amount of time that zoospores stay actively swimming before encystment can vary from 1-24 hours, depending on temperature (Melhus 1915). There has been research indicating that auto-aggregation may also play a role in zoospore behavior, but its role or importance in nature is still undetermined (Savory et al. 2014).

Overall, *Phytophthora* species are well-adapted plant pathogens that have evolved strategies to sense and respond to environmental conditions. Although much has been observed about the response of *Phytophthora* species to changes in the environment and plant host, only few studies have been conducted to explore the molecular basis for these responses. The goal of this study was to further understand the molecular basis for the light, humidity, and nutritional signals that influence sporulation in *Phytophthora* species.

References

Alizadeh, A., Tsao, P.H., 1985. Effect of light on sporangium formation, morphology, ontogeny, and caducity of *Phytophthora capsici* and '*P. palmivora*' MF4 isolates from black pepper and other hosts. Transactions of the British Mycological Society 85, 47–69.

Andersson, B., Sandström, M., Strömberg, A., 1998. Indications of soil borne inoculum of *Phytophthora infestans*. Potato Research 41, 305–310.

Ayers, W.A. 1971. Induction of sporangia in *Phytophthora cinnamomi* by a substance from bacteria and soil. Canadian Journal of Microbiology 17, 1517–1523.

Aylor, D.E., Fry, W.E., Mayton, H., Andrade-Piedra, J.L., 2001. Quantifying the rate of release and escape of *Phytophthora infestans* sporangia from a potato canopy. Phytopathology 91, 1189–1196.

Bashi, E., Ben-Joseph, Y., Rotem, J., 1982. Inoculum potential of *Phytophthora infestans* and the development of potato late blight epidemics *Solanum tuberosum*. Phytopathology 72, 1043–1047.

Beakes, G.W., Glockling, S.L., Sekimoto, S., 2012. The evolutionary phylogeny of the oomycete "fungi." Protoplasma 249, 3–19.

Bourke, P.M. 1964. Emergence of potato blight, 1843–46. Nature 203, 805–808.

Chowdappa, P., Kumar, N.B.J., Madhura, S., Kumar, M.S.P., Myers, K.L., Fry, W.E., Squires, J.N., Cooke, D.E.L., 2013. Emergence of 13_A2 Blue lineage of *Phytophthora infestans* was responsible for severe outbreaks of late blight on tomato in South-West India. Journal of Phytopathology 161, 49–58.

Cohen, Y., Eyal, H., Sadon, T., 1975. Light-induced inhibition of sporangial formation of *Phytophthora infestans* on potato leaves. Canadian Journal of Botany 53, 2680–2686.

Danies, G., Myers, K., Mideros, M.F., Restrepo, S., Martin, F.N., Cooke, D.E.L., Smart, C.D., Ristaino, J.B., Seaman, A.J., Gugino, B.K., Grünwald, N.J., Fry, W.E., 2014. An ephemeral sexual population of *Phytophthora infestans* in the northeastern United States and Canada. PLoS ONE 9, e116354.

Erwin, D.C., Ribeiro, O.K. 1996. Phytophthora diseases worldwide. xii + 562 pp.

Fry, W., 2008. *Phytophthora infestans*: the plant (and R gene) destroyer. Molecular Plant Pathology 9, 385–402.

Fry, W.E., Birch, P.R.J., Judelson, H.S., Grünwald, N.J., Danies, G., Everts, K.L., Gevens, A.J., Gugino, B.K., Johnson, D.A., Johnson, S.B., McGrath, M.T., Myers, K.L., Ristaino, J.B., Roberts, P.D., Secor, G., Smart, C.D., 2015. Five reasons to consider *Phytophthora infestans* a reemerging pathogen. Phytopathology 105, 966–981.

Granke, L.L., Windstam, S.T., Hoch, H.C., Smart, C.D., Hausbeck, M.K., 2009. Dispersal and movement mechanisms of *Phytophthora capsici* sporangia. Phytopathology 99, 1258–1264.

Gevens, A.J., Donahoo, R.S., Lamour, K.H., Hausbeck, M.K. 2007. Characterization of *Phytophthora capsici* from Michigan surface irrigation water. Phytopathology 97, 421–428.

Grünwald, N.J., Flier, W.G., Sturbaum, A.K., Garay-Serrano, E., van den Bosch, T.B.M., Smart, C.D., Matuszak, J.M., Lozoya-Saldaña, H., Turkensteen, L.J., Fry, W.E. 2001. Population structure of *Phytophthora infestans* in the Toluca Valley region of central Mexico. Phytopathology 91, 882–890.

Grünwald, N.J., Sturbaum, A.K., Montes, G.R., Serrano, E.G., Lozoya-Saldaña, H., Fry, W.E., 2006. Selection for fungicide resistance within a growing season in field populations of *Phytophthora infestans* at the center of origin. Phytopathology 96, 1397–1403.

Haas, B.J., Kamoun, S., Zody, M.C., Jiang, R.H.Y., Handsaker, R.E., Cano, L.M., Grabherr, M., Kodira, C.D., Raffaele, S., Torto-Alalibo, T., Bozkurt, T.O., Ah-Fong, A.M.V., Alvarado, L., Anderson, V.L., Armstrong, M.R., Avrova, A., Baxter, L., Beynon, J., Boevink, P.C., Bollmann, S.R., Bos, J.I.B., Bulone, V., Cai, G., Cakir, C., Carrington, J.C., Chawner, M., Conti, L., Costanzo, S., Ewan, R., Fahlgren, N., Fischbach, M.A., Fugelstad, J., Gilroy, E.M., Gnerre, S., Green, P.J., Grenville-Briggs, L.J., Griffith, J., Grünwald, N.J., Horn, K., Horner, N.R., Hu, C.-H., Huitema, E., Jeong, D.-H., Jones, A.M.E., Jones, J.D.G., Jones, R.W., Karlsson, E.K., Kunjeti, S.G., Lamour, K., Liu, Z., Ma, L., Maclean, D., Chibucos, M.C., McDonald, H., McWalters, J., Meijer, H.J.G., Morgan, W., Morris, P.F., Munro, C.A., O'Neill, K., Ospina-Giraldo, M., Pinzón, A., Pritchard, L., Ramsahoye, B., Ren, Q., Restrepo, S., Roy, S., Sadanandom, A., Savidor, A., Schornack, S., Schwartz, D.C., Schumann, U.D., Schwessinger, B., Seyer, L., Sharpe, T., Silvar, C., Song, J., Studholme, D.J., Sykes, S., Thines, M., van de Vondervoort, P.J.I., Phuntumart, V., Wawra, S., Weide, R., Win, J., Young,

C., Zhou, S., Fry, W., Meyers, B.C., van West, P., Ristaino, J., Govers, F., Birch, P.R.J., Whisson, S.C., Judelson, H.S., Nusbaum, C. 2009. Genome sequence and analysis of the Irish potato famine pathogen *Phytophthora infestans*. Nature 461, 393–398.

Harnish, W.N.,1965. Effect of light on production of oospores and sporangia in species of *Phytophthora*. Mycologia 57, 85–90.

Harrison, J.G., Lowe, R. 1989. Effects of humidity and air speed on sporulation of *Phytophthora infestans* on potato leaves. Plant Pathology 38, 585–591.

Hausbeck, M.K., Lamour, K.H. 2004. *Phytophthora capsici* on vegetable crops: research progress and management challenges. Plant Disease 88. 1292–1303.

Hohl, H.R., Iselin, K., 1984. Strains of *Phytophthora infestans* from Switzerland with A2 mating type behaviour. Transactions of the British Mycological Society 83, 529–530.

Kroon, L.P.N.M., Brouwer, H., de Cock, A.W.A.M., Govers, F., 2011. The genus Phytophthora anno 2012. Phytopathology 102, 348–364.

Lamour, K.H., Hausbeck, M.K. 2003. Effect of crop rotation on the survival of *Phytophthora capsici* in Michigan. Plant Disease 87, 841–845.

Lamour, K.H., Mudge, J., Gobena, D., Hurtado-Gonzales, O.P., Schmutz, J., Kuo, A., Miller, N.A., Rice, B.J., Raffaele, S., Cano, L.M., Bharti, A.K., Donahoo, R.S., Finley, S., Huitema, E., Hulvey, J., Platt, D., Salamov, A., Savidor, A., Sharma, R., Stam, R., Storey, D., Thines, M., Win, J., Haas, B.J., Dinwiddie, D.L., Jenkins, J., Knight, J.R., Affourtit, J.P., Han, C.S., Chertkov, O., Lindquist, E.A., Detter, C., Grigoriev, I.V., Kamoun, S., Kingsmore, S.F. 2012a. Genome sequencing and mapping reveal loss of heterozygosity as a mechanism for rapid adaptation in the vegetable pathogen *Phytophthora capsici*. MPMI 25, 1350–1360.

Lamour, K.H., Stam, R., Jupe, J., Huitema, E. 2012b. The oomycete broad-host-range pathogen *Phytophthora capsici*. Molecular Plant Pathology 13, 329–337.

Leonian, L.H. 1922. Stem and fruit blight of peppers caused by *Phytophthora capsici* sp. nov. Phytopathology 12, 401–408 pp.

Li, Y., van der Lee, T. a. J., Evenhuis, A., van den Bosch, G.B.M., van Bekkum, P.J., Förch, M.G., van Gent-Pelzer, M.P.E., van Raaij, H.M.G., Jacobsen,

E., Huang, S.W., Govers, F., Vleeshouwers, V.G. a. A., Kessel, G.J.T., 2012. Population dynamics of *Phytophthora infestans* in the Netherlands reveals expansion and spread of dominant clonal lineages and virulence in sexual offspring. G3 2, 1529–1540.

Li, Y., van der Lee, T., Zhu, J.H., Jin, G.H., Lan, C.Z., Zhu, S.X., Zhang, R.F., Liu, B.W., Zhao, Z.J., Kessel, G., Huang, S.W., Jacobsen, E., 2013. Population structure of *Phytophthora infestans* in China – geographic clusters and presence of the EU genotype Blue_13. Plant Pathology 62, 932–942.

Maltese, C.E., Conigliaro, G., Shaw, D.S., 1995. The development of sporangia of *Phytophthora infestans*. Mycological Research 99, 1175–1181.

Melhus, I.E. 1915. Germination and infection with the fungus of the late blight of potato (*Phytophthora infestans*). Madison, WI: University of Wisconsin, Agricultural Experiment Station.

Mizubuti, E.S.G., Aylor, D.E., Fry, W.E., 2000. Survival of *Phytophthora infestans* sporangia exposed to solar radiation. Phytopathology 90, 78–84.

Mizubuti, E.S.G., Fry, W.E., 1998. Temperature effects on developmental stages of isolates from three clonal lineages of *Phytophthora infestans*. Phytopathology 88, 837–843.

Niederhauser, J.S. 1956. Division of Mycology: The Blight, the Blighter, and the Blighted. Transactions of the New York Academy of Sciences 19, 55–63.

Nielsen, C.J., Ferrin, D.M., Stanghellini, M.E., 2006. Cyclic production of sporangia and zoospores by *Phytophthora capsici* on pepper roots in hydroponic culture. Canadian Journal of Plant Pathology 28, 461–466.

Ribeiro, O.K. 1983. Physiology of asexual sporulation andspore germination in Phytophthora. In: Phytophthora, its Biology, Taxonomy, Ecology, and Pathology. St Paul: MN APS Press, pp. 55–70.

Ristaino, J.B. 2002. Tracking historic migrations of the Irish potato famine pathogen, *Phytophthora infestans*. Microbes and Infection 4, 1369–1377.

Savory, A.I.M., Grenville-Briggs, L.J., Wawra, S., West, P. van, Davidson, F.A., 2014. Auto-aggregation in zoospores of *Phytophthora infestans*: the cooperative roles of bioconvection and chemotaxis. Journal of The Royal Society 11, 20140017.

Schepers, H.T. a. M., Kessel, G.J.T., Lucca, F., Förch, M.G., Bosch, G.B.M. van den, Topper, C.G., Evenhuis, A., 2018. Reduced efficacy of fluazinam against *Phytophthora infestans* in the Netherlands. European Journal of Plant Pathology 1–14.

Schlub, R.L. 1983. Epidemiology of *Phytophthora capsici* on bell pepper. The Journal of Agricultural Science 100, 7–11.

Sujkowski, L.S., Parra, G.R., Gumpertz, M.L., Ristaino, J.B. 2000. Temporal dynamics of Phytophthora blight on bell pepper in relation to the mechanisms of dispersal of primary inoculum of *Phytophthora capsici* in soil. Phytopathology 90, 148–156.

Tani, S., Yatzkan, E., Judelson, H.S., 2004. Multiple pathways regulate the induction of genes during zoosporogenesis in *Phytophthora infestans*. MPMI 17, 330–337.

Tyler, B.M., Tripathy, S., Zhang, X., Dehal, P., Jiang, R.H.Y., Aerts, A., Arredondo, F.D., Baxter, L., Bensasson, D., Beynon, J.L., Chapman, J., Damasceno, C.M.B., Dorrance, A.E., Dou, D., Dickerman, A.W., Dubchak, I.L., Garbelotto, M., Gijzen, M., Gordon, S.G., Govers, F., Grunwald, N.J., Huang, W., Ivors, K.L., Jones, R.W., Kamoun, S., Krampis, K., Lamour, K.H., Lee, M.-K., McDonald, W.H., Medina, M., Meijer, H.J.G., Nordberg, E.K., Maclean, D.J., Ospina-Giraldo, M.D., Morris, P.F., Phuntumart, V., Putnam, N.H., Rash, S., Rose, J.K.C., Sakihama, Y., Salamov, A.A., Savidor, A., Scheuring, C.F., Smith, B.M., Sobral, B.W.S., Terry, A., Torto-Alalibo, T.A., Win, J., Xu, Z., Zhang, H., Grigoriev, I.V., Rokhsar, D.S., Boore, J.L. 2006. Phytophthora genome sequences uncover evolutionary origins and mechanisms of pathogenesis. Science 313, 1261–1266.

van der Horst, M.A., Hellingwerf, K.J. 2004. Photoreceptor proteins, “Star actors of modern times”: A review of the functional dynamics in the structure of representative members of six different photoreceptor families. Accounts of Chemical Research 37, 13–20.

Warren, R.C., Colhoun, J., 1975. Viability of sporangia of *Phytophthora infestans* in relation to drying. Transactions of the British Mycological Society 64, 73–75.

Waterhouse, G.M. 1931. The production of conidia in the genus Phytophthora. Transactions of the British Mycological Society 15, 311–321.

Xiang, Q., Judelson, H.S., 2014. Myb transcription factors and light regulate sporulation in the oomycete *Phytophthora infestans*. PLoS ONE 9, e92086.

Yuen, J.E., Andersson, B., 2013. What is the evidence for sexual reproduction of *Phytophthora infestans* in Europe? Plant Pathology 62, 485–491.

Zentmyer, G.A., 1961. Chemotaxis of zoospores for root exudates. Science 133, 1595–1596.

Zentmyer, G. A., Ribeiro, O.K. 1977. The effect of visible and near-visible radiation on sporangium production by *Phytophthora cinnamomi*. Phytopathology 67: 91–95.

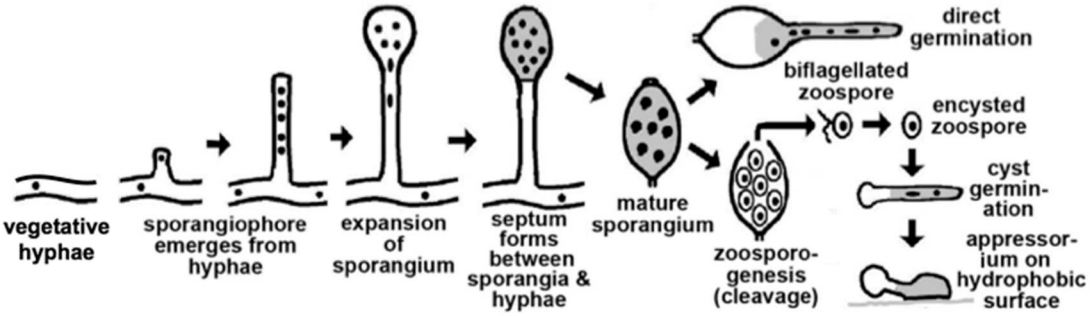

Figure 1.1. Detailed description of the *Phytophthora* asexual life cycle (credit: H.S. Judelson).

Chapter 2: Role of light and cryptochrome proteins in sporulation of Phytophthora species

Introduction

Light is an important signal in the development of many organisms. Light can serve as a source of energy, but can also cause direct damage to DNA. Light also serves as an informational signal for space and time, such as position relative to soil and shade, and the time of day and year. Many organisms have developed sophisticated ways to sense light and regulate development accordingly.

Light in plant-pathogen interactions

In plants, light influences metabolism, growth, development, and physiology (Chen et al., 2004; Darko et al., 2014; Deng, 1994; Ouzounis et al., 2015). As photosynthetic, sessile organisms, light is the energetic driver of plant biomass production, but can also be a signal for external stress (Kangasjärvi et al., 2012; Trotta et al., 2014). Light modulates plant defense responses, such as *R*-gene mediated defense, jasmonate signaling, and salicylic acid-mediated defense responses, including pathogen-associated molecular pattern (PAMP)-triggered immunity, effector-triggered immunity (ETI), and systemic acquired resistance (SAR) responses (Gangappa and Kumar, 2018; Griebel and Zeier, 2008; Karpinski et al., 2003; Kazan and Manners, 2011; Lu et al., 2017; Roden and Ingle, 2009; Stael et al., 2015; Wang et al., 2011). Light also influences pathogen biology, which can have a significant influence in disease outcome and

severity (Adam et al., 2018; Larrondo and Canessa, 2019; Lyu et al., 2016; Marine et al., 2018; Schumacher et al., 2014). This has been shown in several *Phytophthora* pathosystems including *P. infestans* on potato, *P. capsici* on pepper, pumpkin, and tomato, *P. drechsleri* on safflower and pigeon pea, and *P. megasperma* on soybean (Islam et al., 2002; Lebecka and Sobkowiak, 2013; Schumann, 1977; Singh and Chauhan, 1985; Thomas and Allen, 1971; Victoria and Thurston, 1974; Ward and Buzzell, 1983). Zonate, concentric rings radiating from the point of infection are common among *Phytophthora* diseases, both on foliage and fruit. This could be a result of periodicity underlying pathogenesis, or light-regulated biological changes in the pathogen itself.

Light in Phytophthora

Previous studies have shown that light has an effect on the biology of *Phytophthora* species, particularly related to sporulation. Notably, light has been shown to have a differential effect on sporulation in different species. In *P. capsici,* sporangial production is starkly affected by light, with sporulation inhibited in darkness and stimulated in light (Alizadeh and Tsao, 1985; Harnish, 1965). A similar pattern was shown in *P. cactorum*, *P. palmivora*, and *P. lateralis* (Alizadeh and Tsao, 1985; Englander, 1972; Harnish, 1965). In contrast, light will inhibit sporulation of *P. infestans* on potato leaves and on media (Cohen et al., 1975; Lebecka and Sobkowiak, 2013). Visible light also inhibits sporulation of *Phytophthora ramorum* (Englander et al., 2006). In *P. infestans*, although

sporangium production is light-sensitive, sporangiophore production was not shown to be light-sensitive, and green and red light wavelengths showed no effect on sporulation, while blue light did show an effect (Cohen et al., 1975). Light also has an effect on sporulation of downy mildews such as *Peronospora belbahrii* and *Bremia lactucae* (Nordskog et al., 2007). As in *P. infestans*, sporulation of *Peronospora belbahrii* is light-inhibited but sporophore production is not light-sensitive; however, in contrast to *P. infestans*, green, red, and blue single-spectrum wavelengths all decreased sporulation (Cohen et al., 2013). In both *P. belbahrii* and *Bremia lactucae*, this light-related suppression has an interaction with temperature (Cohen et al., 2013; Nordskog et al., 2007).

Previous to this study, little research had been conducted to understand the molecular basis for the light response in *Phytophthora*. Several light-regulated sporulation transcription factor genes have been identified, but the initial photoreceptors have not been identified (Leesutthiphonchai and Judelson, 2018; Xiang and Judelson, 2014). Through domain-level searches of the available *Phytophthora* and oomycete genomes, the only known photoreceptor genes that could be identified were cryptochromes (Xiang and Judelson, 2014).

Cryptochromes

Cryptochromes are a class of flavoproteins that are found in all kingdoms of life. Cryptochromes belong to the photolyase/cryptochrome superfamily, which also contains light-dependent photorepair enzymes known as photolyases (Wang

et al., 2015). Although members of the photolyase/cryptochrome superfamily have similar structure, the functions of these proteins can vary widely. Functions include DNA repair, reception of blue light, red light, and UV-A, transcriptional regulation, circadian rhythm entrainment, and magnetoreception (Gegear et al., 2010; Maeda et al., 2012; Veluchamy and Rollins, 2008; Zoltowski et al., 2019). Some cryptochromes are regulated at the transcript level, while others are regulated post-translationally (Lin and Todo, 2005).

Cryptochrome structure

Cryptochromes have an FAD-binding domain, photolyase homology domain, and a Rossmann-like alpha beta alpha sandwich fold (Chaves et al., 2011; Kim et al., 2014). Animal-type and plant-type cryptochromes have a C-terminal extension that can be active in light signaling, nuclear localization, and protein-protein interactions (Chaves et al., 2011; Lin and Shalitin, 2003; Liu et al., 2011; Thieulin-Pardo et al., 2015). The C-terminal extension in animal-type cryptochromes varies in length and sequence, is intrinsically disordered, and is thought to be critical for function and signaling in some species (Franz et al., 2018; Franz-Badur et al., 2019; Michael et al., 2017; Oldemeyer et al., 2016; Thieulin-Pardo et al., 2015).

All members of the photolyase/cryptochrome protein superfamily have flavin adenine dinucleotide (FAD) as a co-factor (Zhang et al., 2017). Some of the members of this protein family also have a second chromophore, a pterin or

folate such as methenyltetrahydrofolate (MTHF), flavin mononucleotide (FMN), 7,8-didemethyl-8-hydroxy-5-deazariboflavin (F_0), or 8-hydroxy-5-deazaflavin (8-HDF), which acts as an antenna, transferring the excitation energy to the canonical FAD (Göbel et al., 2017; Ozturk, 2017; Öztürk et al., 2007; Selby and Sancar, 2012). The second chromophore binding pocket is generally in the Rossmann fold of the photolyase homology region near the amino terminal, either directly in the groove (as with 8-HDF) or next to it (as with MTHF) (Franz et al., 2018; Sancar, 2003; Scheerer et al., 2015).

Cryptochrome types

Members of the photolyase/cryptochrome family can be divided into two groups: cryptochromes and photolyases. Photolyases use blue light to repair two types of ultraviolet-induced photolesions: cyclobutane pyrimidine dimers (CPDs) or pyrimidine-pyrimidone (6-4) photoproduct (6-4PP) (Liu et al., 2015). Members of the photolyase protein class are grouped by which of these lesions are repaired. However, some cryptochromes are bi-functional and have retained DNA repair activity.

Although cryptochromes were once defined as “proteins with a high degree of sequence homology to DNA photolyase but with no DNA repair activity”, this definition has changed over time as more information has been uncovered about proteins in this family that exhibit DNA repair function (Balland et al., 2009; Chaves et al., 2011; Coesel et al., 2009; Franz-Badur et al., 2019;

Holub et al., 2019; Ozturk, 2017; Pokorny et al., 2008; Selby and Sancar, 2006; Tagua et al., 2015).

Cryptochromes can further be divided into sub-classes: plant-type, DASH-type, and animal-type (Ozturk, 2017; Selby and Sancar, 2006). The sub-classes differ in structure, particularly at the C-terminal extension and FAD binding pocket (Ozturk, 2017). Plant-type cryptochromes have only been found in plants and have been shown to be involved in a range of growth and developmental processes including inhibition of hypocotyl elongation, photoperiodic control of floral initiation, entrainment of the circadian clock, regulation of stomatal opening, guard cell development, inhibition of germination of dormant grain, root growth, plant height, fruit and ovule size, tropic growth, stimulation of cotyledon expansion, apical dominance, apical meristem activity, programmed cell death, suppressing leaf senescence, osmotic stress response, light-dependent stress responses, shade avoidance, and responses to pathogens (as reviewed in Liu et al., 2011; Wang et al., 2018).

DASH-type proteins are named for *Drosophila melanogaster*, *Arabidopsis thaliana*, *Synechocystis*, and *Homo sapiens*, and exist in a wide range of organisms (Brudler et al., 2003; Daiyasu et al., 2004). DASH cryptochromes have photoreceptor activity, and repair single-stranded DNA damage. Cryptochromes in fungi are mostly DASH-type, and serve functions in processes such as circadian regulation, secondary metabolism, and development (Castrillo et al., 2013; Heintzen, 2012; Nsa et al., 2015). However, some researchers have

proposed that because DASH cryptochromes repair DNA, they should be classified as photolyases and not cryptochromes, or placed in a separate category (Balland et al., 2009; Schelvis and Gindt, 2017).

Animal-type cryptochromes were originally characterized in Drosophila, humans, mouse, monarch butterfly, birds, zebrafish, and frogs, but have since been also described in non-animal systems such as algae (Beel et al., 2012; Kim et al., 2014; Michael et al., 2017). Animal-type cryptochromes are most well-known for their role in circadian timekeeping and transcriptional repression, but have also been shown to play roles in regulation of the DNA damage response, cancer progression and glucocorticoid signaling, sexual development in algae, as well as possibly magnetoreception (as reviewed in Michael et al., 2017). Animal-type cryptochromes can be classified further into three groups: type 1, type 2, and type 4. Type 1 cryptochromes are typically photoreceptors involved in circadian timekeeping, type 2 are non-photoreceptive transcriptional repressors, and type 4 are the putative magnetoreceptors.

Blue and red light perception

In plants and microorganisms, blue light is detected by LOV-domain-containing proteins (such as phototropins, aureochromes, and white collar proteins), cryptochromes, or BLUF-domain containing proteins (van der Horst and Hellingwerf, 2004).

In *Chlamydomonas reinhardtii*, red light regulates the sexual cycle, and reception is mediated by an animal-type cryptochrome (Beel et al., 2012; Oldemeyer et al., 2016). However, red light is sensed in most plants and microorganisms by phytochrome proteins. Phytochromes have also been described to sense temperature (Legris et al., 2016). In plants, plant-type cryptochromes Cry1 and Cry2 have been shown to have blue light-independent activity, and specifically red light-dependent activity (Yang et al., 2008). However, it is not hypothesized that the plant cryptochromes directly sense red light, rather that the cryptochromes play a role in mediating the expression of genes related to phytochromes and phytochrome-interacting factors (Yang et al., 2008).

Light control of sporulation in fungi

In fungi, some species within a genus have differential response to light, as we see in Phytophthora. One example is Aspergillus, where *Aspergillus oryzae* has sexual development repressed by light, while sexual development in *Aspergillus nidulans* is stimulated by light (Hatakeyama et al., 2007). In *Aspergillus fumigatus*, single-spectrum blue light and red light were able to inhibit condium germination to the same level as white light (Fuller et al., 2013).

Neurospora crassa is one of the best-studied biological systems for light. However, light sensing in fungi involves many more types of photoreceptors than in *Phytophthora*, such as phytochromes, light-oxygen-voltage (LOV domain proteins), rhodopsins, and opsin-like proteins (Fuller et al., 2015; Z. Wang et al.,

2018). The cryptochrome in *Neurospora* is DASH-type, and does not have primary photoreception function, rather participating in circadian regulation. Knockout and overexpression of the *Neurospora* cryptochrome does not totally interrupt photoreception or the circadian clock, but results in a small phase delay in the circadian rhythm (Froehlich et al., 2010).

A recent large-scale network analysis of pan-proteomes of filamentous eukaryotic plant pathogens and saprobes (including oomycetes and fungi) showed that cryptochrome/photolyase activity is significantly enriched in biotrophic and hemibiotrophic plant pathogens (Pandaranayaka et al., 2019). Although cryptochromes are present in the necrotrophs, the enriched activity in biotrophs and hemibiotrophs indicate that these proteins may play a central role in virulence on plants, with roles that may include photoprotection and photomorphogenesis (Pandaranayaka et al., 2019).

To investigate the molecular basis of the differential response to light relative to sporulation, the available *Phytophthora* genomes were searched for putative photoreceptor proteins. Domain-level searches revealed that of the known types of photoreceptor proteins (van der Horst et al. 2004), only cryptochrome proteins could be found (Xiang and Judelson 2014). The genome of *P. infestans* is predicted to have three cryptochromes proteins: PITG_01718, PITG_16100, and PITG_16104. *Phytophthora capsici* is predicted to have two: Phyca_44729 and Phyca_574436. In this chapter, I describe the effects of manipulating these genes through gene knockdown and overexpression.

Additionally, several studies were conducted to understand the role of light and light quality on sporulation of these two species.

Materials and Methods

Strains

Phytophthora infestans strain 1306, an A1 strain isolated from tomato in California, was maintained on rye-sucrose media at 18°C in the dark (Judelson and Whittaker, 1995). *Phytophthora capsici* strain LT1534, a lab strain created through a cross of LT51 and LT263, backcrossed twice to LT263 to reduce heterozygosity, was maintained on 10% V8 juice agar at 18-23°C in the dark (Hurtado□Gonzales and Lamour, 2009). Experiments were conducted with three biological replicates, unless otherwise noted.

Photoreceptor identification

Domain-level searches were performed against the *Phytophthora infestans* T30-4 reference genome sequence, *P. capsici* LT1534 reference genome sequence, and the genomes of *P. sojae, P. ramorum, P. parasitica, P. cinnamomi,* and *Hyaloperonospora arabidopsidis* (Baxter et al., 2010; Haas et al., 2009; Lamour et al., 2012; Tyler et al., 2006) using BLASTp in FungiDB (FungiDB, http://fungidb.org/) and domain search in InterPro (EMBL-EBI, https://www.ebi.ac.uk/interpro/).

Gene models

Gene models were verified for the putative photoreceptors identified in *P. infestans* and *P. capsici*. DNA was extracted from 7-day-old wild-type *P. infestans* 1306 cultures grown on solid rye-sucrose agar and 7-day-old *P. capsici* LT1534 grown on 10% V8 juice agar, with the Wizard SV DNA extraction kit (Promega Corporation, Madison, WI) or the GeneJet Plant Genomic DNA extraction kit (Thermo Fisher Scientific, Waltham, MA). Genes were amplified from genomic DNA by PCR, cloned into pGEM-T (Promega Corporation, Madison, WI), and sequenced by Sanger sequencing with a 3130 Genetic Analyzer (Applied Biosystems, Foster City, CA). Predicted introns were verified by mapping available Illumina RNA-seq transcript reads to the reference genome (Abrahamian et al., 2016). Once gene models were determined, protein sequences were predicted with the exPASY translate tool (Swiss Institute of Bioinformatics, https://web.expasy.org/translate/).

Cap analysis gene expression sequencing (CAGE-seq) data was generated for *P. infestans* to verify transcription start sites. RNA was prepared by Dr. Audrey Ah-Fong, using the Plant Spectrum Total RNA extraction kit (Sigma-Aldrich, St. Louis, MO). Libraries were prepared and sequenced by GenXPro (Frankfurt, Germany). Initial bioinformatic analysis was performed by Amy Boyd.

Protein domain architecture was predicted with the Conserved Domains Database CD-Search tool using the Pfam v31.0 database, which included 16,709 pre-calculated position-specific scoring matrices (National Center for

Biotechnology Information, https://www.ncbi.nlm.nih.gov/Structure/cdd/wrpsb.cgi). The CD-Search tool uses the reverse position-specific basic local alignment search tool algorithm (RPS-BLAST), which is a variation of the position-specific iterated BLAST.

Phylogeny

Protein sequences of *Phytophthora* cryptochromes and cryptochromes from other organisms were collected from FungiDB, NCBI, and JGI genome databases. The sequences were aligned in SeaView (Pôle Rhône-Alpes de Bioinformatique Site, http://doua.prabi.fr/software/seaview) using the MUSCLE algorithm, then trimmed with the Transitive Consistency Score (TCS) program in the T-Coffee suite (Centre for Genomic Regulation, http://tcoffee.crg.cat/apps/tcoffee/), and a Maximum Likelihood phylogeny was calculated using PhyML in SeaView using the approximate likelihood ratio test to mreasure branch support.

Gene knockdown and overexpression

In *P. infestans*, each gene was targeted for knockdown using homology-based gene silencing. A 500 bp region was selected in each gene, and a hairpin construct was made by cloning the 500 bp homologous sequence into the pSTORA cloning vector, upstream of the Ste20 intron, then the reverse compliment sequence was cloned directly downstream of the Ste20 intron, using

primers listed in Table 2.1. The pSTORA vector is a modified version of the pTOR cloning vector (Ah-Fong et al., 2008). Constructs were confirmed by restriction digest and Sanger sequencing and cloned into DH5α chemically competent cells. Plasmid minipreps were performed with the GeneJet plasmid extraction kit (ThermoFisher, Waltham, MA), and maxipreps were performed with the Nucleobond Maxi kit (Machery-Nagel, Düren, Germany). Additionally, the 500 bp sense region was cloned into the pTOR cloning vector to attempt gene knockdown through sense-mediated post-transcriptional gene silencing. However, none of the transformants from these constructs were silenced for the target gene. Therefore, only hairpin-induced gene silencing transformants were used in the rest of this study.

To assess the effect of overexpression, the full-length gene was cloned behind the strong constitutive promoter ham34, with an added peptide tag using the pTOR cloning vector, using primers listed in Table 2.1. Because each end of the protein could have signaling function, particularly in PITG_01718, constructs were made with a myc-tag (EQKLISEEDL) at the amino terminal, or a FLAG-tag (DYKDDDDK) at the carboxyl end. The genes were amplified from genomic DNA, as no introns are present in any of these genes.

Potential knockdown transformants were screened by qPCR. Initial screening of overexpression transformants was completed with Western blotting. Positives were single nuclear purified via single zoospore selection, and transcript levels were quantified by real time reverse transcription PCR (qRT-

PCR), using primers listed in Table 2.1. PITG_01718 knockdown transformants were also screened by Western blot.

Quantitative real time PCR (qRT-PCR)

RNA was extracted with the Plant Spectrum total RNA kit (Sigma-Aldrich, St. Louis, MO). RNA was treated with RQ1 DNase (Promega Corporation, Madison, WI), and complementary DNA (cDNA) was made using the Maxima first strand synthesis kit (Thermo Scientific, Waltham, MA). qRT-PCR was performed on a Bio-Rad CFX Connect using the Dynamo Sybr Green Hot Start master mix kit (ThermoFisher, Waltham, MA) with a program of 95° C for 15 min, 40 cycles of 94° C for 10 sec, 58°C or 62°C for 20 sec, 72°C for 30 sec, and a melting curve to 95°C. Primers were designed to amplify 100-150 bp fragments towards the 3' end of the gene, outside of the hairpin construct target region, as listed in Table 2.1. The ribosomal protein S3A gene was used as an internal control for both *P. infestans* and *P. capsici*, and three technical replicates were run for every sample. No-reverse transcriptase (RT) controls (DNase-treated RNA with Maxima reaction mix, but no RT enzyme) were run to assess DNA contamination, and negative controls were run to assess contamination of reagents. Primer efficiency was calculated. Fold-change was calculated by the delta-delta-Cq method, and standard error fold-change was calculated.

Western blots

Western blots were performed on 0.45 µm nitrocellulose membranes, using monoclonal M2 anti-FLAG (Sigma-Aldrich, St. Louis, MO) with an anti-mouse secondary antibody (ThermoFisher, Waltham, MA), anti-myc (ThermoFisher, Waltham, MA) with a goat-anti-rabbit secondary antibody (Invitrogen, Carlsbad, CA), or custom anti-PITG_01718 antibodies raised in rabbit and affinity purified using peptide SQTSKKRQREGSDDESKQQ, and the goat-anti-rabbit secondary antibody.

Proteins were extracted from 5-7-day-old cultures grown on solid media. Tissue was scraped from the surface of two 100-mm rye-sucrose plates per isolate with a flamed scalpel, then ground in a ceramic mortar and pestle under liquid nitrogen. Extraction buffer (50mM Tris pH 7.4, 30 mM NaCl, 1% SDS (sodium dodecyl sulfate), 1 mM dithiothreitol, 1mM phenylmethylsulfonyl fluoride, 20% glycerol) was made fresh and added at approximately 1 µl per mg frozen tissue in a screw cap 1.5 ml tube. Tissue in extraction buffer was vortexed at max speed for 30-60 seconds then placed on a rotational shaker at room temperature (22°C) for 10 min at 60 rpm. Tubes were then centrifuged for 10 min at max speed (12,000 ×*g*) in a tabletop microcentrifuge at room temperature. The supernatant was transferred to a new tube, as only soluble protein was used.

Proteins were denatured for 5 minutes at 98°C in a thermal cycler in Laemmli SDS-PAGE gel loading buffer (50 mM Tris pH 6.8, 10% glycerol, 0.01% bromophenol blue, 3% SDS, 5% β-mercaptoethanol). Proteins were separated in

0.75 mm polyacrylamide gels with 10% acrylamide resolving gel and 4% acrylamide stacking gel, in running buffer (25 mM Tris, 192 mM glycine, 0.1% SDS, pH 8.3). Proteins were transferred from the acrylamide gel to nitrocellulose membrane using migration buffer with SDS (25 mM Tris, 192 mM glycine, 0.05% SDS, 20% methanol, pH 8.3) at 4°C.

Gels were stained with Coomassie blue (0.25% w/v Coomassie Brilliant Blue R-250, 50% methanol, 10% acetic acid). Membranes were stained with Ponceau stain (0.5% w/v Ponceau S, 1% glacial acetic acid). Membranes were blocked in 5% milk blocking buffer, washed in Tris-buffered saline with Tween-20, and developed with Amersham ECL western blotting detection reagent (GE Healthcare, Marlborough, MA) in a Li-Cor C-Digit blot scanner (Li-Cor, Lincoln, NE).

Transformation

Transformants were obtained by a modified version of published protoplast methods (Judelson et al., 1991; Vu et al., 2019). Twelve 150 mm rye-sucrose media plates were spread with approximately 200 µl of a 6×10^4 spore suspension and incubated for 10-14 days at 18°C in the dark. The plates were then flooded with sterile water and rubbed with a bent glass rod to dislodge sporangia, and the sporangial suspension was poured through a 50 µm nylon mesh in a ring holder over a 400 ml plastic beaker to remove hyphal fragments. The spore concentration was adjusted with water to 5×10^5 spores/ml, then an

equal volume of clarified amended lima bean agar was added, to a final concentration of 2.5×10^5 spores/ml (Bruck et al., 1980). The spore suspension was amended with 40 units nystatin, 25 µg/ml vancomycin, and 50 µg/ml ampicillin, and distributed to 1-L glass flasks, with approximately 150 ml/flask. Cultures were incubated stationary at 18°C in the dark for 36 hours, until the sporangia germinated and formed a thin mat of young, sparsely branched hyphae. The hyphal mat was dislodged by swirling and collected by pouring the solution through a 50 µm nylon mesh in a ring holder over a 400ml plastic beaker. The hyphal mat was collected with bent flat-paddle forceps and washed with protoplasting buffer (PB; 0.4 M mannitol, 20 mM KCl, 20mM MES pH 5.7, 10mM $CaCl_2$) by one gentle inversion in a 50 ml conical tube, and re-collected on the nylon mesh. The washed hyphal mat was quickly weighed, then moved to a 50ml conical containing 3 ml/gram hyphae of PB with 5 mg/ml of filter-sterilized cellulase (from *Trichoderma reesi*, Sigma-Aldrich, St. Louis, MO) and 10 mg/ml β-glucanase (Vinoflow NCE (Novozymes A/S, Bagsværd, Denmark) or Extralyse (Laffort USA, Petaluma, CA)). Typically, 5 grams of hyphae was harvested and added to 15 ml PB containing 25 mg cellulose and 50 mg β-glucanase. The conical was then wrapped in aluminum foil to protect the enzyme mixture from light, and incubated at room temperature on an orbital shaker at 50 rpm. When the hyphal mat was approximately 80-90% digested, about 45 minutes, the solution was passed through a 40 µm cell strainer (Fisherbrand, Waltham, MA) seated in a 50 ml conical to remove any undigested hyphae. The protoplasts

were then pelleted in the 50 ml conical tube in a swinging bucket centrifuge at 700×g at room temperature for 5 minutes. During this first centrifugation, 30 µg plasmid DNA in 40 µl volume was mixed in a 14ml round bottom polystyrene tube with 60 µl Lipofectin (ThermoFisher, Waltham, MA) and left to incubate at room temperature. The protoplast pellet then had the liquid gently poured off, and was resuspended in 30ml PB and respun. The pellet was then resuspended in 15 ml PB plus 15 ml of MT (1M mannitol, 10mM Tris pH 7.5). The pellet was spun again and resuspended in 30 ml MT plus 10mM $CaCl_2$. The pellet was centrifuged again and resuspended in 4 ml MT plus 10mM $CaCl_2$, to a final concentration of 2-9 $\times 10^7$ protoplasts/ml. One ml of the protoplast suspension was slowly added while turning the tube, to each of 4 polystyrene tubes containing a DNA-liposome mixture, which has been incubating for about 30 minutes. After 4 min, 1 ml 50% polyethylene glycol MW 3350 containing 10 mM Tris pH 7.5 and 25 mM $CaCl_2$ was slowly added while rotating the tube, then inverted once gently. The tube was again incubated for 4 min, then 2 ml clarified rye-sucrose broth containing 1M mannitol (regeneration media) was added and the tube was gently inverted once. After 1 min, 6 ml of regeneration media was added, for a total volume of 10 ml. The 10 ml was then added to a 50 ml conical containing 25 ml regeneration media amended with 40 units nystatin, 25 µg/ml vancomycin, and 50 µg/ml ampicillin, and stored stationary at 18°C in the dark for 24 hours. The regenerated protoplasts were then centrifuged at 1000 ×g for 5 min. The liquid was carefully poured off except for 2 ml, and the pellet was

resuspended in the remaining 2 ml. The regenerated protoplasts were then carefully plated on rye-sucrose agar amended with 8 µg/ml G418 (geneticin) and spread with a bent glass rod. After 5-9 days, individual colonies were moved to 50mm Petri dishes containing rye-sucrose agar amended with 16 µg/ml G418, and maintained on rye-sucrose agar amended with 16 µg/ml G418 thereafter. Per transformation reaction, 35-50 transformants were typically obtained, depending on the specific construct being introduced.

Light treatments

Experiments were conducted in a Percival I-36LLVL environmental control chamber at 18°C. For 60-minute light exposure, cultures were grown under constant dark conditions, then exposed to light for 60 minutes before harvesting. The intensity and light emission spectra of light treatments were measured with an Apogee PS-200 spectroradiometer (Apogee Instruments,.Logan, UT). The light emission spectrum of the white light treatment is shown in Fig. 2.1, and the photon fluence rate was 75 µmol/m^2/sec. Blue and red LED bulbs were used for single-spectrum blue and red light treatments (Fig. 2.1). The photon fluence rate of these single-spectrum lights was set to 100 µmol/m^2/sec using a dimmer. Dark treatments were incubated in the same chamber as light treatments, but light was blocked from cultures using a combination of cardboard, thick black fabric, or black plastic.

CRISPR/Cas9

To assess the role of the putative photoreceptors in *P. capsici*, 5 or 6 single guide RNAs were designed for each of the two genes. The single guide RNAs (sgRNAs) were designed using Eukaryotic Pathogen CRISPR guide RNA/DNA Design Tool (EuPaGDT; University of Georgia, Athens, GA, http://grna.ctegd.uga.edu/), and secondary structure was checked with the RNA structure tool (University of Rochester Medical School, http://rna.urmc.rochester.edu/RNAstructureWeb/). Sequences are listed in Table 2.2. Off-targets were checked using BLASTn against the *P. capsici* LT1534 reference genome in FungiDB (FungiDB, http://fungidb.org/). SgRNA inserts were made by annealed oligos and cloned into the all-in-one pYF515 vector containing the Cas9 enzyme (Fang et al., 2017). Plasmids were prepared as described (shaken at 150 rpm for 12-14 hours), and transformed via protoplast transformation as described above, with a few modifications for *P. capsici*: V8 juice media was substituted for rye-sucrose media, initial inoculum plates were inoculated with three to four 7mm hyphal plugs then incubated for 8-20 days in light, ALBA flask cultures were incubated for 18-24 hours, and transformed protoplasts were incubated for 12-18 hours regeneration before plating.

Infection assays

P. infestans cryptochrome knockdown transformants were checked for pathogenicity on tomato cultivar ‘New Yorker’. Plants were grown in UC Special

Mix at a 12-hour 23°C/18°C light/dark cycle in a Percival E41L2 growth chamber. Detached leaves were inoculated with 7 µl of 2×10^5 sporangia/ml water dropped along the midline of the adaxial leaf surface and incubated on 0.8% water agar in a deep Petri dish under 12-hour light/dark conditions at 18°C in a Percival I-37LLVL growth chamber.

Results

Sporulation

Sporulation in *P. infestans* was repressed by light, while sporulation in *P. capsici* was stimulated by light (Fig. 2.2A,B), under white light versus dark conditions. When exposed to single-spectrum blue light, both species had the same sporulation response to blue light as to broad-spectrum white light (Fig. 2.2C,D), indicating that blue light is sensed by both species and this signal affects sporulation. However, when given single-spectrum red light, sporulation in *P. infestans* responded the same to red light as to white light, but sporulation in *P. capsici* was not changed by red light (Fig. 2.2D).

Phytophthora cryptochromes

Domain-level searches revealed that of the known types of photoreceptor proteins, only cryptochromes are present in the available *Phytophthora* genomes. *Phytophthora infestans* contains 4 Per-ARNT-Sim (PAS) domain-containing proteins: PITG_01203 (mitogen-activated protein kinase), PITG_23006 (hybrid signal transduction histidine kinase), PITG_13826 (hybrid signal transduction

histidine kinase), and PITG_14416 (PAS-domain containing protein). Although two of these PAS-domain containing proteins also contain histidine kinase domains, as would be found in a phytochrome (PITG_23006 and PITG_13826), neither of these *P. infestans* proteins additionally contain the GAF or phytochrome central domain (PHY) domains of a phytochrome (Nagatani, 2010). GAF domains were predicted in 22 *P. infestans* genes, but no PHY domains were predicted in any *Phytophthora* sequence. None of the PAS domains in *P. infestans* are light-oxygen-voltage (LOV) domains, as would be found in phototropins, white collar proteins, vivid proteins, or aureochromes. Two *P. infestans* proteins have PAS-like photoactive yellow protein (PYP)-like domains, PITG_12584 and PITG_12760. However, these are not predicted to be xanthopsins, as the domain is not predicted to be a full PAS domain and the overall predicted protein structures do not have *p*-coumaric acid chromophore binding pockets (Kort et al., 1996; Pellequer et al., 1998; van der Horst et al., 2005). No BLUF domains were found. No rhodopsin or opsin-like G-protein coupled receptors were found.

Phytophthora infestans has three cryptochromes (PITG_01718, PITG_16100, and PITG_16104), while *P. capsici* has two cryptochrome genes (Phyca_44729 and Phyca_574436). Their relationships to each other and cryptochromes from other species are shown in Fig. 2.3. Each of these genomes also has one other member of the cryptochrome/photolyase superfamily, a deoxyribodipyrimidine photolyase that is predicted to have DNA repair activity but

no photoreception/signaling function: PITG_20715 and Phyca_12143 (Fig. 2.3A).

PITG_16100 is an ortholog of Phyca_44729, and PITG_16104 is an ortholog of Phyca_574436. PITG_01718 does not have an ortholog in *P. capsici*, but does have orthologs in *P. parasitica, P. ramorum*, *P. sojae*, and all of the downy mildew pathogens that were included in this phylogeny: *Plasmopara halstedii, Bremia lactucae, Hyaloperonospora arabidopsidis*, and *Peronospora effusa* (Fig. 2.3B). All of the *Phytophthora* genomes contain at least two cryptochromes. Most of the oomycete cryptochromes group together and form two distinct subclades within that group (Fig. 2.3B). The oomycete clade then groups with the known animal-type cryptochromes, which is the subtype of cryptochrome that the oomycete cryptochromes are expected to be (Kim et al., 2014; Xiang and Judelson, 2014). The exception is the Saprolegnialean oomycetes. *Aphanomyces astaci and A. invadans* cryptochromes group directly with the animal-type cryptochromes from stramenopile algae. Interestingly, the rest of the Saprolegnialean oomycetes that were included in this phylogenetic analysis (*Saprolegnia diclina*, *Saprolegnia parasitica*, *Achyla hypogyna*, and *Thraustotheca clavata*) only have proteins that group with the photolyases, not the cryptochromes (Fig. 2.3A). This is notable as the photolyases are not predicted to have photoreception activity, and therefore, the *Saprolegnia diclina*, *Saprolegnia parasitica*, *Achyla hypogyna*, and *Thraustotheca clavata* genomes are not predicted to contain any known or canonical photoreceptors. However, it

is worth nothing that previous studies have indicated that light affects oospore production of *Saprolegnia diclina* and sporangium production in *Saprolegnia parasitica* (Clausz, 1968; Lee, 1962; Szaniszlo, 1965). Therefore, it is possible that the lack of characterized photoreceptor proteins is an artifact of genome sequencing or assembly specific to this set of organisms.

PITG_16104 in the *P. infestans* T30-4 genome assembly was predicted to have two introns, neither of which are supported by our RNA-seq data at any developmental stage. The gene model of PITG_16104 was adjusted accordingly, and a new predicted protein sequence was generated (Table 2.2). Both *P. capsici* gene models (Phyca_574436 and Phyca_44729) as predicted in the LT1534 454-based reference genome database lacked stop codons, and Phyca_44729 also lacked a start codon. The mapped RNA-seq reads for *P. capsici* (discussed in Chapter 3) left the start codon for Phyca_574436 ambiguous, as very few reads covered the most likely start codon. Phyca_574436 has one obvious open reading frame, and the distance from the ambiguous start codon to the next start codon in frame is 339 nucleotides, which is much larger than the average 45 nucleotide 5'UTR in *Phytophthora* genomes. The N-terminal extension of Phyca_574436 is predicted to be the first 336 bases, with the photolyase homology domain predicted to start at amino acid 113. The first 112 amino acids are conserved among *Phytophthora* species, including the *P. infestans* ortholog PITG_16104.

The transcription start sites (TSS) of the *P. infestans* genes were mapped by CAGE-seq, which confirmed the TSS predicted in the T30-4 genome and the 5' UTRs mapped in the RNA-seq of *P. infestans* strain 1306 for all three genes. The TSSs for the *P. capsici* cryptochromes were predicted as the most likely start site based on comparison of orthologous gene model DNA sequences, particularly with the CAGE-seq-confirmed *P. infestans* models, RNA read coverage, and protein sequence conservation among *Phytophthora* species, leading to the protein sequences used in this study (Table 2.2).

Since *P. capsici* appeared to encode fewer cryptochromes than *P. infestans,* we considered the possibility that the public LT1534 assembly was incomplete. However, a new *P. capsici* LT1534 genome assembly generated using long-read PacBio sequencing and Illumina reads still only contained two sequences predicted to encode cryptochrome photoreceptors.

The new *P. capsici* genome assembly showed two distinct alleles for Phyca_44729. This was confirmed by PCR, cloning, and Sanger sequencing. The alleles are distinguished by a 9-base insertion/deletion near the 5' end, a 9-base insertion/deletion in the photolyase homology domain, and an 11-base insertion/deletion at the 3' end that interrupts the stop codon and leads to an alternative stop codon (Fig. 2.4B, Table 2.2).

Structurally, the N-terminal end before the photolyase domain is longer in most *Phytophthora* cryptochromes than in cryptochromes in other organisms, with the exception of PITG_01718 (Fig. 2.4C). However, cryptochrome size and

structure varies in different organisms and with different functions (Lin and Todo, 2005).

Light-regulated expression of cryptochrome genes

Based on qRT-PCR results, gene expression of PITG_16100 and Phyca_44279 were higher under constant white light versus constant dark conditions (2.5 to 3.7-fold and 6 to 10.5-fold, respectively), while PITG_01718 and Phyca_574436 were not differentially expressed in response to light (Fig. 2.5A,B). PITG_16104 had slightly reduced expression under constant light at 2 days post inoculation (30% reduced), but was not differentially expressed at 3 or 4 days post inoculation (Fig. 2.5A).

Because some cryptochromes in other species are induced in response to short bursts of light but level off expression due to acclimatization to the constant light (Schwerdtfeger and Linden, 2001), the expression levels were also checked after 60 minute exposure to white light. When *P. infestans* cultures were grown in the dark for several days then exposed to white light for 60 minutes before harvest, PITG_16100 transcripts were again induced under the light condition (6-fold) as compared to constant dark (Fig. 2.5C). This is a larger fold-change than in constant light (Fig. 2.5A). PITG_01718 transcript levels were not significantly differentially expressed under the short light exposure (Fig. 2.5C). PITG_16104 expression was 45% reduced after 60-minute light exposure, both when harvested at day 4 and day 6 (Fig. 2.5C).

Taken together, these experiments show that PITG_16100 and the *P. capsici* ortholog, Phyca_44729, both have higher transcript levels in light than dark, while expression of PITG_01718 and Phyca_574436 were unchanged, and PITG_16104 had slightly less transcripts detected in light as compared to dark, using ribosomal S3A gene expression as an internal control.

P. infestans cryptochrome knockdowns

Transformants were generated using the constructs and strategies described in Fig. 2.6A. Although both hairpin and sense silencing constructs were made and transformed into *Phytophthora*, only hairpin constructs yielded positives for knockdown or silencing. No sense-mediated knockdown transformants were identified.

One PITG_01718-silenced transformant and two transformants with reduced expression were identified using the hairpin construct (Fig. 2.7A). Expression levels of neighboring genes were checked for off-target silencing effects (Fig. 2.7A). Isolates were single-nuclear purified, and 4-5 single nuclear derivatives per isolate were checked for expression of PITG_01718 (Fig. 2.7B). For the silenced strain, AV9, all four single nuclear derivatives were silenced for PITG_01718, indicating that AV9 was likely homokaryotic. Strain 17 also showed similar expression of PITG_01718 in all of its single-nuclear derivatives. Strain 26, however, had some derivatives were either less-reduced than the original culture, or no longer reduced in expression of PITG_01718 (Fig. 2.7B). This

indicates that strain 26 was likely heterokaryotic, or had some nuclei that reverted to wild-type PITG_01718 expression levels, while maintaining G418 antibiotic resistance. Transformants were grown for 7 days under 12-hour light/dark conditions and checked for sporangia production. All three transformant strains were reduced in sporulation as compared to wild-type strain 1306 (Fig. 2.7C). This experiment was repeated under constant blue light, constant red light, and constant darkness, and reduced sporulation was observed in all three knockdown strains (Fig. 2.7D). Under constant light, constant dark, and 12-hour light/dark conditions, radial growth was only reduced in the silenced strain AV9, as compared to wild type (Fig. 2.7E). All three silenced strains retained pathogenicity on detached tomato leaves, however, AV9 continued to show reduced growth rate as compared to the other strains (Fig. 2.7F). Silenced strain AV9 has distinct colony morphology from wild-type in both light and dark conditions, again showing a slower growth rate as compared to wild-type (Fig. 2.7G).

Transformations targeting PITG_16100 also yielded silenced and knockdown strains. Once seven individual silenced or strong knockdown transformants were identified, all with the hairpin construct, further screening was stopped. Three biological replicates per isolate were checked for off-target gene expression changes in the neighboring genes (Fig. 2.8A). Isolate 5A had a flat colony growth and reduced growth rate as compared to wild-type and the other silenced transformants, and qRT-PCR revealed reduced expression of

PITG_16099, an EF-hand domain-containing protein located immediately to the left of the target gene (Fig. 2.8A). Strain 17 also had reduced expression of PITG_16099. Because any phenotype could therefore not be reliably attributed solely to the reduction of PITG_16100 transcripts, these two strains were excluded from further study. Strains 5A, 18, and 19 had an approximately 40% increase in expression of PITG_16101, an anoctamin-like protein. The remaining PITG_16100-silenced transformants showed normal expression of its flanking genes, and were thus assayed for growth, colony morphology, and sporulation in light versus dark. No growth or sporulation changes were observed (Fig. 2.8B).

Transformations with three different constructs targeting PITG_16104 were performed, and yielded about 12 transformants with reduced transcript levels for PITG_16104 (Fig. 2.9A). Unfortunately, all of these transformants were severely developmentally delayed or stunted, and several died before phenotyping could be performed. Although none of these cultures sporulated well, if at all, qRT-PCR of the neighboring genes showed that expression of a proximal non-coding RNA was significantly reduced in all of the transformants, as was expression of nearby gene PITG_16105, an E3 ubiquitin ligase with a zinc RING finger domain (Fig. 2.9A,B). One transformant also showed slightly reduced expression of PITG_16103, a Major Facilitator Superfamily protein. Because these transformants had off-target alterations in gene expression, any deviation in cultural and sporulation phenotypes from wild-type could not be

reliably attributed to the reduction of PITG_16104 transcripts. No further analysis was conducted.

P. infestans cryptochrome overexpression

Overexpression transformants were generated using constructs described in Fig. 2.6B. Positive transformants were obtained for all three genes (Fig. 2.10). Transformants overexpressing PITG_16100 with the peptide tag were not easy to obtain, as only one positive was identified from 77 screened: 16100-OE-22, which has the N-terminus myc tag (Fig. 2.10A). For PITG_01718, 6 positive transformants were identified from 33 screened, all of which all have the C-terminal FLAG tag. Each isolate was single nuclear purified, and derivatives were again checked by Western blot for production of the target gene with the small peptide tag attached (Fig. 2.10B). For PITG_16104, 5 transformants overexpressing this protein with a C-terminal FLAG tag were identified from 41 screened (Fig. 2.10C). Also, mRNA levels of the target gene and other cryptochromes were quantified for each isolate using RT-qPCR. PITG_16100-OE-22 has an 86-fold increase in expression of PITG_16100 mRNA compared to wild-type, with slight alterations in expression of the other cryptochrome genes, with a 25% reduction of PITG_16104 and 50% increase in transcripts of PITG_01718 (Fig. 2.11A). PITG_16104-OE isolates 35, 36, and 38 have 72-, 66-, and 92-fold increases in expression of PITG_16104, respectively, with about an 80% increase in expression of PITG_01718 and a 2-fold increase in PITG_16100

(Fig. 2.11B). PITG_01718-OE isolates 28, 34, and 35 have 37-, 72-, and 18-fold increases in expression of the target gene PITG_01718, with a 50% increase in expression of PITG_16104, and a 2-fold increase in PITG_16100 (Fig. 2.11C). These strains were phenotyped for growth and sporulation under constant light and constant dark conditions (Fig. 2.12). PITG_01718 transformants OE-28 and OE-34 sporulated the same as wild type in both light and dark, while OE-35 had sporulation reduced in the dark. PITG_16104 transformant OE-35 did not differ from wild type, while OE-36 had a 2-fold increase in darkness, but did not differ from wild type in light, and OE-38 had a 60% decrease in sporulation in both light and dark conditions. PITG_16100 OE-22 sporulation did not differ from wild type in light or dark (Fig. 2.12).

Discussion

Cryptochromes are conserved response proteins that exist in all kingdoms of life, so it is not surprising that *Phytophthora* genomes contain cryptochromes. It is surprising that Saprolegnialean oomycetes (with the exception of *Aphanomyces* spp.) appear not to contain cryptochromes. Although cryptochromes are involved in the circadian clock in many organisms, no evidence has been published to demonstrate a circadian rhythm or any circadian-regulated processes in *Phytophthora* species, or in any oomycete. Circadian rhythms have been identified in photosynthetic stramenopiles, including brown algae, diatoms, and *Nannochloropsis* spp. (Braun et al., 2014; Ragni and D'Alcala, 2007; Schmid et al., 1992; Schmid and Dring, 1992).

It is worth noting that no light-oxygen-voltage (LOV) domains were identified in the *Phytophthora* genomes. LOV domains are in the Per-ARNT-Sim (PAS) domain superfamily and detect blue light through a flavin cofactor (Crosson et al., 2003). Many photoreceptors contain LOV domains, such as vivid and the white collar photoreceptors in fungi, phototropins in plants, and aureochromes in photosynthetic stramenopiles (He et al., 2002; Schwerdtfeger and Linden, 2003; Takahashi et al., 2007). LOV domains are conserved in all kingdoms of life, including bacteria and archaea (Herrou and Crosson, 2011). However, my searches of the stramenopiles only found LOV domains in the photosynthetic stramenopiles. The lack of LOV domains in *Phytophthora* and other oomycetes was confirmed in an extensive search of the InterPro/UniProt database, using a bioinformatic pipeline for identifying LOV domains while excluding false positives (Glantz et al., 2016; Brian Chow, personal communication).

All of the *Phytophthora* genomes contain two or more cryptochromes. Based on the PhyML phylogeny, Phytophthora cryptochromes group into two clades (Fig 2.2). The *P. infestans* and *P. capsici* cryptochromes that have light-responsive transcription are in one clade, and the *P. infestans* and *P. capsici* cryptochromes with constitutive (or nearly constitutive) expression are in the other clade (Fig. 2.2).

Some cryptochromes are constitutively expressed, such as *Arabidopsis thaliana* Cry2, while other cryptochromes have light-regulated gene expression,

such as *Drosophila melanogaster* Cry or *Gallus gallus* Cry1 (Emery et al., 1998; Haque et al., 2002; Wang, 2019; Zuo et al., 2012). Constitutively expressed cryptochromes tend to be regulated by light-dependent post-transcriptional mechanisms (Guo et al., 1999). In *Phytophthora infestans*, PITG_16100 transcription is light-responsive, while PITG_01718 expression is constitutive. PITG_16104 appears to have reduced transcript levels with 60-minute light exposure, and when grown two days in constant light. This may be due to a light-related mechanism for short-term light exposure.

P. capsici strain LT1534 was found to have two distinct alleles for Phyca_44729 (Fig 2.3B). The three changes between the two copies are in the N-terminal extension, photolyase homology domain, and the C-terminal extension. Oomycete cryptochromes have an extended N-terminal region before the photolyase homology domain that is conserved among *Phytophthora* species. The function of this region has not been studied. In making the overexpression transformants, a small peptide tag was put on either end of the protein, and of the 57 transformants generated with the amino terminal myc tag, only one positive was identified attached to PITG_16100. Most of the transformation reactions with PITG_16104 and PITG_01718 overexpression constructs with the 5' myc tag yielded very few to no surviving transformants. This does not indicate that the amino terminal is essential to the protein, as the construct preps could have had an issue. The photolyase homology domain contains the Rossmann fold and in other cryptochromes is where the second

chromophore binds. A 3 amino acid change could affect the folding and binding of the second chromophore, but a second chromophore has not been determined for Phytophthora cryptochromes. The C-terminal extension has been shown in have a role in signaling and localization in other cryptochromes, and the 4 amino acid change due to the indel and alternative stop codon could alter function of the C-terminal extension.

Phytophthora infestans sporulation responds to red light, while *P. capsici* sporulation is not affected by red light. This difference is likely caused by one of two things: *P. capsici* does not sense red light while *P. infestans* does, or both species sense red light, but the signal does not affect sporulation in *P. capsici*. More experiments need to be done to determine the underlying molecular basis for the difference.

A possible biological explanation for the difference is that this is an adaptation to the light color distribution under the plant canopy versus above the plant canopy. Under the plant canopy, the light wavelengths are mainly blue and green with little to no red, while the intensity of red is higher than blue light above the plant canopy (Neff et al., 2000). *P. capsici*, a pathogen of roots, crowns, stems, and mostly fruits that grow shaded by the plant leaves and sit on or near the ground (such as pumpkin, squash, eggplant), would likely be more adapted to below canopy light quality than above canopy light quality. In contrast, *P. infestans* is primarily a foliar pathogen that causes disease on the canopy, or in the above canopy light quality that includes more red light.

It would be worth investigating if the species that were included in the phylogenic analysis that contain a PITG_01718 ortholog (*P. parasitica, P. ramorum*, *P. sojae*, *Plasmopara halstedii, Bremia lactucae, Hyaloperonospora arabidopsidis*, and *Peronospora effusa)* also respond to red light. Because *Plasmopara halstedii, Bremia lactucae, Hyaloperonospora arabidopsidis,* and *Peronospora effusa* are downy mildews, these pathogens are directly exposed to above-canopy light, but since these are obligate pathogens any response to red light may result from signals attributable to the plant. *Peronospora belbahrii*, a downy mildew pathogen of basil, has been described previously as having a sporulation response to red light, which to my knowledge, is the only previous report of an oomycete plant pathogen with a sporulation response to red light (Cohen et al., 2013). A BLASTn search of the publically available *Peronospora belbahrii* genome assembly with the query sequence of PITG_01718 nucleotide sequence results in 4 hits, one of which has an E-value of 0, and is approximately 1500 nucleotides (500 amino acids) on scaffold sc_02239 (CACTHD01000239: 442,315 - 443,843) (Thines et al., 2019). The predicted domain architecture of this protein (using exPASY translate and NCBI cDART CDD-search as described above) results in a protein similar to PITG_01718, with no N-terminal extension before the photolyase homology domain.

Of the Phytophthora cryptochromes, PITG_01718 is structurally the most like the *C. reinhardtii* aCRY red light receptor (Fig. 2.3C). This gene is the most likely candidate for further studies relative to red light reception. Heterologous

expression and UV/Vis spectroscopy would help determine which wavelengths this protein absorbs. I speculate that PITG_01718 may perceive red light.

Although a previous study showed that *P. infestans* sporulation is not affected by red light, it is possible that the red light intensity in the previous study was too weak to elicit an effect (Cohen et al., 1975). The previous study conducted an experiment with several blue light intensities, then chose the lowest effective photon fluence that inhibited sporulation on potato leaves for blue light, and only conducted experiments with red and green light at that rate (15.5 μmol/m^2/sec) (Cohen et al., 1975). However, sunlight and greenhouse lighting are not equal in intensity of blue, red, and green light, and it is possible that the red light effect is elicited under a higher intensity than blue light. In this study, the red and blue intensity was high, with the intention of reaching saturation. Results showed that even at a high intensity, red light did not affect sporulation in *P. capsici* as compared to the dark condition, which we see with blue light and white light. It is worth noting that the white light intensity used in the study by Cohen et al. (1975) was approximately double the intensity that I used here.

In other organisms, such as Arabidopsis or Chlamydomonas, knocking out the red light receptor is not a lethal mutation, but does cause developmental delays and changes. In *Arabidopsis thaliana*, for example, knockout of the phytochrome red light receptors result in developmental delays and increased susceptibility to stress (Monte et al., 2003).

Because knockout strains exist for PITG_01718 and PITG_16100, RNA-seq of these strains, particularly looking at light-induced and dark-induced genes (discussed later in this dissertation) may help identify the genes that cryptochromes regulate in *P. infestans.* In *P. capsici*, the cryptochromes have close neighboring genes, which could make homology-based gene silencing challenging, as the *cis*-spread of heterochromatin from the silenced loci may lead to a change in expression of the neighboring genes. CRISPR/Cas9 genome editing technology may provide a more precise method for knocking out these genes. Although I did not screen enough transformants to find CRISPR-edited positives, the constructs and sequences provided could be used for this purpose.

References

Abrahamian, M., Ah-Fong, A.M.V., Davis, C., Andreeva, K., Judelson, H.S., 2016. Gene expression and silencing studies in *Phytophthora infestans* reveal infection-specific nutrient transporters and a role for the nitrate reductase pathway in plant pathogenesis. PLOS Pathogens 12, e1006097.

Adam, A., Deimel, S., Pardo-Medina, J., García-Martínez, J., Konte, T., Limón, M.C., Avalos, J., Terpitz, U., 2018. protein activity of the *Fusarium fujikuroi* rhodopsins caro and opsa and their relation to fungus–plant interaction. International Journal of Molecular Sciences 19, 215.

Ah-Fong, A.M.V., Bormann-Chung, C.A., Judelson, H.S., 2008. Optimization of transgene-mediated silencing in *Phytophthora infestans* and its association with small-interfering RNAs. Fungal Genetics and Biology 45, 1197–1205.

Alizadeh, A., Tsao, P.H., 1985. Effect of light on sporangium formation, morphology, ontogeny, and caducity of *Phytophthora capsici* and '*P. palmivora*' MF4 isolates from black pepper and other hosts. Transactions of the British Mycological Society 85, 47–69.

Balland, V., Byrdin, M., Eker, A.P.M., Ahmad, M., Brettel, K., 2009. What makes the difference between a cryptochrome and DNA photolyase? A spectroelectrochemical comparison of the flavin redox transitions. Journal of the American Chemical Society 131, 426–427.

Baxter, L., Tripathy, S., Ishaque, N., Boot, N., Cabral, A., Kemen, E., Thines, M., Ah-Fong, A., Anderson, R., Badejoko, W., Bittner-Eddy, P., Boore, J.L., Chibucos, M.C., Coates, M., Dehal, P., Delehaunty, K., Dong, S., Downton, P., Dumas, B., Fabro, G., Fronick, C., Fuerstenberg, S.I., Fulton, L., Gaulin, E., Govers, F., Hughes, L., Humphray, S., Jiang, R.H.Y., Judelson, H., Kamoun, S., Kyung, K., Meijer, H., Minx, P., Morris, P., Nelson, J., Phuntumart, V., Qutob, D., Rehmany, A., Rougon-Cardoso, A., Ryden, P., Torto-Alalibo, T., Studholme, D., Wang, Y., Win, J., Wood, J., Clifton, S.W., Rogers, J., Van den Ackerveken, G., Jones, J.D.G., McDowell, J.M., Beynon, J., Tyler, B.M., 2010. Signatures of adaptation to obligate biotrophy in the *Hyaloperonospora arabidopsidis* genome. Science 330, 1549–1551.

Beel, B., Prager, K., Spexard, M., Sasso, S., Weiss, D., Müller, N., Heinnickel, M., Dewez, D., Ikoma, D., Grossman, A.R., Kottke, T., Mittag, M., 2012. A flavin binding cryptochrome photoreceptor responds to both blue and red light in *Chlamydomonas reinhardtii*. Plant Cell 24, 2992–3008.

Braun, R., Farré, E.M., Schurr, U., Matsubara, S., 2014. Effects of light and circadian clock on growth and chlorophyll accumulation of *Nannochloropsis gaditana*. Journal of Phycology 50, 515–525.

Bruck, R.I., Fry, W.E., Apple, A.E., Mundt, C.C., 1980. Effect of metalaxyl, an acylalanine fungicide, on developmental stages of *Phytophthora infestans*. Phytopathology 70, 597.

Brudler, R., Hitomi, K., Daiyasu, H., Toh, H., Kucho, K., Ishiura, M., Kanehisa, M., Roberts, V.A., Todo, T., Tainer, J.A., Getzoff, E.D., 2003. Identification of a New Cryptochrome Class: Structure, Function, and Evolution. Molecular Cell 11, 59–67. https://doi.org/10.1016/S1097-2765(03)00008-X

Castrillo, M., García-Martínez, J., Avalos, J., 2013. Light-dependent functions of the *Fusarium fujikuroi* CryD DASH cryptochrome in development and secondary metabolism. Applied Environmental Microbiology 79, 2777–2788.

Chaves, I., Pokorny, R., Byrdin, M., Hoang, N., Ritz, T., Brettel, K., Essen, L.-O., van der Horst, G.T.J., Batschauer, A., Ahmad, M., 2011. The Cryptochromes: Blue light photoreceptors in plants and animals. Annual Review of Plant Biology 62, 335–364.

Chen, M., Chory, J., Fankhauser, C., 2004. Light signal transduction in higher plants. Annual Review of Genetics 38, 87–117.

Clausz, J.C., 1968. Factors affecting oogenesis and oospore germination in *Achlya hypogyna*. Journal of the Elisha Mitchell Scientific Society 84, 199–206.

Coesel, S., Mangogna, M., Ishikawa, T., Heijde, M., Rogato, A., Finazzi, G., Todo, T., Bowler, C., Falciatore, A., 2009. Diatom PtCPF1 is a new cryptochrome/photolyase family member with DNA repair and transcription regulation activity. EMBO Reports 10, 655–661.

Cohen, Y., Eyal, H., Sadon, T., 1975. Light-induced inhibition of sporangial formation of *Phytophthora infestans* on potato leaves. Canadian Journal of Botany 53, 2680–2686.

Cohen, Y., Vaknin, M., Ben-Naim, Y., Rubin, A.E., 2013. Light suppresses sporulation and epidemics of *Peronospora belbahrii*. PLoS ONE 8, e81282.

Crosson, S., Rajagopal, S., Moffat, K., 2003. The LOV domain family: photoresponsive signaling modules coupled to diverse output domains. Biochemistry 42, 2–10.

Daiyasu, H., Ishikawa, T., Kuma, K., Iwai, S., Todo, T., Toh, H., 2004. Identification of cryptochrome DASH from vertebrates. Genes Cells 9, 479–495.

Darko, E., Heydarizadeh, P., Schoefs, B., Sabzalian, M.R., 2014. Photosynthesis under artificial light: the shift in primary and secondary metabolism. Philosophical Transactions of the Royal Society B: Biological Sciences 369, 20130243.

Deng, X.-W., 1994. Fresh view of light signal transduction in plants. Cell 76, 423–426.

Emery, P., So, W.V., Kaneko, M., Hall, J.C., Rosbash, M., 1998. CRY, a Drosophila clock and light-regulated cryptochrome, is a major contributor to circadian rhythm resetting and photosensitivity. Cell 95, 669–679.

Englander, L., 1972. Growth and sporulation of *Phytophthora lateralis* in vitro as influenced by the chemical and physical environment. Doctoral dissertation, Oregon State University Library.

Englander, L., Browning, M., Tooley, P.W., 2006. Growth and sporulation of *Phytophthora ramorum* in vitro in response to temperature and light. Mycologia 98, 365–373.

Fang, Y., Cui, L., Gu, B., Arredondo, F., Tyler, B.M., 2017. Efficient genome editing in the oomycete *Phytophthora sojae* Using CRISPR/Cas9, in: Current Protocols in Microbiology. John Wiley & Sons, Inc.

Franz, S., Ignatz, E., Wenzel, S., Zielosko, H., Putu, E.P.G.N., Maestre-Reyna, M., Tsai, M.-D., Yamamoto, J., Mittag, M., Essen, L.-O., 2018. Structure of the bifunctional cryptochrome aCRY from *Chlamydomonas reinhardtii.* Nucleic Acids Research 46, 8010–8022.

Franz-Badur, S., Penner, A., Straß, S., von Horsten, S., Linne, U., Essen, L.-O., 2019. Structural changes within the bifunctional cryptochrome/photolyase CraCRY upon blue light excitation. Scientific Reports 9.

Froehlich, A.C., Chen, C.-H., Belden, W.J., Madeti, C., Roenneberg, T., Merrow, M., Loros, J.J., Dunlap, J.C., 2010. Genetic and molecular characterization of a cryptochrome from the filamentous fungus *Neurospora crassa*. Eukaryotic Cell 9, 738–750.

Fuller, K.K., Loros, J.J., Dunlap, J.C., 2015. Fungal photobiology: visible light as a signal for stress, space and time. Current Genetics 61, 275–288.

Fuller, K.K., Ringelberg, C.S., Loros, J.J., Dunlap, J.C., 2013. The fungal pathogen *Aspergillus fumigatus* regulates growth, metabolism, and stress resistance in response to light. mBio 4, e00142-13.

Gangappa, S.N., Kumar, S.V., 2018. DET1 and COP1 modulate the coordination of growth and immunity in response to key seasonal signals in Arabidopsis. Cell Reports 25, 29-37.

Gegear, R.J., Foley, L.E., Casselman, A., Reppert, S.M., 2010. Animal cryptochromes mediate magnetoreception by an unconventional photochemical mechanism. Nature 463, 804–807.

Glantz, S.T., Carpenter, E.J., Melkonian, M., Gardner, K.H., Boyden, E.S., Wong, G.K.-S., Chow, B.Y., 2016. Functional and topological diversity of LOV domain photoreceptors. PNAS 113, E1442–E1451.

Göbel, T., Reisbacher, S., Batschauer, A., Pokorny, R., 2017. Flavin Adenine Dinucleotide and N5 ,N10 -Methenyltetrahydrofolate are the in planta cofactors of *Arabidopsis thaliana* Cryptochrome 3. Photochemistry and Photobiology 93, 355–362.

Griebel, T., Zeier, J., 2008. Light regulation and daytime dependency of inducible plant defenses in Arabidopsis: Phytochrome signaling controls systemic acquired resistance rather than local defense. Plant Physiology 147, 790–801.

Guo, H., Duong, H., Ma, N., Lin, C., 1999. The Arabidopsis blue light receptor cryptochrome 2 is a nuclear protein regulated by a blue light-dependent post-transcriptional mechanism. The Plant Journal 19, 279–287.

Haas, B.J., Kamoun, S., Zody, M.C., Jiang, R.H.Y., Handsaker, R.E., Cano, L.M., Grabherr, M., Kodira, C.D., Raffaele, S., Torto-Alalibo, T., Bozkurt, T.O., Ah-Fong, A.M.V., Alvarado, L., Anderson, V.L., Armstrong, M.R., Avrova, A., Baxter, L., Beynon, J., Boevink, P.C., Bollmann, S.R., Bos, J.I.B., Bulone, V., Cai, G., Cakir, C., Carrington, J.C., Chawner, M., Conti, L., Costanzo, S., Ewan, R., Fahlgren, N., Fischbach, M.A., Fugelstad, J.,

Gilroy, E.M., Gnerre, S., Green, P.J., Grenville-Briggs, L.J., Griffith, J., Grünwald, N.J., Horn, K., Horner, N.R., Hu, C.-H., Huitema, E., Jeong, D.-H., Jones, A.M.E., Jones, J.D.G., Jones, R.W., Karlsson, E.K., Kunjeti, S.G., Lamour, K., Liu, Z., Ma, L., Maclean, D., Chibucos, M.C., McDonald, H., McWalters, J., Meijer, H.J.G., Morgan, W., Morris, P.F., Munro, C.A., O'Neill, K., Ospina-Giraldo, M., Pinzón, A., Pritchard, L., Ramsahoye, B., Ren, Q., Restrepo, S., Roy, S., Sadanandom, A., Savidor, A., Schornack, S., Schwartz, D.C., Schumann, U.D., Schwessinger, B., Seyer, L., Sharpe, T., Silvar, C., Song, J., Studholme, D.J., Sykes, S., Thines, M., van de Vondervoort, P.J.I., Phuntumart, V., Wawra, S., Weide, R., Win, J., Young, C., Zhou, S., Fry, W., Meyers, B.C., van West, P., Ristaino, J., Govers, F., Birch, P.R.J., Whisson, S.C., Judelson, H.S., Nusbaum, C., 2009. Genome sequence and analysis of the Irish potato famine pathogen *Phytophthora infestans*. Nature 461, 393–398.

Haque, R., Chaurasia, S., Wessel, J., Iuvone, P., 2002. Dual regulation of cryptochrome 1 mRNA expression in chicken retina by light and circadian oscillators. Neuroreport 13, 2247–2251.

Harnish, W.N., 1965. Effect of light on production of oospores and sporangia in species of Phytophthora. Mycologia 57, 85–90.

Hatakeyama, R., Nakahama, T., Higuchi, Y., Kitamoto, K., 2007. Light represses conidiation in koji mold *Aspergillus oryzae*. Bioscience Biotechnology and Biochemistry 71, 1844–1849.

He, Q., Cheng, P., Yang, Y., Wang, L., Gardner, K.H., Liu, Y., 2002. White Collar-1, a DNA binding transcription factor and a light sensor. Science 297, 840–843.

Heintzen, C., 2012. Plant and fungal photopigments. Wiley Interdisciplinary Reviews: Membrane Transport and Signaling 1, 411–432.

Herrou, J., Crosson, S., 2011. Function, structure and mechanism of bacterial photosensory LOV proteins. Nature Reviews Microbiology 9, 713–723.

Holub, D., Kubař, T., Mast, T., Elstner, M., Gillet, N., 2019. What accounts for the different functions in photolyases and cryptochromes: a computational study of proton transfers to FAD. Physical Chemistry Chemical Physics 21, 11956–11966.

Hurtado□Gonzales, O.P., Lamour, K.H., 2009. Evidence for inbreeding and apomixis in close crosses of *Phytophthora capsici*. Plant Pathology 58, 715–722.

Islam, S.Z., Babadoost, M., Honda, Y., 2002. Effect of red light treatment of seedlings of pepper, pumpkin, and tomato on the occurrence of Phytophthora damping-off. HortScience 37, 678–681.

Judelson, H.S., Tyler, B.M., Michelmore, R.W., 1991. Transformation of the oomycete pathogen, *Phytophthora infestans*. MPMI 4, 602–607.

Judelson, H.S., Whittaker, S.L., 1995. Inactivation of transgenes in *Phytophthora infestans* is not associated with their deletion, methylation, or mutation. Current Genetics 28, 571–579.

Kangasjärvi, S., Neukermans, J., Li, S., Aro, E.-M., Noctor, G., 2012. Photosynthesis, photorespiration, and light signalling in defence responses. Journal of Experimental Botany 63, 1619–1636.

Karpinski, S., Gabrys, H., Mateo, A., Karpinska, B., Mullineaux, P.M., 2003. Light perception in plant disease defence signalling. Current Opinion in Plant Biology 6, 390–396.

Kazan, K., Manners, J.M., 2011. The interplay between light and jasmonate signalling during defence and development. Journal of Experimental Botany 62, 4087–4100.

Kim, Y.-M., Choi, J., Lee, H.-Y., Lee, G.-W., Lee, Y.-H., Choi, D., 2014. dbCRY: a Web-based comparative and evolutionary genomics platform for blue-light receptors. Database 2014, bau037–bau037.

Kort, R., Hoff, W.D., Van West, M., Kroon, A.R., Hoffer, S.M., Vlieg, K.H., Crielaand, W., Van Beeumen, J.J., Hellingwerf, K.J., 1996. The xanthopsins: a new family of eubacterial blue-light photoreceptors. EMBO Journal 15, 3209–3218.

Lamour, K.H., Mudge, J., Gobena, D., Hurtado-Gonzales, O.P., Schmutz, J., Kuo, A., Miller, N.A., Rice, B.J., Raffaele, S., Cano, L.M., Bharti, A.K., Donahoo, R.S., Finley, S., Huitema, E., Hulvey, J., Platt, D., Salamov, A., Savidor, A., Sharma, R., Stam, R., Storey, D., Thines, M., Win, J., Haas, B.J., Dinwiddie, D.L., Jenkins, J., Knight, J.R., Affourtit, J.P., Han, C.S., Chertkov, O., Lindquist, E.A., Detter, C., Grigoriev, I.V., Kamoun, S., Kingsmore, S.F., 2012. Genome sequencing and mapping reveal loss of heterozygosity as a mechanism for rapid adaptation in the vegetable pathogen *Phytophthora capsici*. MPMI 25, 1350–1360.

Larrondo, L.F., Canessa, P., 2019. The clock keeps on ticking: Emerging roles for circadian regulation in the control of fungal physiology and pathogenesis, in: Rodrigues, M.L. (Ed.), Fungal Physiology and Immunopathogenesis, Current Topics in Microbiology and Immunology. Springer International Publishing, pp. 121–156.

Lebecka, R., Sobkowiak, S., 2013. Host–pathogen interaction between *Phytophthora infestans* and *Solanum tuberosum* following exposure to short and long daylight hours. Acta Physiology Plant 35, 1131–1139.

Lee, P.C., 1962. Some effects of pH, temperature and light on the production of Zoosporagia in Saprolegnia parasitica Coker. University of Richmond, Master's Thesis 49.

Leesutthiphonchai, W., Judelson, H.S., 2018. A MADS-box transcription factor regulates a central step in sporulation of the oomycete *Phytophthora infestans*. Molecular Microbiology 110, 562–575.

Legris, M., Klose, C., Burgie, E.S., Costigliolo, C., Neme, M., Hiltbrunner, A., Wigge, P.A., Schäfer, E., Vierstra, R.D., Casal, J.J., 2016. Phytochrome B integrates light and temperature signals in Arabidopsis. Science 354, 897–900.

Lin, C., Shalitin, D., 2003. Cryptochrome structure and signal transduction. Annual Review of Plant Biology 54, 469–496.

Lin, C., Todo, T., 2005. The cryptochromes. Genome Biology 6, 220.

Liu, H., Liu, B., Zhao, C., Pepper, M., Lin, C., 2011. The action mechanisms of plant cryptochromes. Trends in Plant Science 16, 684–691.

Liu, Z., Wang, L., Zhong, D., 2015. Dynamics and mechanisms of DNA repair by photolyase. Phys Chem Chem Phys 17, 11933–11949.

Lu, H., McClung, C.R., Zhang, C., 2017. Tick tock: Circadian regulation of plant innate immunity. Annual Review of Phytopathology 55, 287–311.

Lyu, X., Shen, C., Fu, Y., Xie, J., Jiang, D., Li, G., Cheng, J., 2016. The microbial opsin homolog Sop1 is involved in *Sclerotinia sclerotiorum* development and environmental stress response. Frontiers in Microbiology 6.

Maeda, K., Robinson, A.J., Henbest, K.B., Hogben, H.J., Biskup, T., Ahmad, M., Schleicher, E., Weber, S., Timmel, C.R., Hore, P.J., 2012. Magnetically sensitive light-induced reactions in cryptochrome are consistent with its proposed role as a magnetoreceptor. PNAS 109, 4774–4779.

Marine, S.C., Baudoin, A., Hong, C.X., 2018. Effect of initial darkness duration on the pathogenicity of *Calonectria pseudonaviculata* on boxwood. Plant Pathology 67, 735–740.

Michael, A.K., Fribourgh, J.L., Gelder, R.N.V., Partch, C.L., 2017. Animal cryptochromes: divergent roles in light perception, circadian timekeeping and beyond. Photochemistry and Photobiology 93, 128–140.

Monte, E., Alonso, J.M., Ecker, J.R., Zhang, Y., Li, X., Young, J., Austin-Phillips, S., Quail, P.H., 2003. Isolation and characterization of phyC mutants in arabidopsis reveals complex crosstalk between phytochrome signaling pathways. The Plant Cell 15, 1962–1980.

Nagatani, A., 2010. Phytochrome: structural basis for its functions. Current Opinion in Plant Biology 13, 565–570.

Neff, M.M., Fankhauser, C., Chory, J., 2000. Light: an indicator of time and place. Genes and Development 14, 257–271.

Nordskog, B., Gadoury, D.M., Seem, R.C., Hermansen, A., 2007. Impact of diurnal periodicity, temperature, and light on sporulation of *Bremia lactucae*. Phytopathology 97, 979–986.

Nsa, I.Y., Karunarathna, N., Liu, X., Huang, H., Boetteger, B., Bell-Pedersen, D., 2015. A novel cryptochrome-dependent oscillator in *Neurospora crassa*. Genetics 199, 233–245.

Oldemeyer, S., Franz, S., Wenzel, S., Essen, L.-O., Mittag, M., Kottke, T., 2016. Essential role of an unusually long-lived tyrosyl radical in the response to red light of the animal-like cryptochrome aCRY. Journal of Biological Chemistry 291, 14062–14071.

Ouzounis, T., Rosenqvist, E., Ottosen, C.-O., 2015. Spectral effects of artificial light on plant physiology and secondary metabolism: A review. HortScience 50, 1128–1135.

Ozturk, N., 2017. Phylogenetic and functional classification of the photolyase/cryptochrome family. photochemistry and photobiology 93, 104–111.

Öztürk, N., Song, S.-H., Özgür, S., Selby, C.P., Morrison, L., Partch, C., Zhong, D., Sancar, A., 2007. Structure and function of animal cryptochromes. Cold Spring Harbor Symposium on Quantitative Biology 72, 119–131.

Pandaranayaka, E.P., Frenkel, O., Elad, Y., Prusky, D., Harel, A., 2019. Network analysis exposes core functions in major lifestyles of fungal and oomycete plant pathogens. BMC Genomics 20, 1020.

Pellequer, J.-L., Wager-Smith, K.A., Kay, S.A., Getzoff, E.D., 1998. Photoactive yellow protein: A structural prototype for the three-dimensional fold of the PAS domain superfamily. PNAS 95, 5884–5890.

Pokorny, R., Klar, T., Hennecke, U., Carell, T., Batschauer, A., Essen, L.-O., 2008. Recognition and repair of UV lesions in loop structures of duplex DNA by DASH-type cryptochrome. PNAS 105, 21023–21027.

Ragni, M., D'Alcala, M.R., 2007. Circadian variability in the photobiology of *Phaeodactylum tricornutum*: pigment content. J. Plankton Res. 29, 141–156.

Roden, L.C., Ingle, R.A., 2009. Lights, rhythms, infection: The role of light and the circadian clock in determining the outcome of plant–pathogen interactions. Plant Cell 21, 2546–2552.

Sancar, A., 2003. Structure and function of DNA photolyase and cryptochrome blue-light photoreceptors. Chemistry Reviews 103, 2203–2238.

Scheerer, P., Zhang, F., Kalms, J., Stetten, D. von, Krauß, N., Oberpichler, I., Lamparter, T., 2015. The class III cyclobutane pyrimidine dimer photolyase structure reveals a new antenna chromophore binding site and alternative photoreduction pathways. Journal of Biological Chemistry 290, 11504–11514.

Schelvis, J.P.M., Gindt, Y.M., 2017. A review of spectroscopic and biophysical-chemical studies of the complex of cyclobutane pyrimidine dimer photolyase and cryptochrome DASH with substrate DNA. Photochemistry and Photobiology 93, 26–36.

Schmid, R., Dring, M.J., 1992. Circadian rhythm and fast responses to blue light of photosynthesis in Ectocarpus (Phaeophyta, Ectocarpales) : I. Characterization of the rhythm and the blue-light response. Planta 187, 53–59.

Schmid, R., Forster, R., Dring, M.J., 1992. Circadian rhythm and fast responses to blue light of photosynthesis in Ectocarpus (Phaeophyta, Ectocarpales) : II. Light and CO2 dependence of photosynthesis. Planta 187, 60–66.

Schumacher, J., Simon, A., Cohrs, K.C., Viaud, M., Tudzynski, P., 2014. The transcription factor BcLTF1 regulates virulence and light responses in the necrotrophic plant pathogen *Botrytis cinerea*. PLOS Genetics 10, e1004040.

Schumann, G., 1977. Light intensity as a factor in field evaluations of general resistance of potatoes to *Phytophthora infestans*. Phytopathology 77, 1400.

Schwerdtfeger, C., Linden, H., 2003. VIVID is a flavoprotein and serves as a fungal blue light photoreceptor for photoadaptation. The EMBO Journal 22, 4846–4855.

Schwerdtfeger, C., Linden, H., 2001. Blue light adaptation and desensitization of light signal transduction in *Neurospora crassa*. Molecular Microbiology 39, 1080–1087.

Selby, C.P., Sancar, A., 2012. The second chromophore in Drosophila photolyase/cryptochrome family photoreceptors. Biochemistry 51, 167–171.

Selby, C.P., Sancar, A., 2006. A cryptochrome/photolyase class of enzymes with single-stranded DNA-specific photolyase activity. PNAS 103, 17696–17700.

Singh, U.P., Chauhan, V.B., 1985. Relationship between field levels and light and darkness on the development of Phytophthora blight of pigeon pea (*Cajanus cajan* (L.) Millsp.). Journal of Phytopathology 114, 160–167.

Stael, S., Kmiecik, P., Willems, P., Van Der Kelen, K., Coll, N.S., Teige, M., Van Breusegem, F., 2015. Plant innate immunity – sunny side up? Trends in Plant Science 20, 3–11.

Szaniszlo, P.J., 1965. A study of the effect of light and temperature on the formation of oögonia and oöspheres in *Saprolegnia diclina*. Journal of the Elisha Mitchell Scientific Society 81, 10–15.

Tagua, V.G., Pausch, M., Eckel, M., Gutiérrez, G., Miralles-Durán, A., Sanz, C., Eslava, A.P., Pokorny, R., Corrochano, L.M., Batschauer, A., 2015. Fungal cryptochrome with DNA repair activity reveals an early stage in cryptochrome evolution. PNAS 112, 15130–15135.

Takahashi, F., Yamagata, D., Ishikawa, M., Fukamatsu, Y., Ogura, Y., Kasahara, M., Kiyosue, T., Kikuyama, M., Wada, M., Kataoka, H., 2007. AUREOCHROME, a photoreceptor required for photomorphogenesis in stramenopiles. PNAS 104, 19625–19630.

Thieulin-Pardo, G., Avilan, L., Kojadinovic, M., Gontero, B., 2015. Fairy “tails”: flexibility and function of intrinsically disordered extensions in the photosynthetic world. Frontiers in Molecular Bioscience 2.

Thines, M., Sharma, R., Rodenburg, S.Y.A., Gogleva, A., Judelson, H.S., Xia, X., Hoogen, J. van den, Kitner, M., Klein, J., Neilen, M., Ridder, D. de, Seidl, M.F., Ackerveken, G.V. den, Govers, F., Schornack, S., Studholme, D.J., 2019. The genome of *Peronospora belbahrii* reveals high heterozygosity, a low number of canonical effectors and CT-rich promoters. bioRxiv 721027.

Thomas, C.A., Allen, E.H., 1971. Light and antifungal polyacetylene compounds in relation to resistance of safflower to *Phytophthora drechsleri*. Phytopathology 61, 1459–1461.

Trotta, A., Rahikainen, M., Konert, G., Finazzi, G., Kangasjärvi, S., 2014. Signalling crosstalk in light stress and immune reactions in plants. Philosophical Transactions of the Royal Society of London B, Biological Sciences 369, 20130235.

Tyler, B.M., Tripathy, S., Zhang, X., Dehal, P., Jiang, R.H.Y., Aerts, A., Arredondo, F.D., Baxter, L., Bensasson, D., Beynon, J.L., Chapman, J., Damasceno, C.M.B., Dorrance, A.E., Dou, D., Dickerman, A.W., Dubchak, I.L., Garbelotto, M., Gijzen, M., Gordon, S.G., Govers, F., Grunwald, N.J., Huang, W., Ivors, K.L., Jones, R.W., Kamoun, S., Krampis, K., Lamour, K.H., Lee, M.-K., McDonald, W.H., Medina, M., Meijer, H.J.G., Nordberg, E.K., Maclean, D.J., Ospina-Giraldo, M.D., Morris, P.F., Phuntumart, V., Putnam, N.H., Rash, S., Rose, J.K.C., Sakihama, Y., Salamov, A.A., Savidor, A., Scheuring, C.F., Smith, B.M., Sobral, B.W.S., Terry, A., Torto-Alalibo, T.A., Win, J., Xu, Z., Zhang, H., Grigoriev, I.V., Rokhsar, D.S., Boore, J.L., 2006. Phytophthora genome sequences uncover evolutionary origins and mechanisms of pathogenesis. Science 313, 1261–1266.

van der Horst, M.A., Hellingwerf, K.J., 2004. Photoreceptor proteins, “Star actors of modern times”: a review of the functional dynamics in the structure of representative members of six different photoreceptor families. Accounts of Chemical Research 37, 13–20.

van der Horst, M.A., Laan, W., Yeremenko, S., Wende, A., Palm, P., Oesterhelt, D., Hellingwerf, K.J., 2005. From primary photochemistry to biological function in the blue-light photoreceptors PYP and AppA. Photochemistry and Photobiological Science 4, 688–693.

Veluchamy, S., Rollins, J.A., 2008. A CRY-DASH-type photolyase/cryptochrome from *Sclerotinia sclerotiorum* mediates minor UV-A-specific effects on development. Fungal Genetics and Biology 45, 1265–1276.

Victoria, J.I., Thurston, H.D., 1974. Light intensity effects on lesion size caused by *Phytophthora infestans* on potato leaves. Phytopathology 64, 753–754.

Vu, A.L., Leesutthiphonchai, W., Ah-Fong, A.M.V., Judelson, H.S., 2019. Defining transgene insertion sites and off-target effects of homology-based gene silencing informs the application of functional genomics tools in *Phytophthora infestans*. MPMI 32, 915–927.

Wang, J., Du, X., Pan, W., Wang, X., Wu, W., 2015. Photoactivation of the cryptochrome/photolyase superfamily. Journal of Photochemistry and Photobiology C: Photochemistry Reviews 22, 84–102.

Wang, Q., Zuo, Z., Wang, X., Liu, Q., Gu, L., Oka, Y., Lin, C., 2018. Beyond the photocycle — how cryptochromes regulate photoresponses in plants? Current Opinion in Plant Biology, Cell signalling and gene regulation 2018 45, Part A, 120–126.

Wang, S., 2019. Secretion and delivery of virulence proteins from *Phytophthora infestans* to its host (Ph.D.). University of Dundee Library.

Wang, W., Barnaby, J.Y., Tada, Y., Li, H., Tör, M., Caldelari, D., Lee, D., Fu, X.-D., Dong, X., 2011. Timing of plant immune responses by a central circadian regulator. Nature 470, 110–114.

Wang, Z., Wang, J., Li, N., Li, J., Trail, F., Dunlap, J.C., Townsend, J.P., 2018. Light sensing by opsins and fungal ecology: NOP-1 modulates entry into sexual reproduction in response to environmental cues. Molecular Ecology 27, 216–232.

Ward, E.W.B., Buzzell, R.I., 1983. Influence of light, temperature and wounding on the expression of soybean genes for resistance to *Phytophthora megasperma* f.sp. *glycinea*. Physiological Plant Pathology 23, 401–409.

Xiang, Q., Judelson, H.S., 2014. Myb transcription factors and light regulate sporulation in the oomycete *Phytophthora infestans*. PLoS ONE 9, e92086.

Yang, Y.-J., Zuo, Z.-C., Zhao, X.-Y., Li, X., Klejnot, J., Li, Y., Chen, P., Liang, S.-P., Yu, X.-H., Liu, X.-M., Lin, C.-T., 2008. Blue-light-independent activity of Arabidopsis cryptochromes in the regulation of steady-state levels of protein and mRNA expression. Molecular Plant 1, 167–177.

Zhang, M., Wang, L., Zhong, D., 2017. Photolyase: Dynamics and electron-transfer mechanisms of DNA repair. Archives of Biochemistry and Biophysics 632, 158–174.

Zoltowski, B.D., Chelliah, Y., Wickramaratne, A., Jarocha, L., Karki, N., Xu, W., Mouritsen, H., Hore, P.J., Hibbs, R.E., Green, C.B., Takahashi, J.S., 2019. Chemical and structural analysis of a photoactive vertebrate cryptochrome from pigeon. PNAS 116, 19449–19457.

Zuo, Z.-C., Meng, Y.-Y., Yu, X.-H., Zhang, Z.-L., Feng, D.-S., Sun, S.-F., Liu, B., Lin, C.-T., 2012. A study of the blue-light-dependent phosphorylation, degradation, and photobody formation of Arabidopsis CRY2. Molecular Plant 5, 726–733.

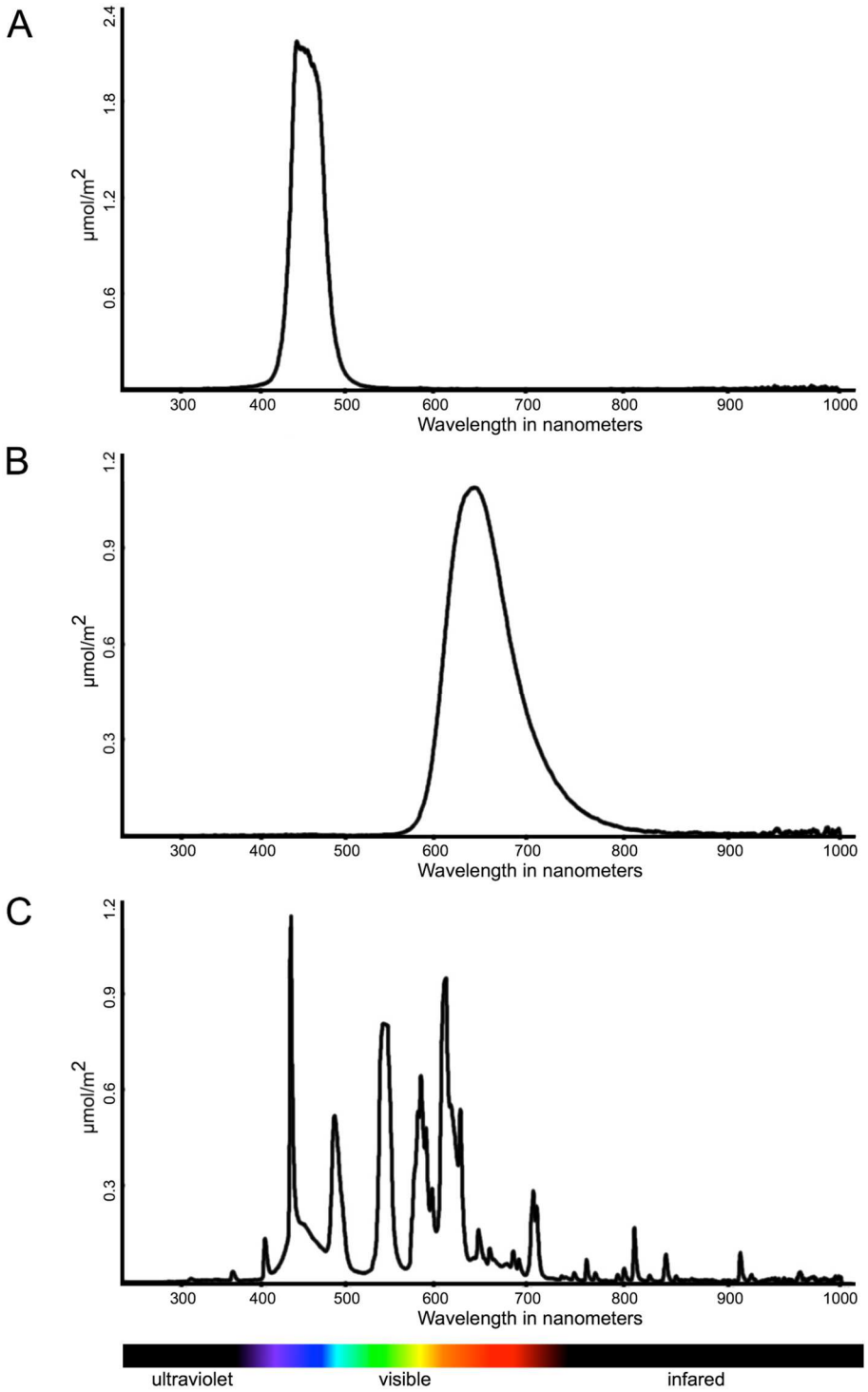

Figure 2.1. Light emission spectra of A) blue light treatment, B) red light treatment, and C) white light treatment.

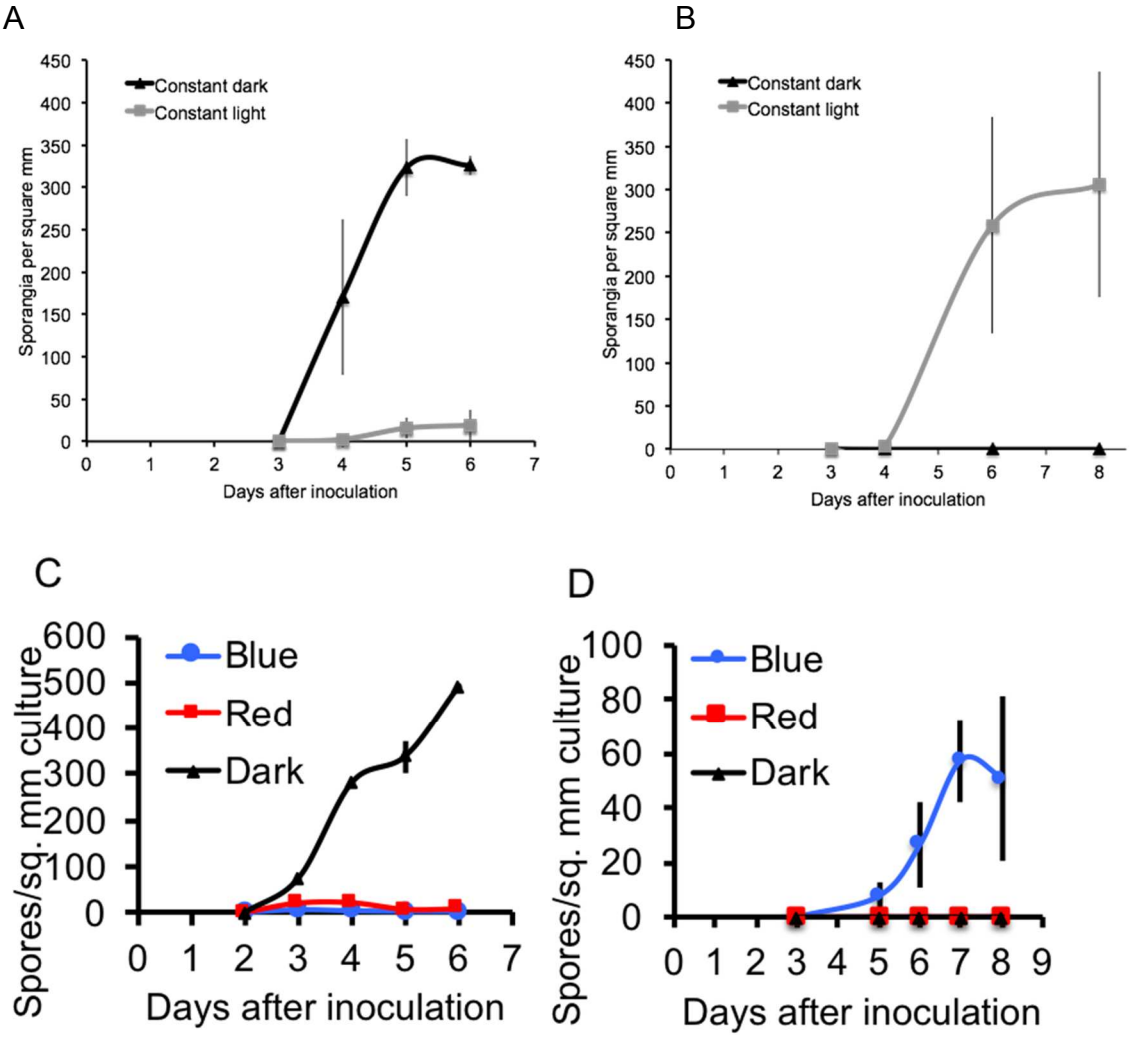

Figure 2.2. Effect of light on sporulation in A) *P. infestans*, B) *P. capsici*.,C) *P. infestans*, and D) *P. capsici*.

A

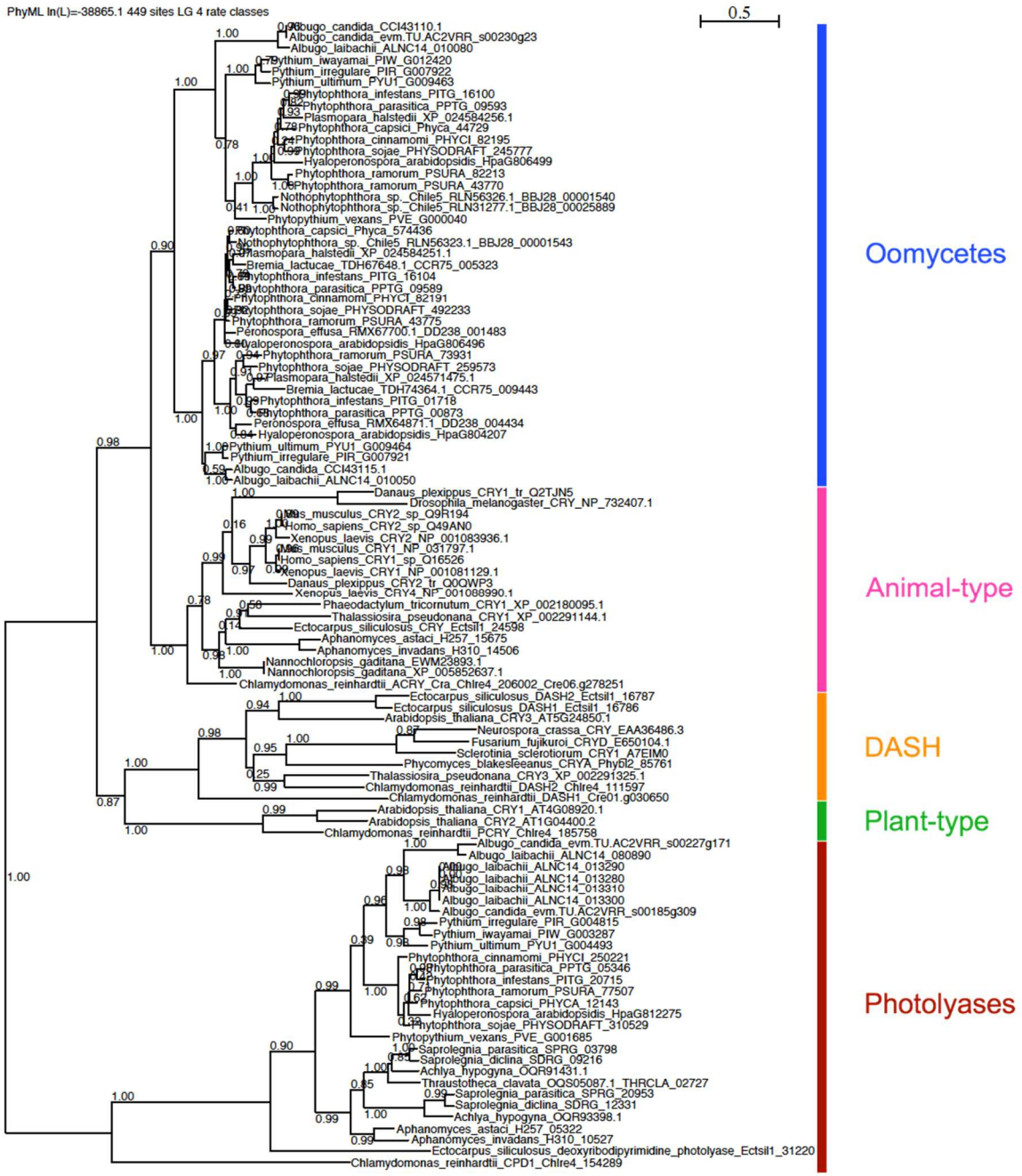
PhyML ln(L)=-38865.1 449 sites LG 4 rate classes
0.5
Albugo_candida_CCI43110.1
Albugo_candida_evm.TU.AC2VRR_s00230g23
Albugo_laibachii_ALNC14_010080
Pythium_iwayamai_PIW_G012420
Pythium_irregulare_PIR_G007922
Pythium_ultimum_PYU1_G009463
Phytophthora_infestans_PITG_16100
Phytophthora_parasitica_PPTG_09593
Plasmopara_halstedii_XP_024584256.1
Phytophthora_capsici_Phyca_44729
Phytophthora_cinnamomi_PHYCI_82195
Phytophthora_sojae_PHYSODRAFT_245777
Hyaloperonospora_arabidopsidis_HpaG806499
Phytophthora_ramorum_PSURA_82213
Phytophthora_ramorum_PSURA_43770
Nothophytophthora_sp._Chile5_RLN56326.1_BBJ28_00001540
Nothophytophthora_sp._Chile5_RLN31277.1_BBJ28_00025889
Phytopythium_vexans_PVE_G000040
Phytophthora_capsici_Phyca_574436
Nothophytophthora_sp._Chile5_RLN56323.1_BBJ28_00001543
Plasmopara_halstedii_XP_024584251.1
Bremia_lactucae_TDH67648.1_CCR75_005323
Phytophthora_infestans_PITG_16104
Phytophthora_parasitica_PPTG_09589
Phytophthora_cinnamomi_PHYCI_82191
Phytophthora_sojae_PHYSODRAFT_492233
Phytophthora_ramorum_PSURA_43775
Peronospora_effusa_RMX67700.1_DD238_001483
Hyaloperonospora_arabidopsidis_HpaG806496
Phytophthora_ramorum_PSURA_73931
Phytophthora_sojae_PHYSODRAFT_259573
Plasmopara_halstedii_XP_024571475.1
Bremia_lactucae_TDH74364.1_CCR75_009443
Phytophthora_infestans_PITG_01718
Phytophthora_parasitica_PPTG_00873
Peronospora_effusa_RMX64871.1_DD238_004434
Hyaloperonospora_arabidopsidis_HpaG804207
Pythium_ultimum_PYU1_G009464
Pythium_irregulare_PIR_G007921
Albugo_candida_CCI43115.1
Albugo_laibachii_ALNC14_010050
Danaus_plexippus_CRY1_tr_Q2TJN5
Drosophila_melanogaster_CRY_NP_732407.1
Mus_musculus_CRY2_sp_Q9R194
Homo_sapiens_CRY2_sp_Q49AN0
Xenopus_laevis_CRY2_NP_001083936.1
Mus_musculus_CRY1_NP_031797.1
Homo_sapiens_CRY1_sp_Q16526
Xenopus_laevis_CRY1_NP_001081129.1
Danaus_plexippus_CRY2_tr_Q0QWP3
Xenopus_laevis_CRY4_NP_001088990.1
Phaeodactylum_tricornutum_CRY1_XP_002180095.1
Thalassiosira_pseudonana_CRY1_XP_002291144.1
Ectocarpus_siliculosus_CRY_Ectsil1_24598
Aphanomyces_astaci_H257_15675
Aphanomyces_invadans_H310_14506
Nannochloropsis_gaditana_EWM23893.1
Nannochloropsis_gaditana_XP_005852637.1
Chlamydomonas_reinhardtii_ACRY_Cra_Chlre4_206002_Cre06.g278251
Ectocarpus_siliculosus_DASH2_Ectsil1_16787
Ectocarpus_siliculosus_DASH1_Ectsil1_16786
Arabidopsis_thaliana_CRY3_AT5G24850.1
Neurospora_crassa_CRY_EAA36486.3
Fusarium_fujikuroi_CRYD_E650104.1
Sclerotinia_sclerotiorum_CRY1_A7EIM0
Phycomyces_blakesleeanus_CRYA_Phybl2_85761
Thalassiosira_pseudonana_CRY3_XP_002291325.1
Chlamydomonas_reinhardtii_DASH2_Chlre4_111597
Chlamydomonas_reinhardtii_DASH1_Cre01.g030650
Arabidopsis_thaliana_CRY1_AT4G08920.1
Arabidopsis_thaliana_CRY2_AT1G04400.2
Chlamydomonas_reinhardtii_PCRY_Chlre4_185758
Albugo_candida_evm.TU.AC2VRR_s00227g171
Albugo_laibachii_ALNC14_080890
Albugo_laibachii_ALNC14_013290
Albugo_laibachii_ALNC14_013280
Albugo_laibachii_ALNC14_013310
Albugo_laibachii_ALNC14_013300
Albugo_candida_evm.TU.AC2VRR_s00185g309
Pythium_irregulare_PIR_G004815
Pythium_iwayamai_PIW_G003287
Pythium_ultimum_PYU1_G004493
Phytophthora_cinnamomi_PHYCI_250221
Phytophthora_parasitica_PPTG_05346
Phytophthora_infestans_PITG_20715
Phytophthora_ramorum_PSURA_77507
Phytophthora_capsici_PHYCA_12143
Hyaloperonospora_arabidopsidis_HpaG812275
Phytophthora_sojae_PHYSODRAFT_310529
Phytopythium_vexans_PVE_G001685
Saprolegnia_parasitica_SPRG_03798
Saprolegnia_diclina_SDRG_09216
Achlya_hypogyna_OQR91431.1
Thraustotheca_clavata_OQS05087.1_THRCLA_02727
Saprolegnia_parasitica_SPRG_20953
Saprolegnia_diclina_SDRG_12331
Achlya_hypogyna_OQR93398.1
Aphanomyces_astaci_H257_05322
Aphanomyces_invadans_H310_10527
Ectocarpus_siliculosus_deoxyribodipyrimidine_photolyase_Ectsil1_31220
Chlamydomonas_reinhardtii_CPD1_Chlre4_154289
Oomycetes
Animal-type
DASH
Plant-type
Photolyases

B

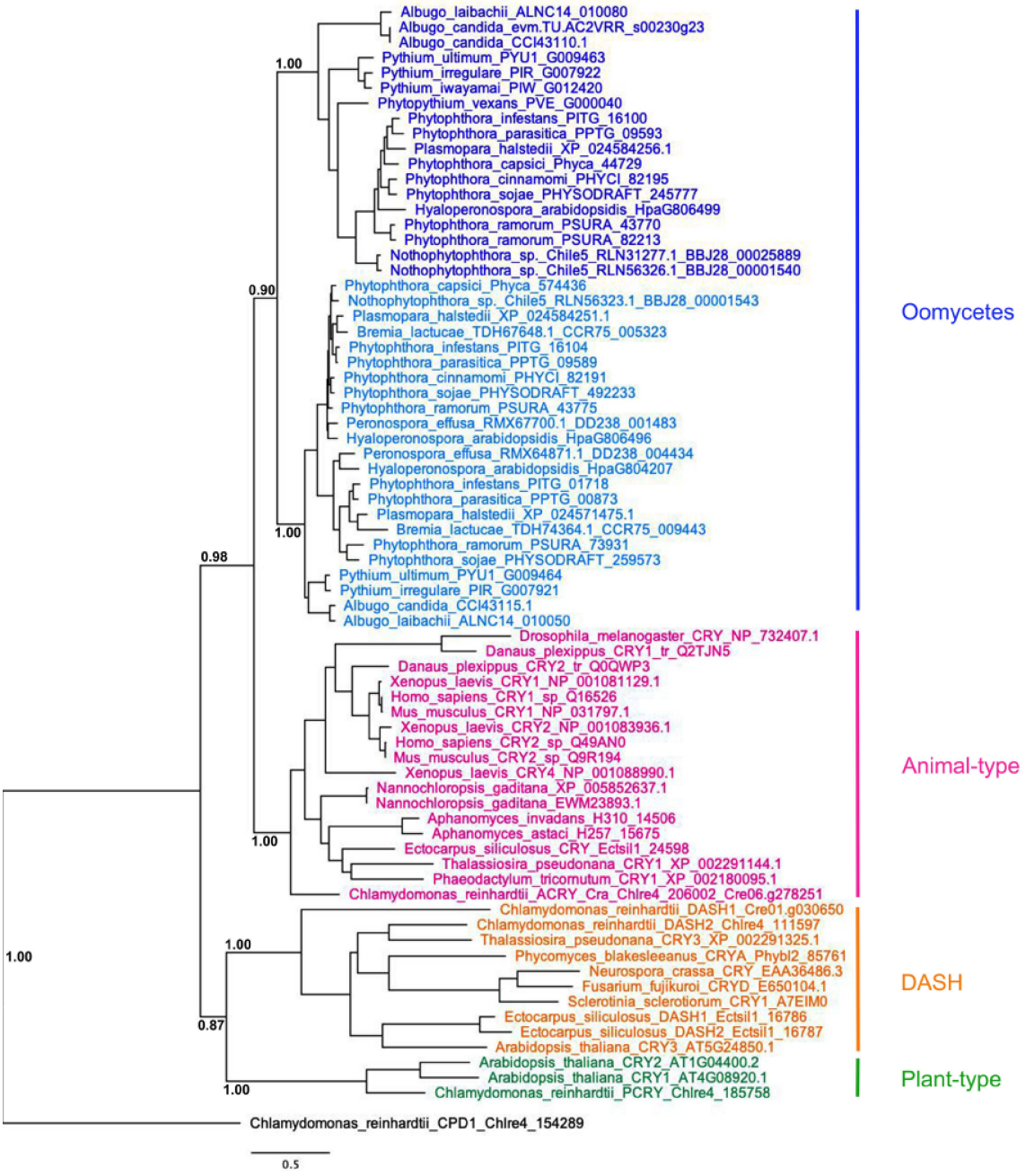

Figure 2.3. Phylogeny of A) *Phytophthora* cryptochrome/photolyase superfamily proteins and characterized proteins from other systems, and B) the *Phytophthora* cryptochrome/photolyase superfamily proteins and characterized proteins from other systems that are predicted to be cryptochromes.

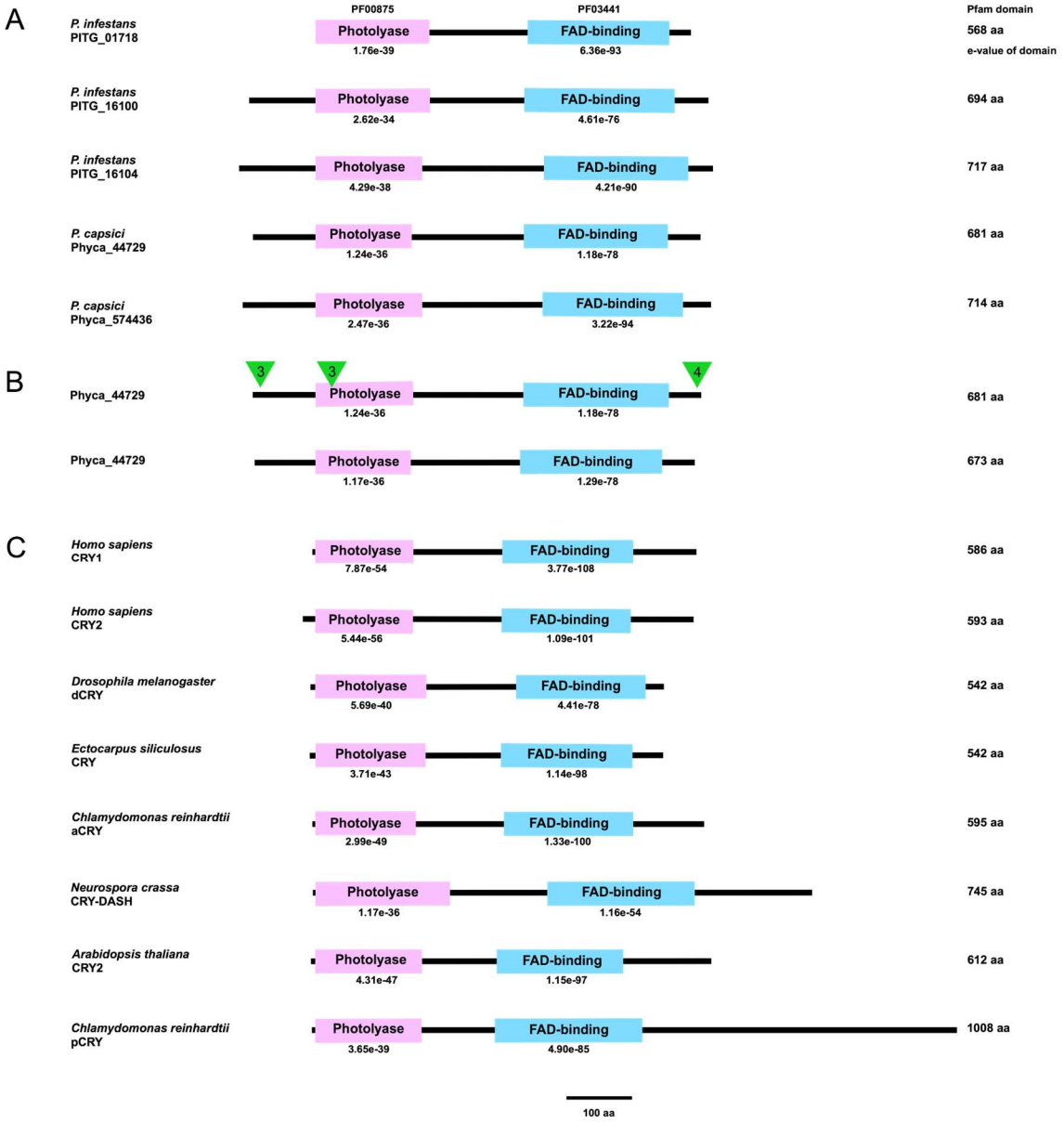

Figure 2.4. Predicted domain architecture of A) *Phytophthora infestans* and *Phytophthora capsici* cryptochromes, B) *P. capsici* Phyca_44729 distinct alleles, and C) cryptochromes from other organisms. Green triangles represent the location and number of amino acids that are lacking in the other allele.

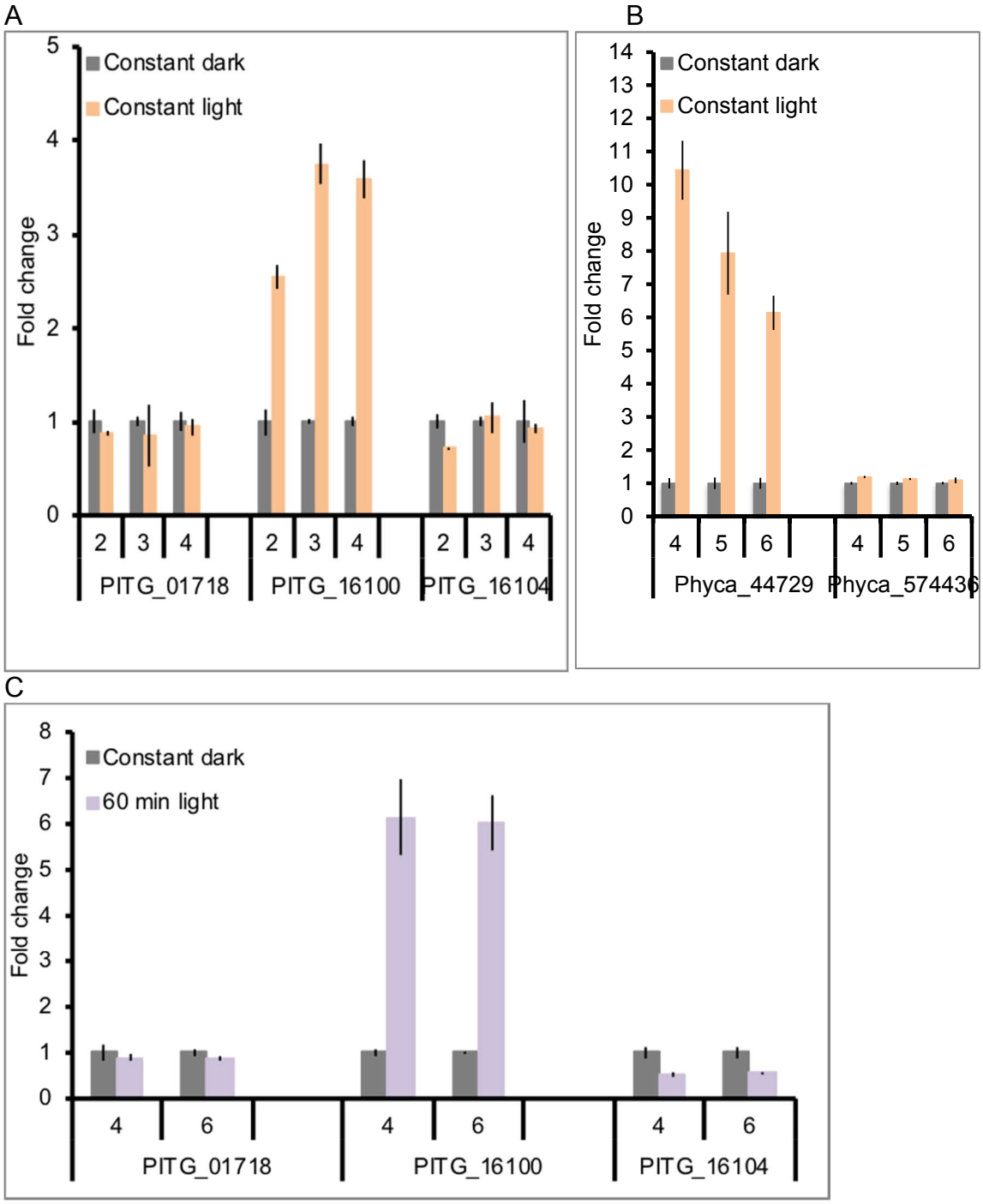

Figure 2.5. Effect of constant light on gene expression of the cryptochrome proteins in A) *P. infestans*, and B) *P. capsici*. C) Effect of 60 minute light exposure on cryptochrome expression in *P. infestans*, as compared to constant dark.

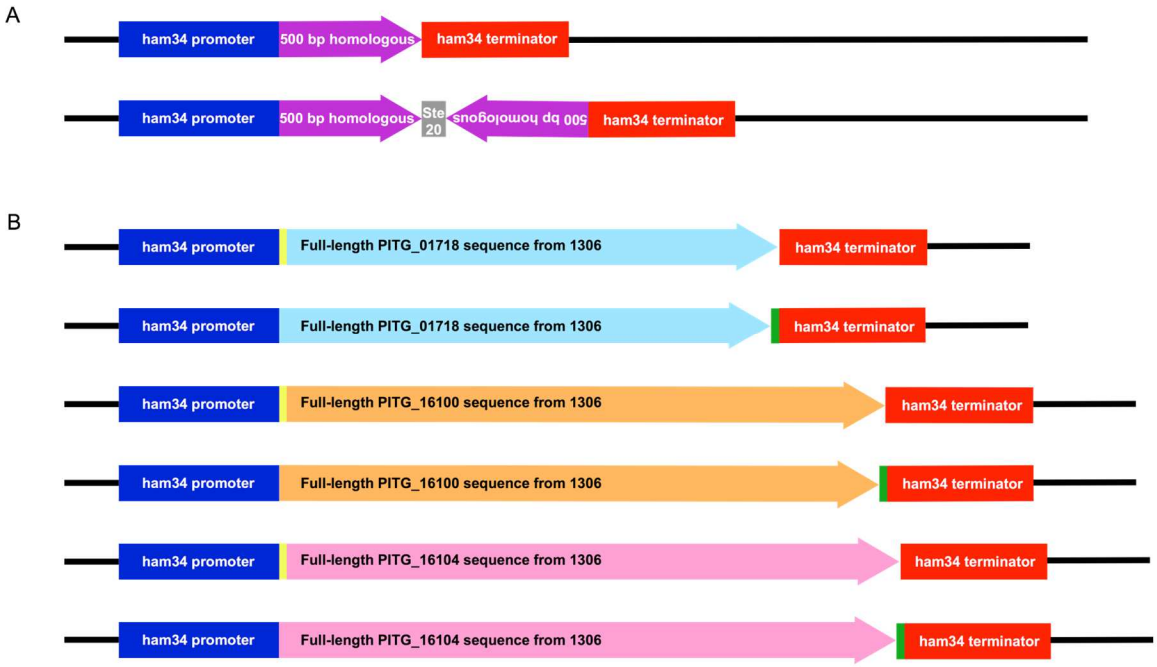

Figure 2.6. Linearized maps of A) silencing constructs, and B) overexpression constructs for the predicted cryptochromes in *P. infestans*. Yellow band represents a myc-tag, and green band represents a FLAG-tag, black line is the plasmid backbone, which contains a nptII gene (not shown).

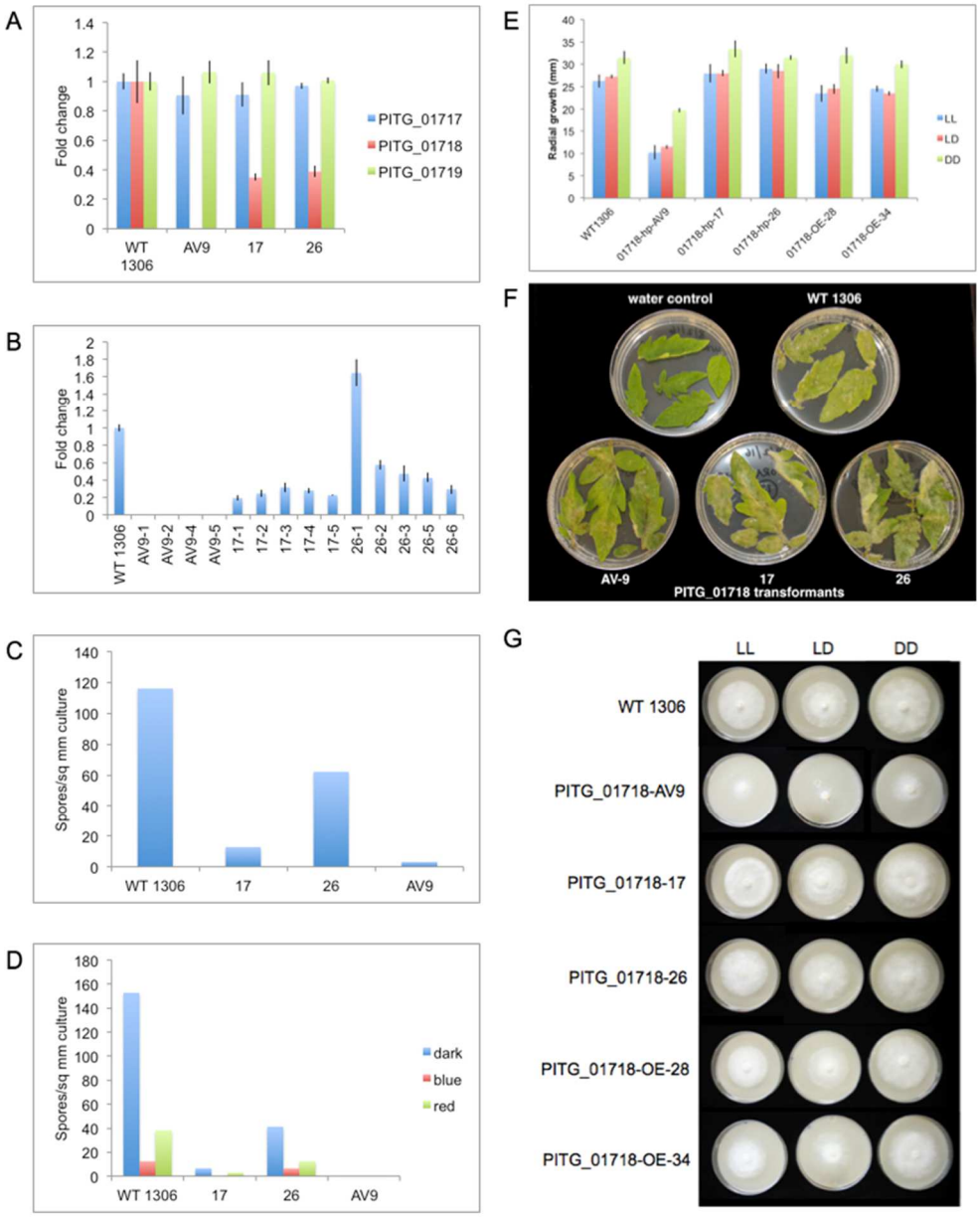

Figure 2.7. A) Expression of PITG_01718 and neighboring genes PITG_01717 and PITG_01719 in silenced and knockdown transformants AV-9, 17, and 26. B) Expression of PITG_01718 in single zoospore derivatives of silenced and knockdown transformants. C) Sporulation of PITG_01718 silenced and knockdown transformants under 12-hour light/dark, and D) Sporulation of PITG_01718 silenced and knockdown transformants under constant red light, constant blue light, or constant dark conditions. E) Radial culture growth under constant light (LL), 12-hour light/dark (LD), and constant dark (DD). F) Plant infection, and G) Cultural growth on rye media under constant light (LL), 12-hour light/dark (LD), and constant dark (DD).

A

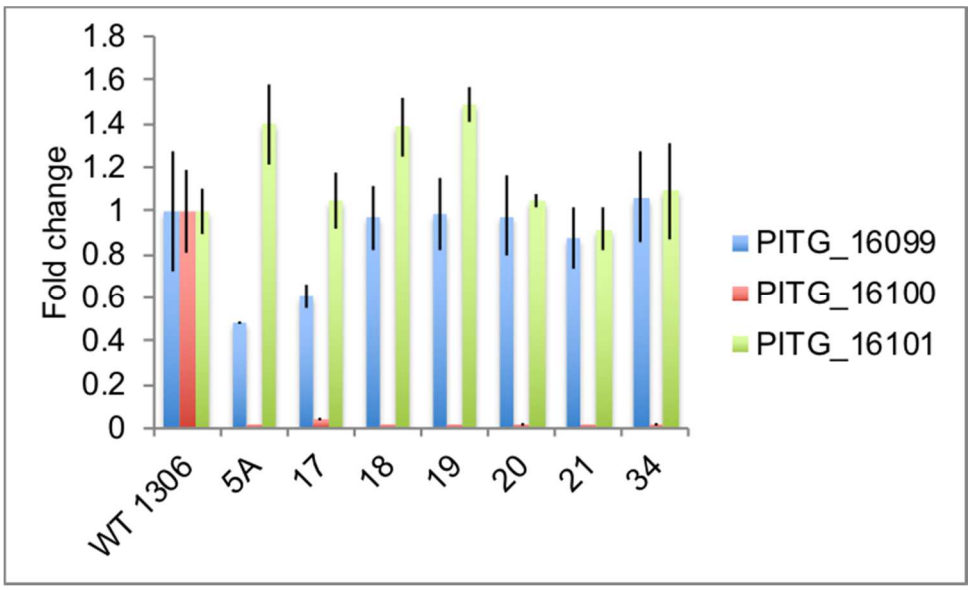

B

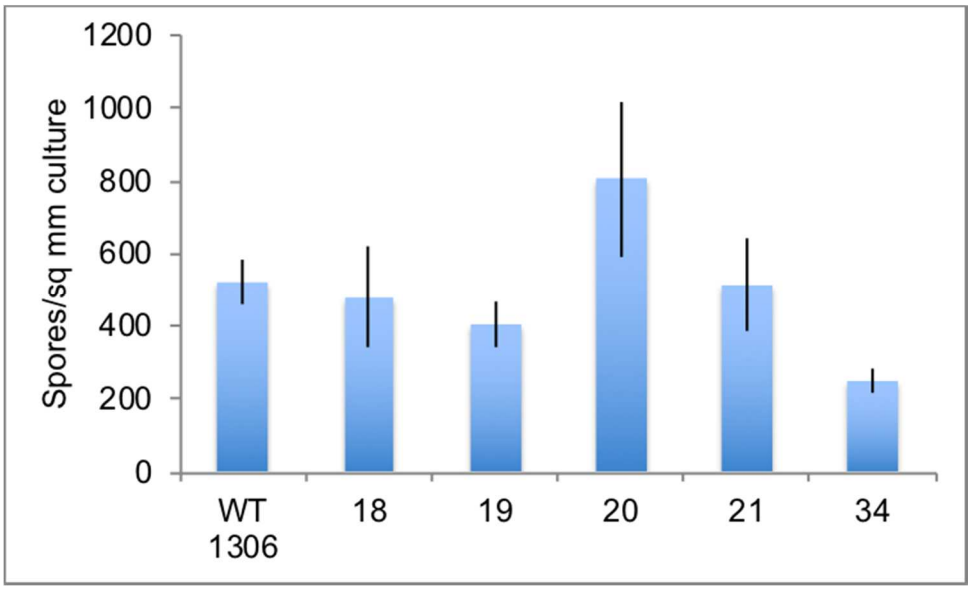

Figure 2.8. A) Expression of PITG_16100 and neighboring genes PITG_16099 and PITG_16101 in PITG_16100 silenced and knockdown strains. B) Sporulation of silenced and knockdown transformants under constant dark conditions.

A

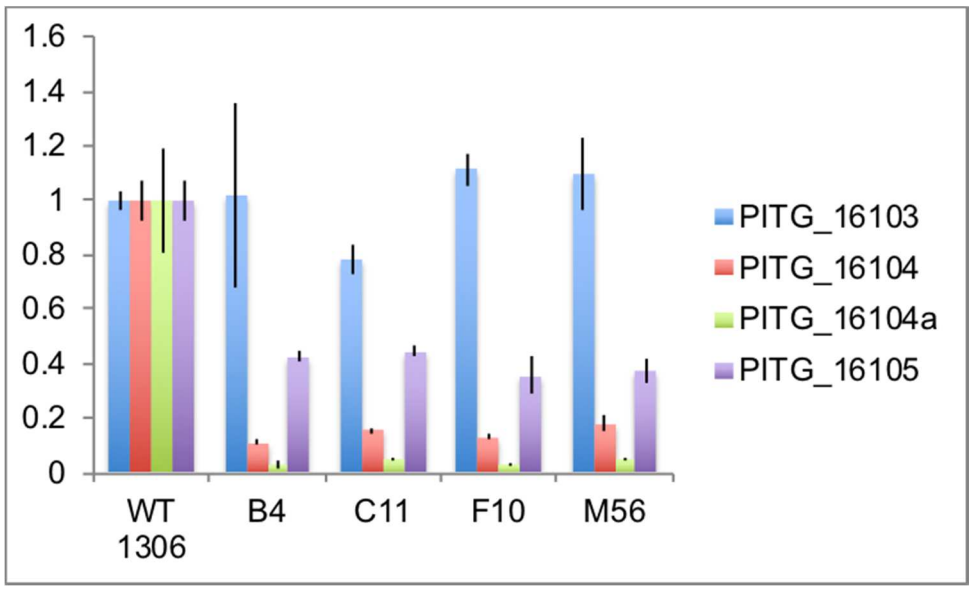

B

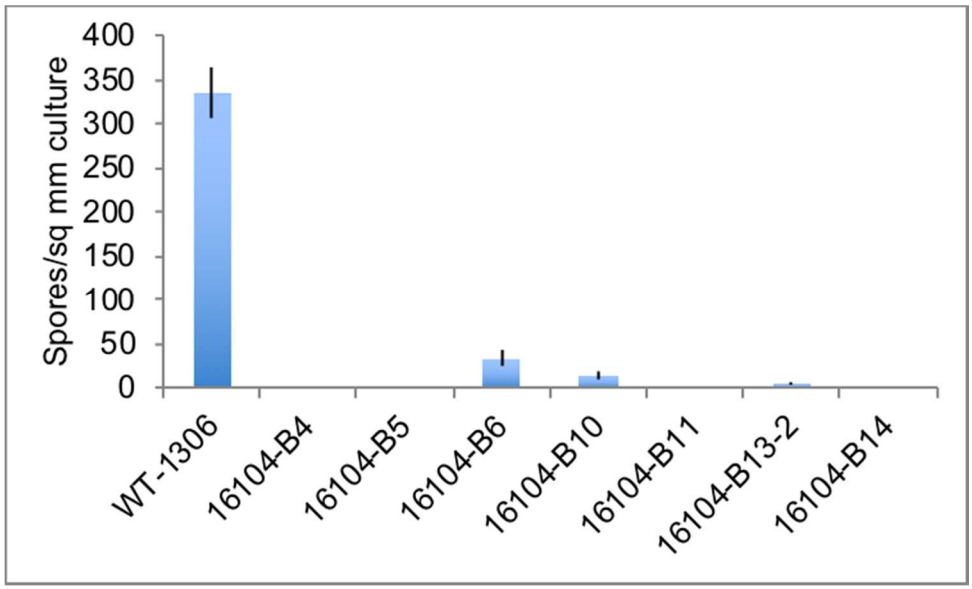

Figure 2.9 A) Expression of PITG_16104 and neighboring genes, including PITG_16104a, non-coding RNA, in PITG_16104 knockdown strains. B) Sporulation of PITG_16104 knockdown strains.

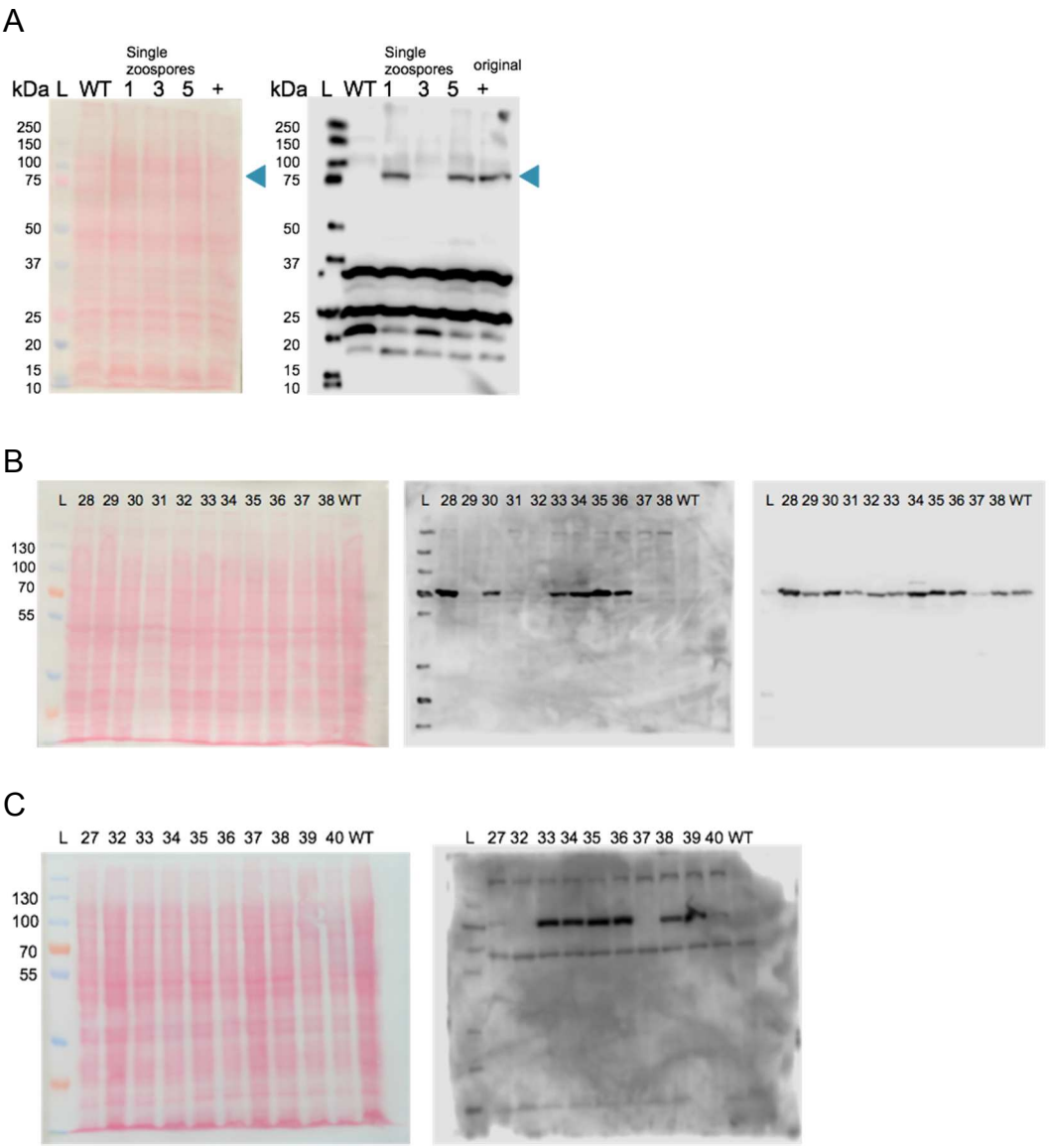

Figure 2.10. Western blots of overexpression transformants A) PITG_16100-5'myc, B) PITG_01718-3'FLAG, and C) PITG_16104-3'FLAG.

A

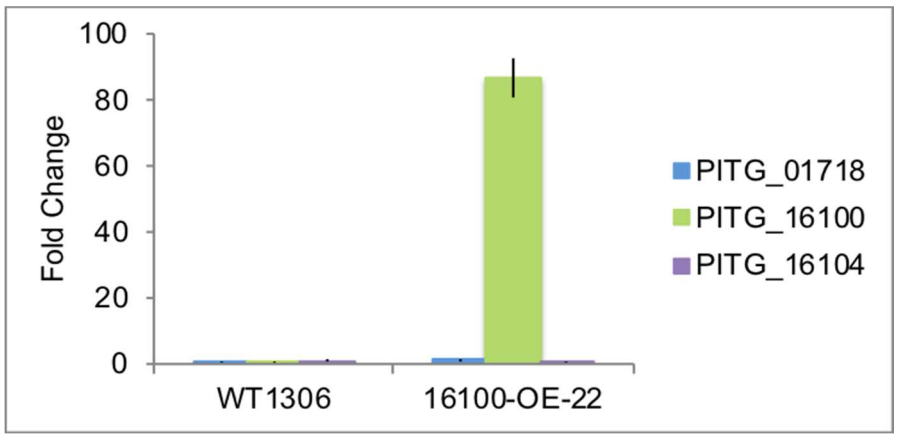

B

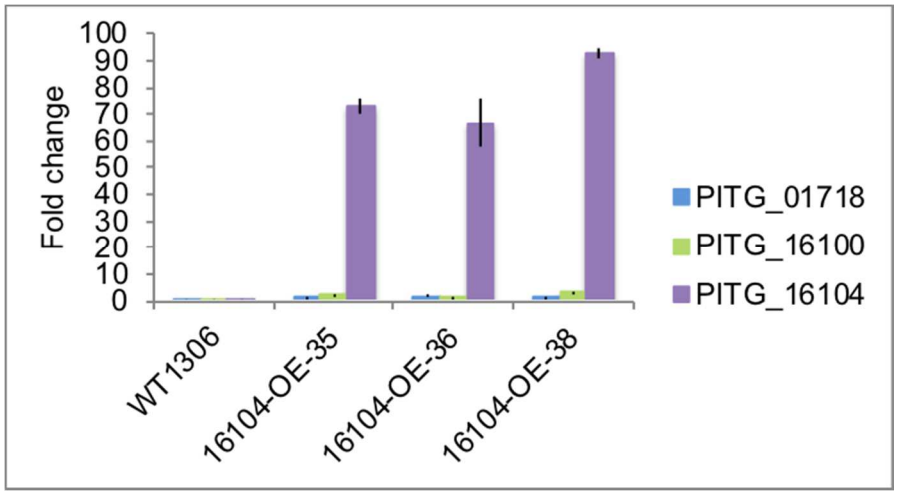

C

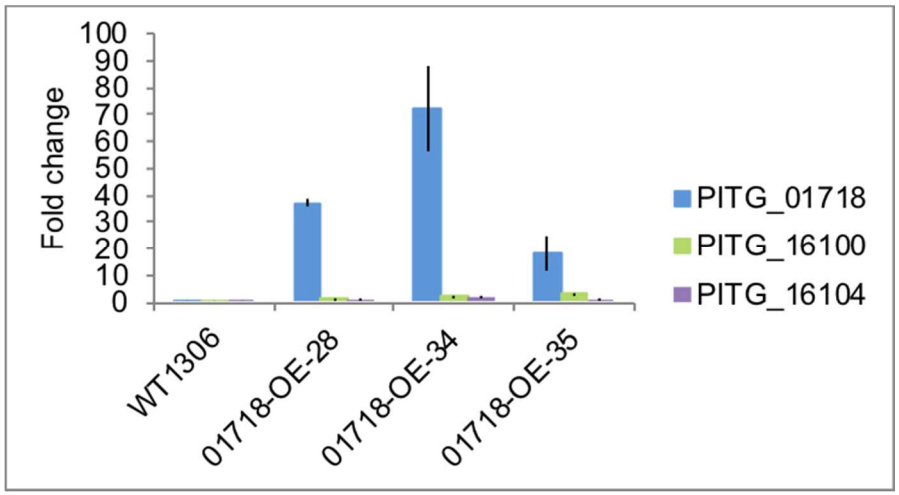

Figure 2.11. Gene expression of overexpression transformants for all three cryptochrome genes for A) PITG_16100, B) PITG_16104, and C) PITG_01718.

A

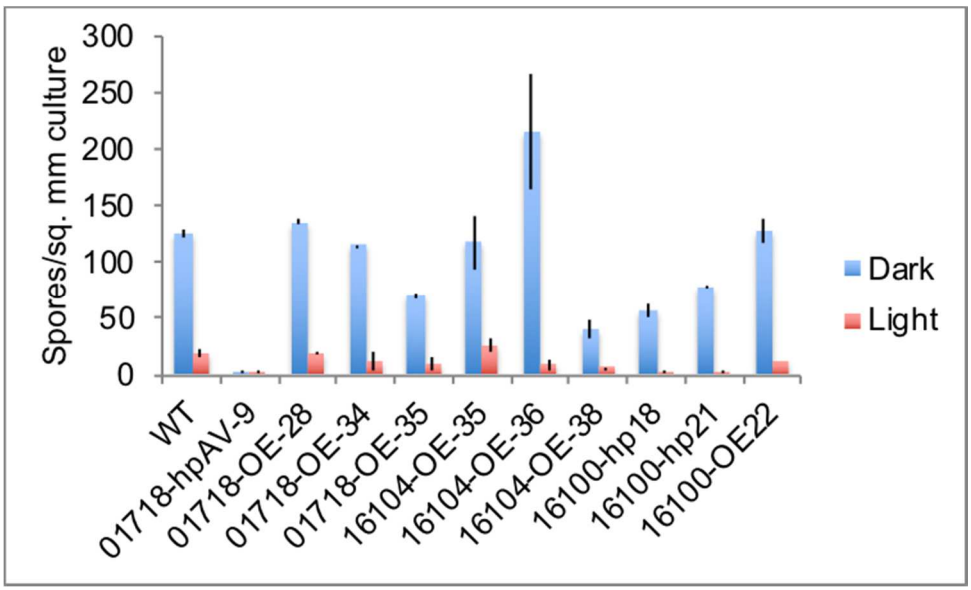

B

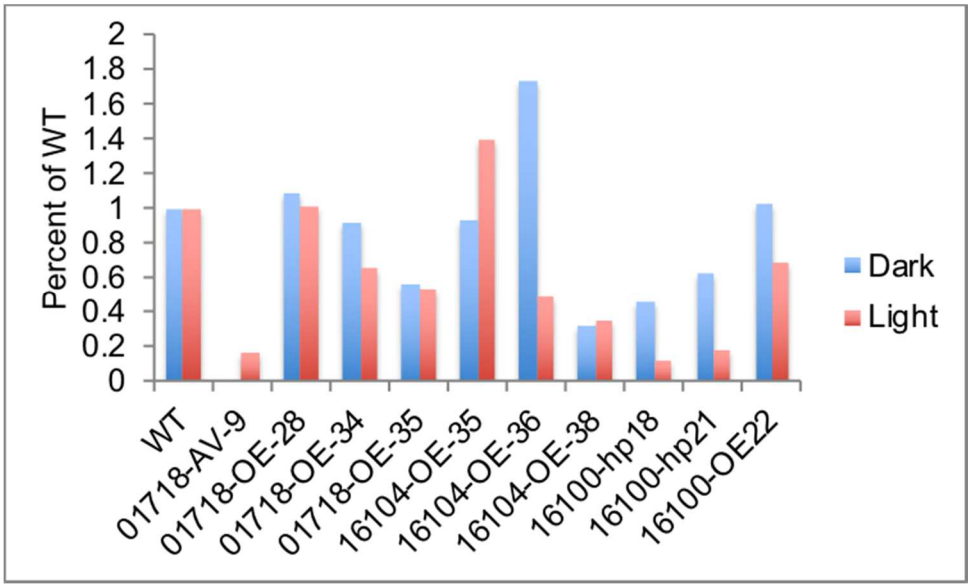

Figure 2.12. Sporulation of overexpression and knockdown strains under constant dark and constant light conditions expressed as A) spores per square mm culture, and B) sporulation percent of wild type.

Table 2.1 Primers used in this chapter.

Primer	Sequence	Experiment
16104OE-3-FLAG-F	AAGACTAGTATGACGGATCGCACTCTCCCG	Overexpression
16104OE-3-FLAG-R	AGCGGCCGCCTACTTGTCGTCGTCGTCCTTGTAGTCCTGCGTAGACTCTTCGGA	Overexpression
16104OE-5-MYC-F	CCAACTAGTATGGAGCAGAAGCTGATCTCGGAGGAGGACCTGACGGATCGCACTCTCCCGC	Overexpression
16104OE-5-MYC-R	TGCGGCCGCCTACTGCGTAGACTCTTCGG	Overexpression
01718OE-3-FLAG-F	GCAACTAGTATGAAGGTGCTTCTTTGGTT	Overexpression
01718OE-3-FLAG-R	AGCGGCCGCCTACTTGTCGTCGTCGTCCTTGTAGTCCTGCTGCTTCGACTCGT	Overexpression
01718OE-5-MYC-F	TCGACTAGTATGGAGCAGAAGCTGATCTCGGAGGAGGACCTGAAGGTGCTTCTTTGGTTCCG	Overexpression
01718OE-5-MYC-R	CGCGGCCGCCTACTGCTGCTTCGACTCGT	Overexpression
16100OE-3-FLAG-F	CCTACTAGTATGACCAGGAAGCGGCAA	Overexpression
16100OE-3-FLAG-R	CGCGGCCGCTCACTTGTCGTCGTCGTCCTTGTAGTCCTCGGGCTGCGAGATCGA	Overexpression
16100OE-5-MYC-F	TCGACTAGTATGGAGCAGAAGCTGATCTCGGAGGAGGACCTGACCAGGAAGCGGCAACG	Overexpression
16100OE-5-MYC-R	CGCGGCCGCTCACTCGGGCTGCGAGAT	Overexpression
PITG_16104pcrR	GCGGCGTCTAGCGTTGATTC	Overexpression
PITG_01718pcrR	GCCACACGGTCTTGATCACT	Overexpression
PITG_16100pcrR	CGTCCTTCCAGCACTGCAAC	Overexpression
PITG_01718s-Fm	GCCCATCGATTGCCATCCCCCACGAGAAAGCACA	Silencing
PITG_01718s-Rn	TGGCCATTAAGGCCTGGCGCGACCGTGGCAATGGTA	Silencing
PITG_16100s-Ff	GCCCATCGATACCACAACGCTGAGTGCTTACCTGA	Silencing
PITG_16100s-Rn	TGGCCATTAAGGCCCGTCGCTCCTCGAAGCCACGAA	Silencing
PITG_16104s-Ff	AAGTATCGATACTCTCCCGCTTTCTGCGCCAC	Silencing
PITG_16104s-Rn	TGGCCATTAAGGCCTTGACGCCGCACAGCATGATCT	Silencing

PITG_16104ant-F-n	GCCTCTAGATTGACGCCGCACAGCATGATCTT	Silencing
PITG_16104ant-R-n	AATGCGGCCGCACTCTCCCGCTTTCTGCGC	Silencing
PITG_01718ant-F-n	TCCTCTAGATGGCGCGACCGTGGCAATGGTAGAA	Silencing
PITG_01718ant-R-n	TTAGCGGCCGCCTGCCATCCCCCACGAGAAA	Silencing
PITG_16100ant-F-n	GCCTCTAGACGTCGCTCCTCGAAGCCACGAA	Silencing
PITG_16100ant-R-n	ATTGCGGCCGCACCACAACGCTGAGTGCTTA	Silencing
s16104-F	ACCTTAATTAATCTGCCCAGTGAGCTCTACCAA	Silencing
s16104-R	AATGCTAGCGAAGCTGTCCGTCCAAGCTCACAG	Silencing
as16104-F	GCCTCTAGAGAAGCTGTCCGTCCAAGCTC	Silencing
as16104-R	AATGCGGCCGCTCTGCCCAGTGAGCTCTA	Silencing
ham34-F-544	CGACCTTCACTCTCACCGAC	Plasmid confirmation
ham34-R-41	TCTGCAACTTCGCACTCAGT	Plasmid confirmation
16104RT-F148	ATACGTTCCAGCACTCAGCA	qRT-PCR
16104RT-R148	ACTTCGACGCATAGCGATCTT	qRT-PCR
01718RT-F151	TCTATGAGCCGTGGAAAGCC	qRT-PCR
01718RT-R151	CCATACTGGCCGTTGGCATA	qRT-PCR
16100RT-F154	CTGACTGCCTCATCGGGAAA	qRT-PCR
16100RT-R154	TCTTCAGTTTGGGTGCGTGT	qRT-PCR
PITG_16099F	GCTGTGTTGTAGGGGGCTTT	qRT-PCR
PITG_16099R	TGCTCAGTTGTCTGCTCACC	qRT-PCR
PITG_16101F	TGCAAGAAAGCGCAGTGAGA	qRT-PCR
PITG_16101R	TCAGGTCGTGCAGATTGGTG	qRT-PCR
PITG_16103F	GCTCATCGGTGGCTACTTCT	qRT-PCR
PITG_16103R	AGCTCAGCCTCCTCCAGATA	qRT-PCR
16104aRT-F	ATTCTGCAAGATGCGCGTTC	qRT-PCR
16104aRT-R	TCGCTGTCTTCCTCGTCGTT	qRT-PCR
16104RT-F	ATCATCTAGCACGTCACTCGGTA	qRT-PCR
16104RT-R	CTAGCACTAAGCCACAGCCAG	qRT-PCR
PITG_16105F	GAGACGACGAGGAGTTCCCA	qRT-PCR
PITG_16105R	GGGAATGAGTCGAGCAGTGG	qRT-PCR

PITG_01717F	GCTGCCTATTCTCCAGGTCA	qRT-PCR
PITG_01717R	TTGCAGTACCCAGTGAGAGG	qRT-PCR
PITG_01719F	CACAACGTGCGTGAGATGAG	qRT-PCR
PITG_01719R	AACCTTGCCGTTCGGGTAAA	qRT-PCR
Pc_44729F-146	CAATTACCGTCATGTGGCGT	qRT-PCR
Pc_44729R-146	GCTGTACCTTCAATGGTGCG	qRT-PCR
Pc_44729F-160	AAGAGGGGCAGCTTACTTCC	qRT-PCR
Pc_44729R-160	GAACTGGCCTTGTTGATCCCA	qRT-PCR
Pc_574436F-149	TCCTTACACGGGGTGACCTA	qRT-PCR
Pc_574436R-149	GTACACCCGGAAGTAAGCCG	qRT-PCR
Pc_574436F-160	ACCGTCGACATTTGGCAAGAA	qRT-PCR
Pc_574436R-160	CGGATAGTCTTTGCCGATCAGA	qRT-PCR
RiboS3A_F	TAAGACGACGGACGGATAC	qRT-PCR
RiboS3A_R	AGGCACAAACTTCAGGAATAG	qRT-PCR

Table 2.2. Predicted protein sequences of cryptochromes in *P. infestans* and *P. capsici.*

Species	Gene ID	Protein sequence	Predicted molecular weight
P. infestans	PITG_01718	MKVLLWFRRDLRLHDNLALNAALQHIEEAKSDVELISLYIIHRPQIMRCG ANRFQFVLESVADLSGALAERGSKLVVAKGDSIQVLRRVLPAWDITHM FFDGVCEPYAVERDDRALALAKSLGVQTHVTKGYNLYDLEVVIASHSG KAPKTYQRFLKAVGAQPTPREPIPTPETLPSPTRKHSELYEQIANYWK DRKLSDEEKEDDLEERERQIDQIAGPEHDFTLPDLTYFGYETPEKHSFI YGGEQKALEMLKNYCSDQDRVALFEKPKTSPAQIPPTPSTTVLSPYMF YGCLSPRTFYHQVRSIQRGRKKVSVPPVSLIGQLLWRDFYHCHGRAN PYFDKMEESSTCLQVNWRYHTIPENEEDLSDDDKLARSQFEAWRDG RTGFPWIDAIMIQLKEEGWMHHLARHSVACFLTRGDLYISWVRGLEVF QERLIDHDWSLNAGNWLWLSSSYFFTAYFRVYSPISFGKKSDPEGLFI KKYIPALKNFPAKYIYEPWKAPLTLQHAAGCRIGKDYPTPIIEHKTAMKR CVEGLKMSYANGQYGIPPTSQTSKKRQREGSDDESKQQ*	65.5 kDa
P. infestans	PITG_16100	MTRKRQRSASVRHVDDHPTPQRRHNATQNDVNGEADLTTPPRQDNA ENANNNGPSITSPTITVTSSLNVLDGEVTTKVETVKDDDEQAKVNVALP KRRAIVWFRRDLRIHDNLALDAAMRAQMQLQKAGDEEMALLPIYILHR PKRQRCGPVRFQFLLEAIEDLARSIAKLDGRLLVLSGDAEEVLRTVIAA WGVTDLFFEAGVAHYAVDRDNRVRAIAKSLDVNVTTIRGVTLYNPHEII RLNSGQAPTDYERLLEITEKMPQPTQPIPAPVKLLNAACFSTDKLFSLL EDVCQQNPSEADVIAGVAGDVKKTESELFVAPPLTAFGLTPPTPHAPLI GGESAAMKRLDDFCEDERRVGQFEKPKTSPVSIDGPSTTTLSAYLSF GCLSAREFFYRIMFIQLQYPHRPGLPTQVTLEGQLMWREFFYCYMCG TRNFDSQELNPSCKQIDWRLLNEYYVSHPEYDEQEPKKVTEADEKLA MRQLQCWKDGRTGFPWIDAVMRQINQEGWTHHAGRHAVACFLTRG VLYISWLRGATYFQEKMIDLDWPINVGNWLWVSASCFFTNYRRMASP STFPQRWDQQGQFIRKYIPALRNMPDKYVFEPWKAPLKVQRDADCLI GKNYPFPIVDSKLAMSRCIAGMSRSFSDSDTESTTSSLTSTRTQTEDA	78.6 kDa

		EADGSSPWSGDDMCYNYRVPGSISQPE*	
P. infestans	PITG_16104	MTDRTLPLSAPLLPTEGTNNDAADDADLVDFASSLLDAADPDSELPES TLDAATLDAVHAAINAPRELASEAISTSDLPVGSQQQQSTVEEEKKESI PSESLPATDSGGGSDDEIRILVWFRRDLRLHDNLAISAALDWIKQEEEK IPGRKVVFIPLYIVHRPKIMLCGVNRFQFLLESVSDLADALAARGSRLVV ARGDGVQVLRRLLPAWRISHLFFDAASEPFAIDRDNRAVALARQLGVE THVTHGYTLYDLDAVIAGNNGEPPKTYTAFLRALAMQPKPPKPLPTPE KVPAPVYLPSELYQQVIDYWQNRLKPDSVTQSDVKEEKTEDETVKQD FEADDDPQEKAKHLDEIAGPEQQFTLPEVTDFGFVAPERHPFIYGGEQ IALGILRDYCRNEGRVVKFEKPKTSPAQTTPSASTTSLSPYLYFGSISP RTFLHHVRGIQEHHAKALSATPVSLDGQLLWREFFHCHGRANAYFDK MEESPTCLQIDWRWHTIPEREEDMTDDDKLARSQFQAWIDGQTGFP WIDAIMIQLKEEGWMHHLARHSVACFLTRGDLYISWVRGLEVFQERLI DHDWSINCGNWLWLSASYFFSAYFRVYSPSTFGKKWDPEGLFIRKYV PALSKMPVKYIYEPWKAPMTVQHAAGCLIGKDYPFPIVDHKIAMRRSM AGMKKSYALNEYGTPPAPNPPSSPRFKRPRENSASSSETSEESTQ*	80.8 kDa
P. capsici	Phyca_574436	MTDHSQPPPTPPLPPEDPNEASDDTDLVNFASSLLDAADPDSQLPES ALDAATLDAVHAAINAPQESPPERNILEVQGDPHATVAEEQREPIPSEI DPETASERIDQDEVRILMWFRRDLRLHDNLALTEALELVKQQEEKMKQ TTGRKVVFIPLYIVHRPKIMLCSVNRFQFMLESVSDLADALAARGSRLV VARGDGVQVLRRLLPAWRITHLFFDAASEPFAIARDNRAVALATRLGV QTRVTHGYTLYDLDAVISGNDGEPPKTYTAFLRSLAMQPKPPKPLPTP EQVPALVYLPSELYQQVADYWKNRLKPDPVGQTDVKEEKTEEEEVKQ EEEDDPKEKAKQLEEIGGPEQQFTLPEVTDFGYEAPERHPFIYGGEQI ALSILRDYCRNEGRVVKFEKPKTSPAQTTPSASTTSLSPYLYFGCISPR TFLHHVQGIQEHHAKALSATPVSLDGQLLWREFFHCHGRANPYFDKM EESPTCLQIDWRWHTIPEKEEDMTDDDKLARSQFKAWTDGQTGFPWI DAIMIQLKEEGWMHHLARHSVACFLTRGDLYISWVRGLEVFQERLIDH DWSINAGNWLWLSSSYFFSAYFRVYSPSTFGKKWDPEGLFIRKYVPA LSKMPVKYIYEPWKAPVTVQHAAGCLIGKDYPFPIVDHKIATRRCMEG MKKSYAINQYGTPPVPKHPSSPRLKRQRENSSSSSETSEESTQG*	81.1 kDa

P. capsici	Phyca_44729	MARKRQRSVSTENSDDVHQLETPVQNTLEVAEEEDDWIEFIDGNSND PSIMSAQSSFVLDGELQTEAVDSNVQEDNSELDTNAKQSDVDVTLPK RRAVVWFRRDLRLHDNLALDAAIRAQQQLQKTEEMALLPIYILHRPKHL RCGPMRFQFLLEAIEDLAKSIDKLHGRLLVLRGEAEEVLRVVMEAWGV TDLFFEAGVMSYAVERDDRVKAIARTLNVKVTAIRGVTLYDPNEIIRLN GGKPPTDYERLLEITENMPQPAQPIAAPVKLKNAAALSTSQLVKLLKDF CKQDPSTANSIVGGTVDAEKADSELFVVPVLAVFGMEQPDPHTPLVG GESEALKRLEEFCKDKRRVGLFEKPKTSPVAINAPSTTALSAYLCFGCL SAREFFYRIMFIQLQFPLRPGPTQVTLEGQLMWREFFYCYACGTPNFA SQERNPGCKQIEWRLRDEAHVTNPEYDQPVPLDADEKLALRQLQCW KDGRTGFPWIDAVMRQINQEGWTHHAGRHAAACFLTRGVLYISWLR GAAYFQEKLVDMDWPMNIGNWLWVSASCFFSNYRHVASPSRFPQR WDQQGQFIRKYIPALRNMPDKFVHEPWNAPLKVQRDAGCLIGKDYPF PIVDSKLAMSRCIAGMSLAYSDSETDSTASSVSSSRTQTEDADTGGSS PWSADDMCYNYRGSQP*	77.0 kDa
P. capsici	Phyca_44729 alternative allele	MARKRQRSVSTENSDDVHQLVQNTLEVAEEEDDWIEFIDGNSNDPSI MSAQSSFVLDGELQTEAVDSNVQEDNSELDTNAKQSDVDVTLPKRRA VVWFRRDLRLHDNLALDAAIRAQQKTEEMALLPIYILHRPKHLRCGPM RFQFLLEAIEDLAKSIDKLHGRLLVLRGEAEEVLRVVMEAWGVTDLFFE AGVMSYAVERDDRVKAIARTLNVKVTAIRGVTLYDPNEIIRLNGGKPPT DYERLLEITENMPQPAQPIAAPVKLKNAAALSTSQLVKLLKDFCKQDPS TANSIVGGTVDAEKADSELFVVPVLAVFGMEQPDPHTPLVGGESEALK RLEEFCKDKRRVGLFEKPKTSPVAINAPSTTALSAYLCFGCLSAREFFY RIMFIQLQFPLRPGPTQVTLEGQLMWREFFYCYACGTPNFASQERNP GCKQIEWRLRDEAHVTNPEYDQPVPLDADEKLALRQLQCWKDGRTG FPWIDAVMRQINQEGWTHHAGRHAAACFLTRGVLYISWLRGAAYFQE KLVDMDWPMNIGNWLWVSASCFFSNYRHVASPSRFPQRWDQQGQF IRKYIPALRNMPDKFVHEPWNAPLKVQRDAGCLIGKDYPFPIVDSKLA MSRCIAGMSLAYSDSETDSTASSVSSSRTQTEDADTGGSSPWSADD MCYNYRRS*	76.1 kDa

* represents stop codon

Table 2.3 *P. capsici* sgRNAs

Gene	Position	sgRNA name	Sequence
Phyca_44729	49	44729_49_revcom	ACGATCCACTTCCAAGCACAAGG
Phyca_44729	276	44729_276_revcom	CTCTGAGCACTCATAATGGAGGG
Phyca_44729	417	44729_417_revcom	CGTGCAGTCTCAAGTCCCGACGG
Phyca_44729	547	44729_547	ATTTACGGTGTGGCCCCATGCGG
Phyca_44729	1422	44729_1422	GCTGTAAACAGATCGACTGGAGG
Phyca_44729	2121	44729_2121_revcom	CACATATCGTCCGCACTCCAAGG
Phyca_574436	353	574436_2	TGTGGTTCCGACGAGACCTGCGG
Phyca_574436	378	574436_27	GCACGATAACCTGGCACTGACGG
Phyca_574436	919	574436_190_revcom	TCTCGAGCATGAACTGGAAGCGG
Phyca_574436	1491	574436_1140	GCACACGATTCCAGAGAAAGAGG
Phyca_574436	1558	574436_1207	GCTTGGACGGATGGTCAGACCGG

Chapter 3: Humidity and light-regulated gene expression in *Phytophthora infestans* and *Phytophthora capsici*

Introduction

The ability to sense and respond to environmental conditions is critical for many organisms, including *Phytophthora* species. Environmental conditions play an influential role in plant disease incidence and severity, with a large role in severity of epidemics. This environmental influence on plant disease has informed plant production practices as early as Ancient Greece (Agrios, 2005). Environmental conditions are used to inform decision support systems for *Phytophthora* diseases, such as BLITECAST or BlightPro, but also inform cultural best practices for disease avoidance, such as water management to decrease periods of high humidity (Harrison, 1992; Krause et al., 1975; Lehsten et al., 2017; Raposo, 1993; Seijo-Rodríguez et al., 2018; Small et al., 2015).

Environmental factors, particularly light and humidity, affect physiology of both pathogen and host. However, limited research has been conducted to understand the effect of light on *Phytophthora* biology at the molecular level, and humidity research has been hampered by ineffective methods to accurately measure and control humidity at the plant or media surface (Harrison, 1992).

Humidity

Humidity has a profound effect on sporulation of *Phytophthora* species (Crosier, 1934). Humidity, rainfall, and frequency of wet days are three of the top

four factors that influence occurrence of *Phytophthora* diseases in the field (Utrata, 1980). Although light and temperature have an interactive effect relative to sporulation in *Phytophthora* and other oomycetes, humidity has not been shown to have an interactive effect with light or temperature (Minogue and Fry, 1981; Nordskog et al., 2007). In plants, humidity has independent regulatory functions, and controls some processes that are independent of light and temperature (Mwimba et al., 2018).

Light

Light is an important signal for space, time, and stress. In *Phytophthora*, light regulates sporulation, and has a differential effect on various species of *Phytophthora*, as discussed in Chapter 2. Little is known about which processes other than sporulation are light-responsive, which sporulation genes are light-responsive, or where in the sporulation cascade light has an effect. Additionally, little research has been conducted to understand the difference in short-term illumination (48 hours or less) versus long-term illumination in *Phytophthora* species.

Understanding transcriptional shifts relative to environment is important for understanding how the organism is adapting at the molecular level. However, gene expression changes under differential environmental conditions has not been thoroughly explored in *Phytophthora* species.

Materials and Methods

Strains

Phytophthora infestans strain 1306, an A1 strain isolated from tomato in California, was maintained on rye-sucrose media at 18°C in the dark (Judelson and Whittaker, 1995). *Phytophthora capsici* strain LT1534, a lab strain created through a cross of LT51 and LT263, backcrossed twice to LT263 to reduce heterozygosity, was maintained on 10% V8 juice agar at 18-24°C in the dark (Hurtado Gonzales and Lamour, 2009).

Light treatment

For the experiments with *Phytophthora infestans* and *Phytophthora capsici* under constant light and constant dark conditions with two timepoints, the white light treatment was the same as described in Chapter 2 (Fig. 2.2). For *P. infestans*, pre-sporulation cultures were harvested at 2-days post inoculation, and actively sporulating cultures were harvested at 4-days post inoculation. For *P. capsici*, pre-sporulation cultures were harvested at 4-days post inoculation, and actively sporulating cultures were harvested at 6-days post inoculation. These experiments involved the collection of two biological replicates. Cultures were grown face-up, with the Petri dishes directly on the wire rack in a single layer in a Percival I-36LLVL incubator outfitted with cool-white fluorescent lighting, kept at a constant 18°C. Photon fluence rate was measured at the media surface, under the Petri dish lid, using an Apogee PS-200 spectroradiometer (Apogee

Instruments, Logan, UT), and was approximately 75 μmol/m^2/sec. Cultures exposed to continuous darkness were stored in individual cardboard boxes inside a polystyrene box covered in light-tight black fabric in the same incubator at the same time. The use of individual cardboard boxes prevented the later (4- and 6-day incubated) cultures from any incidental light exposure during the harvest of the earlier (2- and 4-day incubated) cultures.

In the experiments that were originally published in Xiang and Judelson (2014), and used for RNA-seq analysis in this study, plates were stored upside down inside sealed polystyrene moisture chambers, housed in a Percival I-37LLVL incubator outfitted with cool-white fluorescent lighting, at a constant 18°C temperature (Xiang and Judelson, 2014). Using the same Apogee PS-200 spectroradiometer as above, the photon fluence rate at the time of the experiment was measured at 32 μmol/m^2/sec; the media and polystyrene box lid decreased that intensity at the surface of the culture by approximately half since my measurements and calculations indicated that the photon fluence rate was around 15 μmol/m^2/sec. Cultures exposed to continuous darkness were stored in light-tight black plastic bags in the same incubator at the same time.

Humidity treatment

P. infestans cultures were grown on rye-sucrose media with 0.8% agar with a polycarbonate membrane placed on the agar surface. Plates were spore inoculated with 200 μl of a spore suspension of 2×10^5 spores/ml in sterile water.

Plates were incubated for two days under high humidity in a polystyrene box in the dark. At 48 hours after inoculation, the first timepoint was harvested. Plates were then split into two plastic incubation chambers: a chamber with low humidity (34% relative humidity) or a chamber with high humidity (99-100% relative humidity).

High and low humidity conditions were achieved by using plastic incubation chambers with a compressed air input line. The low humidity set-up had a compressed air line directly to the chamber, while the high humidity chamber had a series of three water bubbler humidifier cups between the compressed air regulator and the chamber. The humidity in the low humidity chamber was maintained around 34% relative humidity, while the high humidity chamber was maintained at 99-100% relative humidity, with the same rate of air flow (3.5 liters/minute) in both chambers. Humidity was measured with traceable meters purchased from Thermo Fisher. Samples were collected every 24 hours from each humidity chamber for 3 days. At 3 days after moving (5 days after inoculation), the low humidity chamber was converted to a high humidity chamber by adding three water bubbler humidifier cups between the compressed air regulator and the chamber of the low humidity chamber, and samples were collected ever 12 hours (Fig. 3.1).

RNA isolation and library preparation

Total RNA was extracted with the Sigma Plant Spectrum Total RNA kit (Product number STRN10-1KT, Sigma-Aldrich, St. Louis, MO). RNA quality was assessed by agarose gel electrophoresis, and with a Bioanalyzer 2100 using the RNA nano kit (Agilent Technologies, Santa Clara, CA). Library preparation was conducted with the TruSeq kit (Illumina, San Diego, CA).

Sequencing

RNA sequencing was conducted by 100-nt paired-end read sequencing on an Illumina HiSeq4000 at University of California-Davis Genome Center DNA Technologies and Expression Analysis Core (UC-Davis, Davis, CA) or by 75-nt single-end reads on an Illumina NextSeq500 at CoFactor Genomics (St. Louis, MO).

Data analysis

P. infestans reads were mapped to the *P. infestans* T30-4 reference genome sequence using Bowtie2 and Tophat (Haas et al., 2009; Langmead et al., 2009). *P. capsici* reads were mapped to the *P. capsici* LT1534 reference genome sequence also using Bowtie2 and Tophat (Lamour et al., 2012). The SystemPipeR pipeline was used to run EdgeR to generate trimmed-M-means-normalized counts per million (CPM) gene expression values (Robinson et al., 2010). For the cyclic light/dark study, DESeq2 was additionally run to generate

DESeq2-normalized counts (Love et al., 2014). Reads per kilobase of transcript per million mapped reads (RPKM) gene expression was also calculated for all datasets. Differentially expressed genes were identified through comparison of normalized or CPM or RPKM values, with a false discovery rate (FDR) cutoff of 0.05, and a *P*-value cut off of 0.01. GO term analysis was conducted with GOHyperGAll (Horan et al., 2008). Heat maps were generated with per-gene-normalized values and average Euclidian distance clustering of rows with Partek Genomics Suite (Partek, St. Louis, MO). *P. capsici* orthologs of *P. infestans* genes were identified using reciprocal best BLAST using *P. capsici* LT1534 reference genome gene models and *P. infestans* T30-4 gene models.

Results

Humidity-related gene expression in *P. infestans*

RNA sequencing yielded an average of 105,793,553 reads per library for each of the 36 libraries, with about 80-85% of reads mapping to the *P. infestans* T30-4 genome. A total of 13,884 genes were expressed with a CPM over 1 in any condition (Fig. 3.2). Approximately one-third of genes in this dataset show steady expression (<1.3-fold change) under both conditions (Fig 3.2).

Further analysis identified 1216 genes that increase in expression by 2-fold as the culture grew under low humidity (Fig. 3.3). Since no sporulation was occurring in these cultures, I refer to these as "aging-related" genes although it is possible that some could reflect early-induced sporulation phenomena. GO term analysis of this data set showed that overrepresented gene ontology terms

included microtubule motor activity, cilium, and potassium ion transport (Table 3.1).

To identify sporulation-associated genes, comparisons were made of the sporulating versus non-sporulating cultures: low humidity versus high humidity days 3, 4, and 5, low humidity day 5 to “low to high humidity” day 5.5, and low humidity day 5 to “low to high humidity” day 6. Lists were compiled, and aging-related genes were removed. This resulted in the identification of 1332 sporulation-associated genes (Fig. 3.4). Many of the genes that are highly expressed in the actively-sporulating high humidity samples at 5.5 and 6 days after inoculation increased expression in the low humidity-grown cultures shifted to high humidity, indicating that these genes may be controlled by a factor directly downstream of the humidity response mechanism (Fig. 3.4). GO term analysis of this set of 1332 genes included some known sporulation-related genes, such as cilia-related genes.

Sets of known, well-characterized sporulation-related genes, i.e. those encoding cilia, mastigoneme, Bardet-Biedel syndrome (BBS), and intraflagellar transport (IFT) proteins, were examined separately to ascertain which genes are turned on under low humidity, and which turned on expression when the low humidity-grown cultures were shifted to high humidity to remove the sporulation repression (Fig 3.5)(Blackman et al., 2011; Judelson et al., 2009, 2012). While approximately one-third of the cilia-related genes were not differentially expressed in sporulating (high humidity) cultures, two-thirds exhibited increased

expression in sporulating cultures (Fig. 3.5A). The mastigoneme and BBS genes all had increased expression in the sporulating cultures, including both the high humidity sporulating cultures and the cultures shifted from low-to-high humidity (Fig. 3.5B,C). While expression in the latter was not as high as in the cultures treated with constant high humidity, the relative ratio of mRNA level to sporangia concentration in the cultures were similar. The mastigoneme and BBS genes had increased expression early in the high-humidity sporulation time course, and also increased in the first 12 and 24 hours after the low humidity samples were exposed to high humidity, which is consistent with these genes being turned on early in the sporulation cascade (Fig. 3.5B, C). The twelve IFT genes showed a very slight increase in expression in the cultures shifted from low to high humidity induced-sporulation genes, albeit lower than observed in the constant high-humidity cultures (Fig. 3.5D).

Effect of long-term illumination on gene expression in *P. infestans* and *P. capsici*

As discussed in Chapter 2, growth under constant light or dark conditions results in normal sporulation in constant dark for *P. infestans* and sporulation in only constant light for *P. capsici* (Fig. 2.1C, D). RNA sequence analysis of *P. infestans* at day 2 (pre-sporulation) and day 4 (active sporulation), using two biological replicates each, resulted in an average of 30 million reads per sample, with approximately 87% alignment to the *P. infestans* T30-4 genome, with 13,179 genes expressed with a CPM over 1 in any condition. RNA analysis of *P. capsici*

at day 4 (pre-sporulation) and day 6 (active sporulation), using two biological replicates each, resulted in an average of 27 million reads per sample, with approximately 86% alignment to the *P. capsici* LT1534 genome, and 14,643 genes expressed with a CPM over 1 in any condition.

Analysis of the *P. infestans* day 4 constant light (non-sporulating) and day 4 constant dark (sporulating) samples identified only 194 differentially expressed genes with a 2-fold change threshold: 130 genes expressed higher in the dark and 64 genes expressed higher in the light condition. By comparison, in the humidity experiment described earlier 1498 differentially expressed genes with a 2-fold change threshold were identified between the day 4 high humidity and low humidity samples: 1285 higher in the former, and 213 higher in the latter. GO term enrichment analysis of the 194 differentially expressed genes between the *P. infestans* day 4 constant light and constant dark cultures resulted in no enriched GO terms. Analysis of selected sporulation-related gene sets (cilia, mastigoneme, BBS, and IFT) showed that nearly all were expressed similarly in the non-sporulating constant light and sporulating constant dark conditions at day 4, with slightly higher expression in the non-sporulating cultures (Fig. 3.6A,B,C,D). There were, however, several cilia genes that are higher in the sporulating cultures than in the non-sporulating cultures (Fig. 3.6A). This indicates these sporulation genes were already turned on in the *P. infestans* cultures exposed to light, indicating that the light-related step is likely later in the

sporulation cascade- after the cilia, mastigoneme, BBS, and IFT sporulation genes are first turned on (Fig. 3.6).

Differential expression analysis of the *P. capsici* cultures grown under constant light or constant dark conditions, harvested at day 4 (pre-sporulation) or day 6 (active sporulation) sets differed from the results in *P. infestans* in several ways. First, as described in Chapter 2, *P. capsici* sporulates in constant light and not constant dark. At day 6, 505 genes were found to be differentially expressed at least 2-fold in constant light versus constant dark, with 379 genes expressed higher in constant light and 126 expressed higher in the constant dark. This is 2.5 times more genes differentially expressed than identified in *P. infestans*, with 3 times as many genes with increased expression in the sporulating cultures as compared to the non-sporulating culture of the same time point.

Analysis of selected sporulation-related gene categories (cilia, mastigoneme, BBS, IFT) in the *P. capsici* constant light and constant dark cultures showed that many of these sporulation genes are expressed higher in the sporulating cultures than the non-sporulating cultures (Fig. 3.7). Although higher expression of sporulation genes in sporulating cultures, and lower expression in non-sporulating cultures is the intuitive or expected result, this is in contrast to *P. infestans*, where the sporulation genes were on in both sporulating and non-sporulating cultures. However, interestingly, both *P. infestans* and *P. capsici* have very similar expression of the cilia genes in constant light at the early and later timepoints, regardless of sporulation (Fig. 3.6A, Fig. 3.7A).

Expression of the cilia genes under constant dark conditions in *P. infestans* versus *P. capsici* was somewhat similar in the two species, but the change in expression from the non-sporulating early timepoint to the sporulating later timepoint was starker in *P. infestans* than the two non-sporulating timepoints in *P. capsici*, indicating a likely association with sporulation in this case (Fig. 3.6A, Fig. 3.7A).

Approximately 30% of the cilia genes were expressed at higher levels in the sporulating cultures of *P. capsici* (Fig. 3.7A). All three of the mastigoneme genes were expressed higher in the sporulating cultures (Fig. 3.7B). Three of the 7 BBS genes were expressed higher in the sporulating cultures, and 8 of the 12 IFT genes are expressed higher in the sporulating cultures, with 1 of the 12 IFT genes expressed higher in the non-sporulating day 6 culture as compared to the sporulating day 6 culture (Fig. 3.7C, 3.7D). This expression pattern is in contrast to the expression of the orthologs of these genes in *P. infestans,* where none of these genes were expressed higher in the sporulating *P. infestans* cultures as compared to the non-sporulating cultures at the later timepoint (day 4). The expression pattern observed in *P. capsici* is more similar to the *P. infestans* humidity-regulated sporulation observed in *P. infestans*, where all of the mastigoneme and BBS, and 9 of the 12 IFT genes and two-thirds of the cilia genes were expressed higher in the sporulating (high humidity) cultures (Fig. 3.5).

To further investigate the differences in expression of sporulation-related genes in the *P. infestans* and *P. capsici* light-regulated sporulation cultures under constant light or constant dark, the 1332 *P. infestans* humidity-related sporulation genes (Fig. 3.4) from the differential humidity datasets, along with the 1129 *P. capsici* orthologs were analyzed in the *P. infestans* and *P. capsici* constant light versus constant dark datasets. TMM-normalized CPM values were used and data was per-gene-normalized per species. When looking at all of these genes together, *P. infestans* again has little differential expression in the sporulating versus non-sporulating day 4 cultures, with slightly higher expression of the sporulation-associated genes in the non-sporulating cultures (Fig. 3.8A). In *P. capsici*, however, 85% of these sporulation-associated genes were expressed higher in the sporulating versus non-sporulating day 6 cultures (Fig. 3.8B). When analyzing a subset of the 1332 genes with the strongest sporulation-related expression in the humidity set, a clade calculated by Euclidean clustering and selected visually (to reduce noise), only 15 of 60 genes in *P. infestans* had 2-fold higher expression in the sporulating versus non-sporulating cultures (Fig. 3.8C, Table 3.2). In *P. capsici*, all 48 of the orthologs were expressed higher in the sporulating cultures as compared to the non-sporulating cultures, with strong expression in only the day 6 constant light sporulating cultures (Fig. 3.8D).

Cyclic light/dark gene expression in *P. infestans*

RNA was also sequenced from *P. infestans* cultures grown under constant light, constant dark, and 12-hour light/dark cycles on media, and on tomato leaves under 12-hour light/dark cycles. This used tissue samples previously used for other experiments by Xiang and Judelson (Xiang and Judelson, 2014). Cultures on media were sampled every 12 hours at 2 days after inoculation, then 3 to 7.5 days after inoculation, and *in planta* cultures were harvested every 4 hours from 2 days after inoculation to 6 days after inoculation. RNA sequencing of media-grown cultures had an average 25 million reads per sample, with an average of 86% mapping to the *P. infestans* T30-4 genome sequence. *In planta* cultures were sequenced to an average of 77 million reads per sample, with 10-80% reads mapping to *P. infestans;* this value increased progressively during the experiment, reflecting the proliferation of the pathogen within plant tissue. Approximately 15,984 genes were expressed in any condition with a DESeq2-normalized counts >20, and RPKM>1 (Fig. 3.9). DESeq2-normalized counts and RPKM were used with this dataset, in contrast to the TMM-normalized CPM values with FDR and *P*-value calculations as above, as this dataset has single replicates. Visualization of the overall expression patterns of genes shows 9 large groups of distinct expression patterns (Fig. 3.9). This includes genes that are highly expressed early in plant infection but are steadily expressed in media, genes that are high early in media, but are low early *in planta*, genes that are expressed high early and decrease over time in both media and *in planta*, genes

that appear to be light-regulated with a cyclic pattern in the 12-hour light/dark set, genes that are higher in the dark media and likely contain sporulation genes, and four other groups with gene expression that changes only slightly over time in the different conditions.

Analysis of the 230 *P. infestans* transcription factors expressed in these datasets showed that several transcription factors have differential expression under constant light, as compared to constant dark, as compared to 12-hour light/dark. A few were expressed higher in the dark sporulating cultures. This included both in constant dark samples and tissue harvested during the dark period of the 12-hour cyclic light/dark cultures, including Myb2R3 and MADS (Fig. 3.10). As discussed in Chapter 2, photoreception in *Phytophthora* is still poorly understood, and we know that in fungi, transcription factors are important in photoreception. In this dataset, 4 transcription factors have slightly elevated expression in light, however, none of these genes have a consistent light-associated (sporulation-independent) gene expression pattern that would be expected for a photoreceptor, which would be low in constant dark, high early in constant light, and consistently higher in the light period that dark period in the 12-hour light dark cycle (Fig. 3.10).

When looking for light-associated or dark-associated gene expression across all genes, 176 genes were identified with a 2-fold change threshold from light to dark or dark to light in the 12-hour light/dark cyclic cultures (Fig. 3.11). Although it may appear that more than 176 genes were cyclic in the overall

heatmap (Fig. 3.9), most of the genes that appear cyclic change very little (approximately 10% change). The 2-fold change threshold used for identification of this gene set was arrived at using trial and error. When a low fold change threshold of 1.25-fold change,was applied (25% change), 2141 genes were cyclic, with 674 higher in light, and 1467 higher in dark. However, GO term analysis returned no statistically-significant results, indicating that this set of genes likely contains more noise than signal. When using a 1.8-fold change threshold, GO term analysis again returns no statistically-significant results, indicating that this set of genes likely contains more noise than signal. The genes that appear cyclic in the overall heat map may be an artifact due to lack of replication. However, biologically, gene expression changes of less than 2-fold change can be significant, and there are biologically relevant genes included in the lower fold-change threshold cyclic gene sets but excluded from the 2-fold change set (i.e. Myb2R3 and MADS). Moreover, depending on mRNA half-lives, changes in *de novo* transcription may be more dramatic than changes in mRNA abundance. Nevertheless perhaps since noise increases as the threshold lowers, a 2-fold change was the lowest fold-change threshold that resulted in enriched GO terms.

In this 2-fold change threshold set of 176 light- or dark-associated genes, 53 genes are light-associated (higher in light) and 123 are dark-associated (higher in dark). GO term analysis of the 53 light-associated genes showed enrichment of histone kinase activity, response to UV, glycine catabolic process,

chromatin-mediated maintenance of transcription, regulation of double-strand break repair, and condensed nuclear chromosome (Table 3.3). As many of these terms are light-related, these results were somewhat expected. GO term analysis of the 123 dark-associated genes showed enrichment of mainly general growth-related terms such as cell wall disassembly, cell wall organization or biogenesis, beta-glucan metabolic process, and glycosyl bonds cell wall macromolecule metabolism (Table 3.4). This result was less expected.

Because sporulation in *P. infestans* is higher in the dark, differential expression of sporulation genes and enrichment of sporulation-related GO terms was expected, but not found. Known sporulation-associated genes (cilia, mastigoneme, BBS, and IFT) were then analyzed for expression (Fig. 3.12). Many cilia genes have slightly elevated expression in the dark phase of the 12-hour cyclic light cultures, with an expression increase of approximately 50%; note that this is below the 2-fold threshold used in Fig. 3.11. None of the cilia genes show increased expression in constant dark compared to constant light (Fig. 3.12A). Several cilia genes have an increase in expression in the *in planta* cultures from 3.5 days after inoculation to 3 days, 20 hours, which is a dark period and early in sporulation (Fig. 3.12A). All 4 mastigoneme genes have the same expression pattern in *P. infestans* under constant light and constant dark conditions (Fig. 3.12B). The mastigoneme genes have approximately an increase in expression in the dark in the cyclic light/dark cultures, and have a strong increase in expression in the *in planta* cultures 3 days, 8 hours post inoculation to

4 days post inoculation, which spans both light and dark conditions, and is the same time as the earliest and strongest increase in sporulation (Fig. 3.12B). The BBS genes show a similar expression pattern as the mastigoneme genes in this dataset, but with a lower degree of gene expression increase (Fig. 3.12C). Five of the IFT genes have a similar expression pattern in all 4 conditions, and the other 8 IFT genes have a similar expression pattern to the BBS genes (Fig. 3.12D).

Several additional known sporulation genes were also examined for expression- Pks1, Myb2R1, Myb2R3, Myb2R4, Cdc14, and MADS (Fig. 3.13). Although qRT-PCR results had shown Pks1 to have a similar sporulation-related expression pattern to Myb2R1 and Myb2R3, these results show an opposite pattern (Xiang and Judelson, 2014). Myb2R1 expression increases 20% in the dark period of the 12-hour light/dark media cultures when sporulation is slightly increased, but expression is similar in the constant light and constant dark conditions, although sporulation is higher in the constant dark samples (Fig. 3.13). Myb2R1 also has slightly higher expression in the dark period of the *in planta* samples when sporulation is observed. Myb2R3 has 40% higher expression in the dark period of the cyclic media samples, when sporulation is increased, however, like Myb2R1, expression is similar in constant light and constant dark, regardless of sporulation levels. *In planta*, Myb2R3 has increased expression in the dark, when sporulation is higher, with a stronger increase in expression when sporulation is first observed around 3.5 days after inoculation

(Fig. 3.13). However, Pks1 expression in the 12h light/dark media samples is opposite to Myb2R1 and Myb2R3, with 30-60% higher expression in the light, when sporulation is lower. Pks1 expression *in planta* is higher in the later timepoints while sporulation is occurring, but does not show a distinct light-related expression pattern (Fig. 3.13). Myb2R4 expression is approximately 10% higher in the dark period of the cyclic 12h light/dark media samples, but has a strong increase *in planta* early in sporulation in the dark. Cdc14 does not show a light- or dark-related expression pattern, but increases over time in all conditions. MADS expression is 60-80% higher in the dark period of the 12h light/dark cycle in media, and also shows an increase in the dark period *in planta* (Fig. 3.13). Cryptochrome PITG_16100 expression was included as a control for light, as its expression is increased in light, which was confirmed by qPCR in chapter 2.

Discussion

Humidity-related sporulation

Based on the gene expression and sporulation patterns of *P. infestans* cultures grown under differential humidity, humidity likely regulates an early step in the sporulation cascade, before the formation of the sporangiophore. Mid- to early sporulation genes, such as the cilia, mastigoneme, and BBS genes that turn on at day 4 under high humidity do not turn on in the low humidity non-sporulating cultures (Fig. 3.5). This model is supported by the observation that cultures in the low humidity condition showed flat growth until exposure to high humidity. The repression of sporulation by humidity is likely an adaptation to the

fact that *Phytophthora* sporangia are sensitive to damage by drying, therefore, spore production timed for high humidity increases the likelihood of survival of the spore (Warren and Colhoun, 1975).

Effect of long-term illumination on sporulation

Although constant light represses sporulation as compared to constant dark in *P. infestans*, none of the mastigoneme, BBS, or IFT genes were differentially expressed in the non-sporulating or reduced-sporulation constant light condition as compared to the sporulating constant-dark-grown cultures. This was observed in two independent experiments with different lighting qualities and 5-fold different light intensities that were conducted several years apart, conducted by two independent researchers (Dr. Quijun Xiang and myself), (Fig. 3.6, 3.12). The results show that in the constant-light (long-term illumination) sporulation-repressed cultures, sporulation genes are turned on, although mature sporangia are not observed. It is likely that the repression signal from constant light is late in the sporulation cascade. Previous studies have reported that when light conditions repress sporulation in *P. infestans* and the downy mildew *Peronospora belbahrii*, the production of the sporangiophore is not affected (Cohen et al., 1975, 2013). This would be consistent with a repression signal late in the sporulation cascade.

Early sporulation genes, such as Cdc14 or MADS in *P. infestans*, are typically expressed before and during the sporangiophore initial stage, so a

repression of the genes post-production of the sporangiophore, would have these genes and some genes downstream of these early regulators already turned on (Ah Fong and Judelson, 2003; Leesutthiphonchai and Judelson, 2018). Both Cdc14 (PITG_18578) and MADS (PITG_07059) are turned fully on in the constant light cultures with little to no sporulation observed. Cdc14 in particular has higher expression in the non-sporulating constant light cultures as compared to the sporulating constant dark cultures (Fig. 3.13). I speculate that the light repression of sporulation that occurs post-production of the sporangiophore may be related to the pumping of the protoplasm from the sporangiophore shaft to the sporangiophore tip, or formation of the basal plug, as these processes occur after the sporangiophore is produced, and after the ballooning of the tip. The ballooning or expansion of the sporangiophore tip was shown to still occur in light-related sporulation-repressed *Peronospora belbahrii* downy mildew cultures (Cohen et al., 2013), though it is only speculation that the light repression would also be after the tip ballooning in *P. infestans* as well.

Effect of 12-hour cyclic light dark

Conclusions from the cyclic light-dark study should be drawn with caution, as this experiment was single replicate and statistical support is therefore lacking. This is particularly an issue in determining the significance of shifts in gene expression, such as the 20% increase in the expression of Myb2R1 (Fig.

3.13). Although this is a small change, and far below the typical 2-fold change threshold used in RNA-seq analysis,

Overall model

Based on the data in the two *P. infestans* RNA-seq datasets presented in this chapter, this expression pattern of MADS is consistent with my hypothesis that light regulates sporulation in *P. infestans* in two independent ways: an early, short exposure signal upstream of genes that are expressed pre-sporangiophore initial, and a later post-sporangiophore dark signal that is needed to break the repression of sporulation caused by constant light (Fig. 3.13).

The hypothesis that light regulates sporulation in two independent ways is also consistent with observations in *P. capsici*. In *P. capsici*, the long-term illumination sporulation-repression does not occur, as light stimulates sporulation in *P. capsici*. However, long-term darkness does repress sporulation in *P. capsici*, and a light signal can be used to break the constant-dark-related sporulation repression. The observation that, in contrast to *P. infestans*, sporulation genes are not fully turned on in the dark-related sporulation-repressed *P. capsici* cultures is consistent with the hypothesis that there is a short exposure to light, like a qualitative “switch” that will turn sporulation on. Likely this is the expression of a single gene, such as a transcription factor, that then turns on a set of genes. The gene expression patterns indicate that the dark-related sporulation-repression is likely not a repression, but a lack of

induction. I base this statement on the fact that in *P. infestans*, the sporulation cascade is turned on and many parts of the sporulation process occur, including the production of the sporangiophore. However, in *P. capsici*, early sporulation genes do not fully turn on then the process is stalled or inhibited in the non-sporulating cultures as they do in *P. infestans*. The *P. capsici* early sporulation genes turn on in response to light, and no do not turn on in the absence of light. The *P. capsici* data presented in this chapter is limited, but consistent with the hypothesis that there is a short burst of light signal that is a quantitative presence or absence “switch”, and a long-term sporulation repression that requires constant light, but is not seen in *P. capsici*.

References

Agrios, G., 2005. Plant Pathology, 5th ed. ed. Academic Press.

Ah Fong, A.M.V., Judelson, H.S., 2003. Cell cycle regulator Cdc14 is expressed during sporulation but not hyphal growth in the fungus-like oomycete *Phytophthora infestans*. Molecular Microbiolology 50, 487–494.

Blackman, L.M., Arikawa, M., Yamada, S., Suzaki, T., Hardham, A.R., 2011. Identification of a mastigoneme protein from *Phytophthora nicotianae*. Protist 162, 100–114.

Cohen, Y., Eyal, H., Sadon, T., 1975. Light-induced inhibition of sporangial formation of *Phytophthora infestans* on potato leaves. Canadian Journal of Botany 53, 2680–2686.

Cohen, Y., Vaknin, M., Ben-Naim, Y., Rubin, A.E., 2013. Light suppresses sporulation and epidemics of *Peronospora belbahrii*. PLoS ONE 8, e81282.

Crosier, W., 1934. Studies in the biology of *Phytophthora Infestans* (Mont.) de Bary. Cornell University.

Haas, B.J., Kamoun, S., Zody, M.C., Jiang, R.H.Y., Handsaker, R.E., Cano, L.M., Grabherr, M., Kodira, C.D., Raffaele, S., Torto-Alalibo, T., Bozkurt, T.O., Ah-Fong, A.M.V., Alvarado, L., Anderson, V.L., Armstrong, M.R., Avrova, A., Baxter, L., Beynon, J., Boevink, P.C., Bollmann, S.R., Bos, J.I.B., Bulone, V., Cai, G., Cakir, C., Carrington, J.C., Chawner, M., Conti, L., Costanzo, S., Ewan, R., Fahlgren, N., Fischbach, M.A., Fugelstad, J., Gilroy, E.M., Gnerre, S., Green, P.J., Grenville-Briggs, L.J., Griffith, J., Grünwald, N.J., Horn, K., Horner, N.R., Hu, C.-H., Huitema, E., Jeong, D.-H., Jones, A.M.E., Jones, J.D.G., Jones, R.W., Karlsson, E.K., Kunjeti, S.G., Lamour, K., Liu, Z., Ma, L., Maclean, D., Chibucos, M.C., McDonald, H., McWalters, J., Meijer, H.J.G., Morgan, W., Morris, P.F., Munro, C.A., O'Neill, K., Ospina-Giraldo, M., Pinzón, A., Pritchard, L., Ramsahoye, B., Ren, Q., Restrepo, S., Roy, S., Sadanandom, A., Savidor, A., Schornack, S., Schwartz, D.C., Schumann, U.D., Schwessinger, B., Seyer, L., Sharpe, T., Silvar, C., Song, J., Studholme, D.J., Sykes, S., Thines, M., van de Vondervoort, P.J.I., Phuntumart, V., Wawra, S., Weide, R., Win, J., Young, C., Zhou, S., Fry, W., Meyers, B.C., van West, P., Ristaino, J., Govers, F., Birch, P.R.J., Whisson, S.C., Judelson, H.S., Nusbaum, C., 2009. Genome sequence and analysis of the Irish potato famine pathogen *Phytophthora infestans*. Nature 461, 393–398.

Harrison, J.G., 1992. Effects of the aerial environment on late blight of potato foliage–a review. Plant Pathology 41, 384–416.

Horan, K., Jang, C., Bailey-Serres, J., Mittler, R., Shelton, C., Harper, J.F., Zhu, J.-K., Cushman, J.C., Gollery, M., Girke, T., 2008. Annotating genes of known and unknown function by large-scale coexpression analysis. Plant Physiology 147, 41–57.

Hurtado□Gonzales, O.P., Lamour, K.H., 2009. Evidence for inbreeding and apomixis in close crosses of *Phytophthora capsici*. Plant Pathology 58, 715–722.

Judelson, H.S., Narayan, R.D., Ah-Fong, A.M.V., Kim, K.S., 2009. Gene expression changes during asexual sporulation by the late blight agent *Phytophthora infestans* occur in discrete temporal stages. Molecular Genetics and Genomics 281, 193–206.

Judelson, H.S., Shrivastava, J., Manson, J., 2012. Decay of genes encoding the oomycete flagellar proteome in the downy mildew *Hyaloperonospora arabidopsidis*. PLoS ONE 7, e47624.

Judelson, H.S., Whittaker, S.L., 1995. Inactivation of transgenes in *Phytophthora infestans* is not associated with their deletion, methylation, or mutation. Current Genetics 28, 571–579.

Krause, R.A., Massie, L.B., Hyre, R.A., 1975. Blitecast: a computerized forecast of potato late blight. Plant Disease Reporter 59, 95–98.

Lamour, K.H., Mudge, J., Gobena, D., Hurtado-Gonzales, O.P., Schmutz, J., Kuo, A., Miller, N.A., Rice, B.J., Raffaele, S., Cano, L.M., Bharti, A.K., Donahoo, R.S., Finley, S., Huitema, E., Hulvey, J., Platt, D., Salamov, A., Savidor, A., Sharma, R., Stam, R., Storey, D., Thines, M., Win, J., Haas, B.J., Dinwiddie, D.L., Jenkins, J., Knight, J.R., Affourtit, J.P., Han, C.S., Chertkov, O., Lindquist, E.A., Detter, C., Grigoriev, I.V., Kamoun, S., Kingsmore, S.F., 2012. Genome sequencing and mapping reveal loss of heterozygosity as a mechanism for rapid adaptation in the vegetable pathogen *Phytophthora capsici*. MPMI 25, 1350–1360.

Langmead, B., Trapnell, C., Pop, M., Salzberg, S.L., 2009. Ultrafast and memory-efficient alignment of short DNA sequences to the human genome. Genome Biology 10, R25.

Leesutthiphonchai, W., Judelson, H.S., 2018. A MADS-box transcription factor regulates a central step in sporulation of the oomycete *Phytophthora infestans*. Molecular Microbiology 110, 562–575.

Lehsten, V., Wiik, L., Hannukkala, A., Andreasson, E., Chen, D., Ou, T., Liljeroth, E., Lankinen, Å., Grenville-Briggs, L., 2017. Earlier occurrence and increased explanatory power of climate for the first incidence of potato late blight caused by *Phytophthora infestans* in Fennoscandia. PLOS ONE 12, e0177580.

Love, M.I., Huber, W., Anders, S., 2014. Moderated estimation of fold change and dispersion for RNA-seq data with DESeq2. Genome Biology 15.

Minogue, K.P., Fry, W.E., 1981. Effect of temperature, relative humidity, and rehydration rate on germination of dried sporangia of *Phytophthora infestans*. Phytopathology 71, 1181–1184.

Mwimba, M., Karapetyan, S., Liu, L., Marqués, J., McGinnis, E.M., Buchler, N.E., Dong, X., 2018. Daily humidity oscillation regulates the circadian clock to influence plant physiology. Nature Communications 9, 1–10.

Nordskog, B., Gadoury, D.M., Seem, R.C., Hermansen, A., 2007. impact of diurnal periodicity, temperature, and light on sporulation of *Bremia lactucae*. Phytopathology 97, 979–986.

Raposo, R., 1993. Evaluation of potato late blight forecasts modified to include weather forecasts: a simulation analysis. Phytopathology 83, 103.

Robinson, M.D., McCarthy, D.J., Smyth, G.K., 2010. edgeR: a Bioconductor package for differential expression analysis of digital gene expression data. Bioinformatics 26, 139–140.

Seijo-Rodríguez, A., Escuredo, O., Rodríguez-Flores, M.S., Seijo, M.C., 2018. Improving the use of aerobiological and phenoclimatological data to forecast the risk of late blight in a potato crop. Aerobiologia 34, 315–324.

Small, I.M., Joseph, L., Fry, W.E., 2015. Evaluation of the BlightPro decision support system for management of potato late blight using computer simulation and field validation. Phytopathology 105, 1545–1554.

Utrata, A., 1980. Agrometeorological conditions determining the occurrence of potato blight (*Phytophthora infestans*) in Poland. EPPO Bulletin 10, 75–81.

Warren, R.C., Colhoun, J., 1975. Viability of sporangia of *Phytophthora infestans* in relation to drying. Transactions of the British Mycological Society 64, 73-IN5.

Xiang, Q., Judelson, H.S., 2014. Myb transcription factors and light regulate sporulation in the oomycete *Phytophthora infestans*. PLoS ONE 9, e92086.

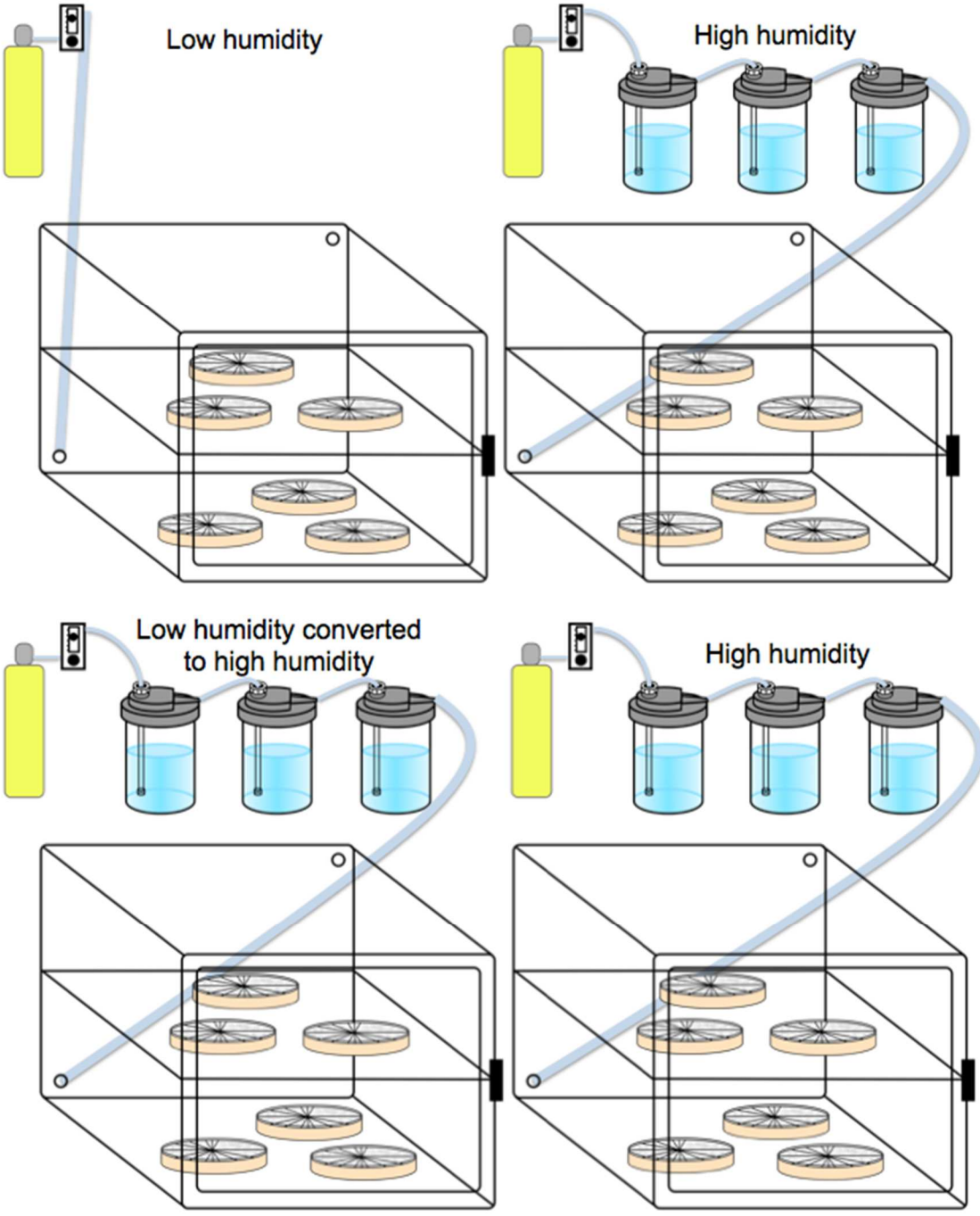

Figure 3.1. Schematic diagram of humidity control.

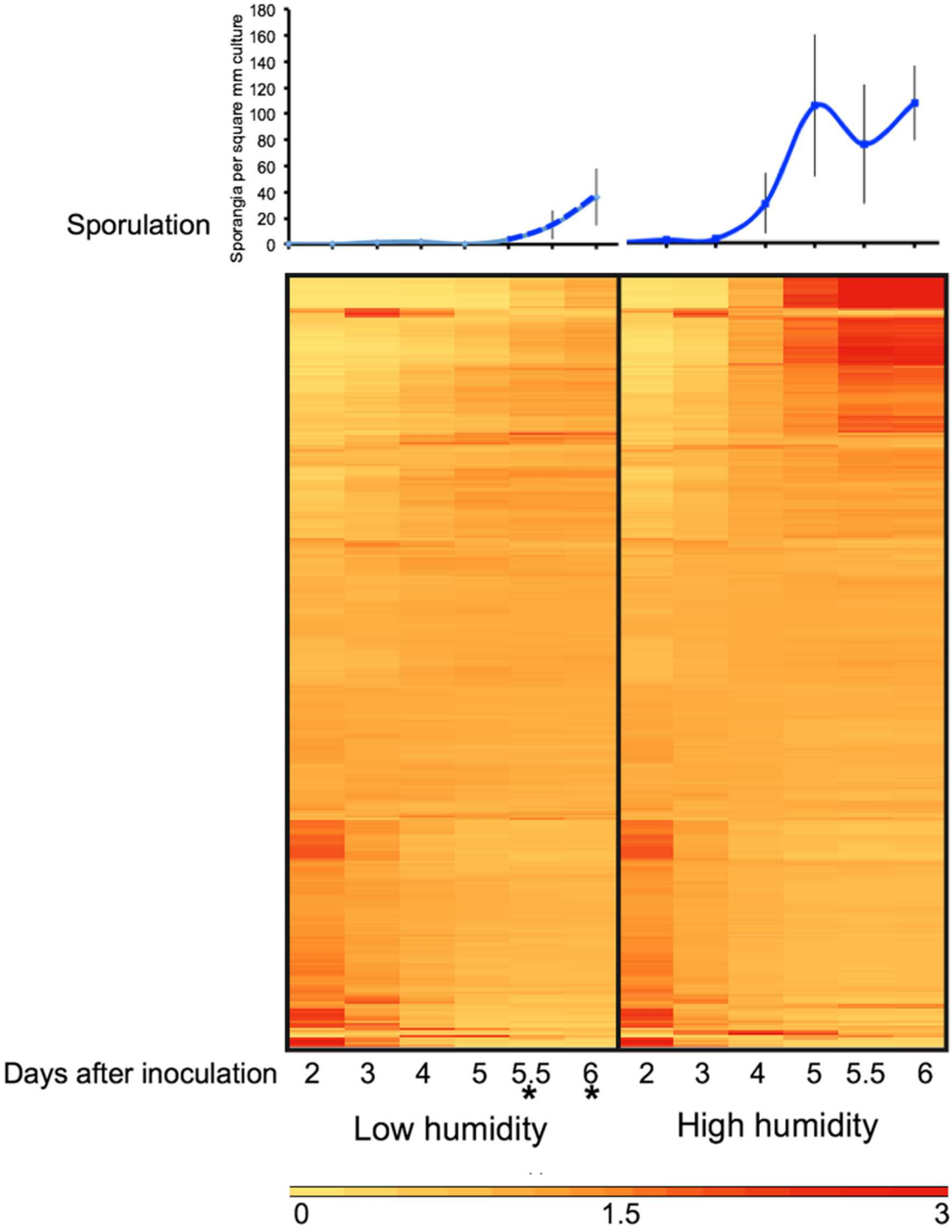

Figure 3.2. Expression of all *P. infestans* genes under high and low humidity conditions. Top panel represents sporulation of each sample. Asterisk represents low humidity cultures that were shifted to high humidity.

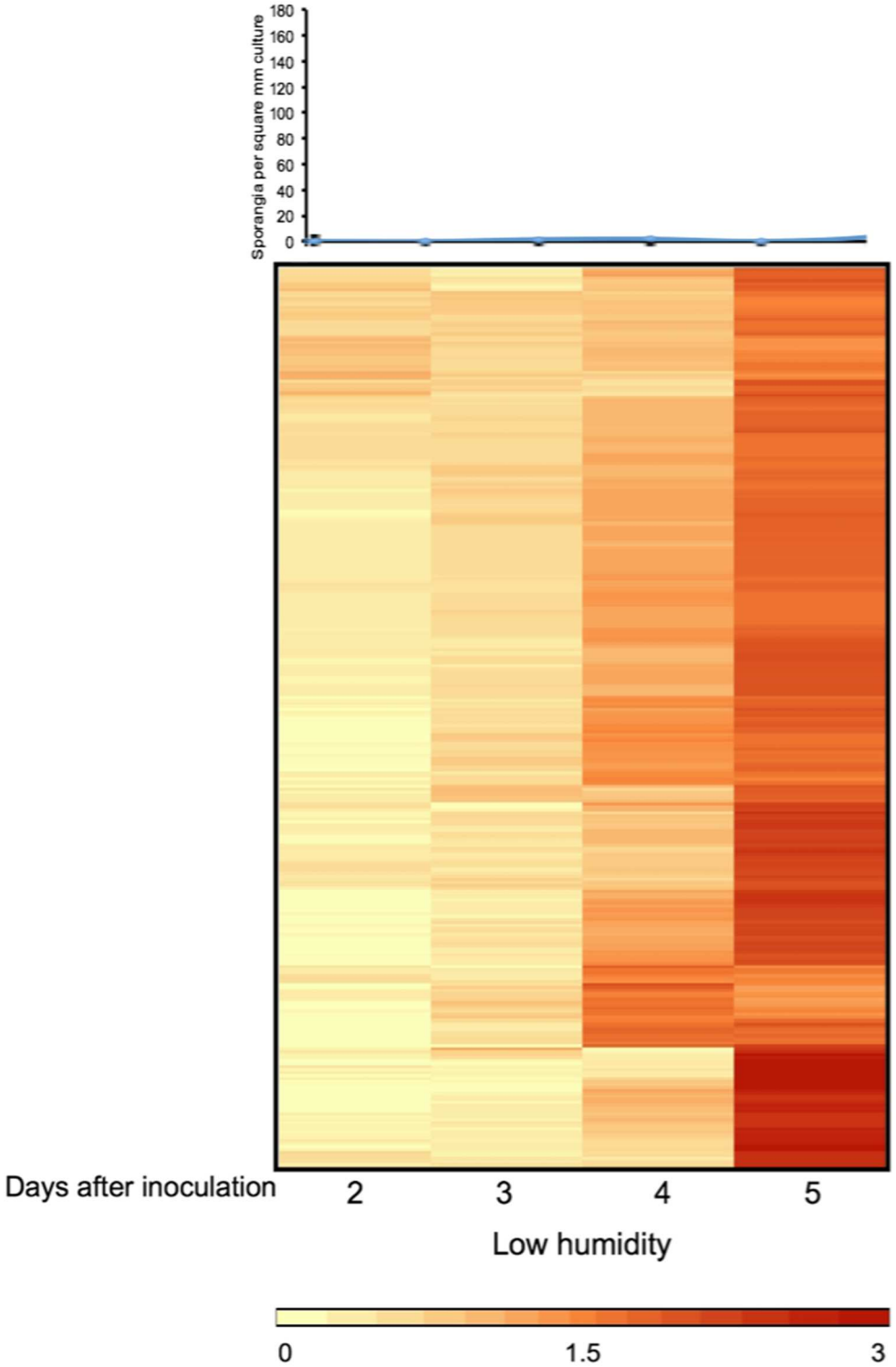

Figure 3.3. Expression of aging-related genes in *P. infestans* cultures under low humidity from days 2-5 after inoculation. Top panel represents sporulation.

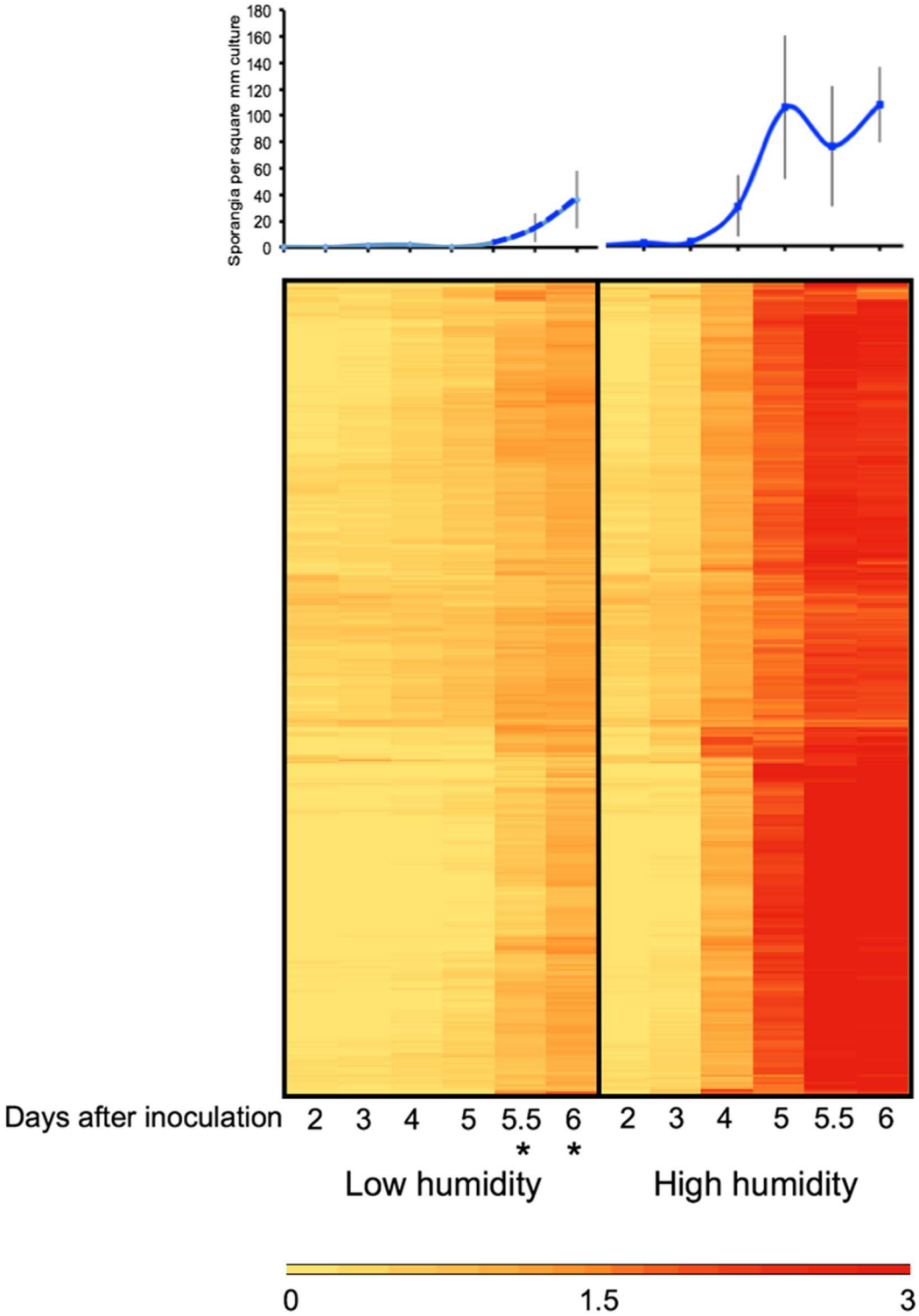

Figure 3.4. Expression of 1332 sporulation-associated genes in *P. infestans*. Top panel represents sporulation of each sample. Asterisk represents low humidity cultures that were exposed to high humidity.

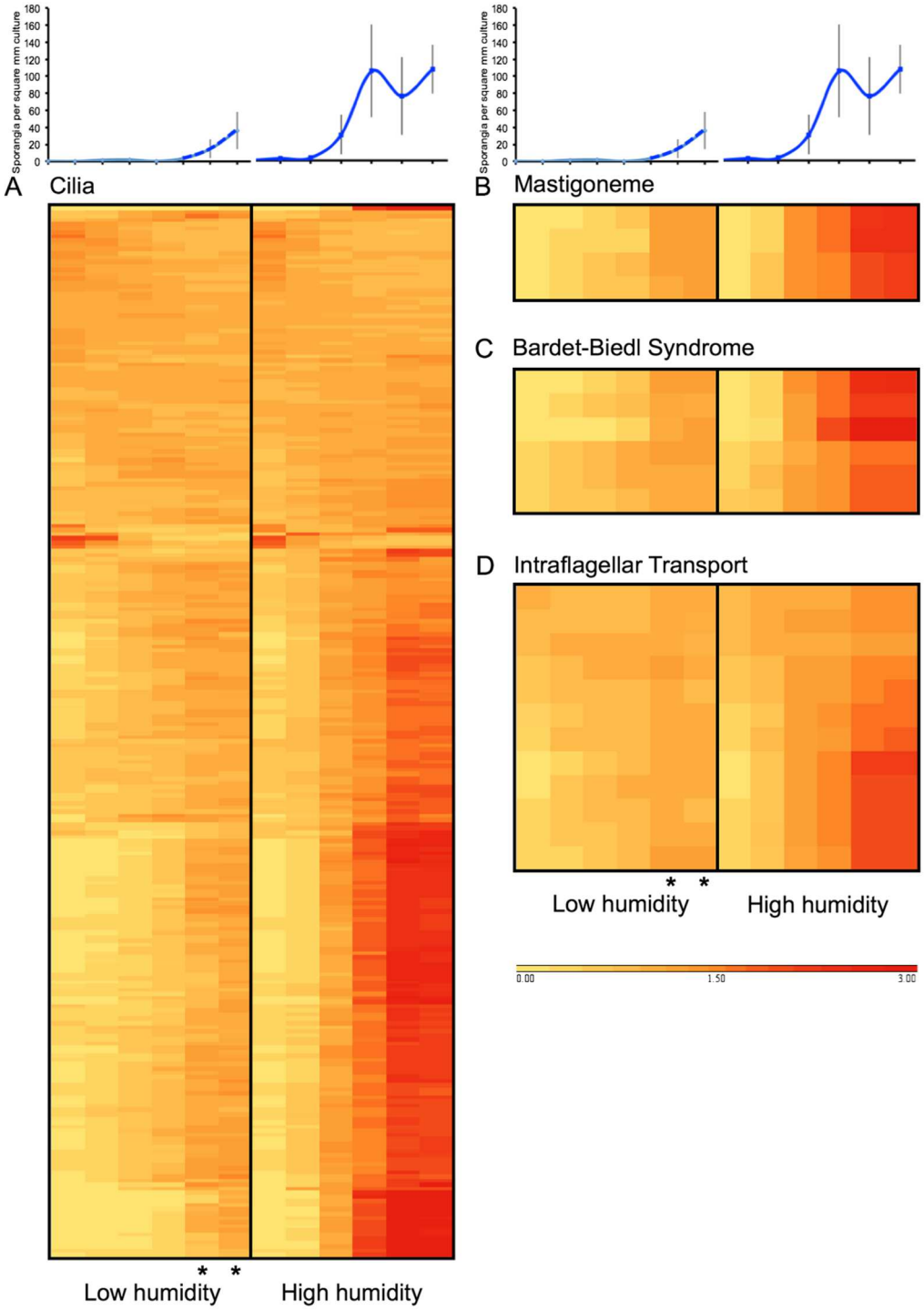

Figure 3.5. Expression of *P. infestans* genes in the categories A) cilia, B) masitgoneme, C) Bardet-Biedl Syndrome, and intraflagellar transport genes in *P. infestans* under high and low humidity from days 2-6 after inoculation. Top panel represents sporulation of each sample. Asterisk represents low humidity cultures that were shifted to high humidity.

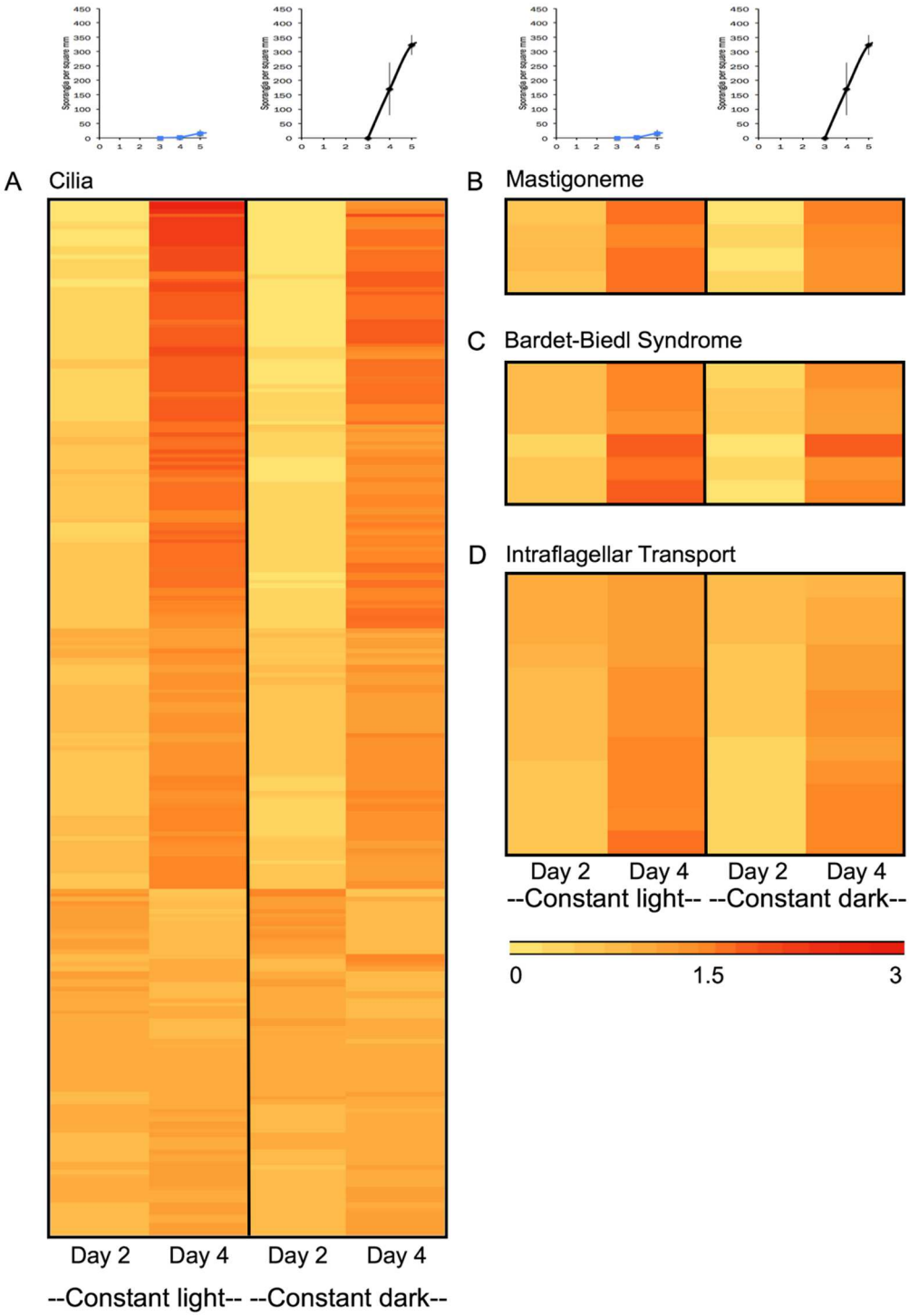

Figure 3.6. Expression of genes in categories A) cilia, B) mastigoneme, C) Bardet-Biedl Syndrome (BBS), and D) intraflagellar transport (IFT) in *P. infestans* under constant light or constant dark conditions. Top panel represents sporulation of each sample.

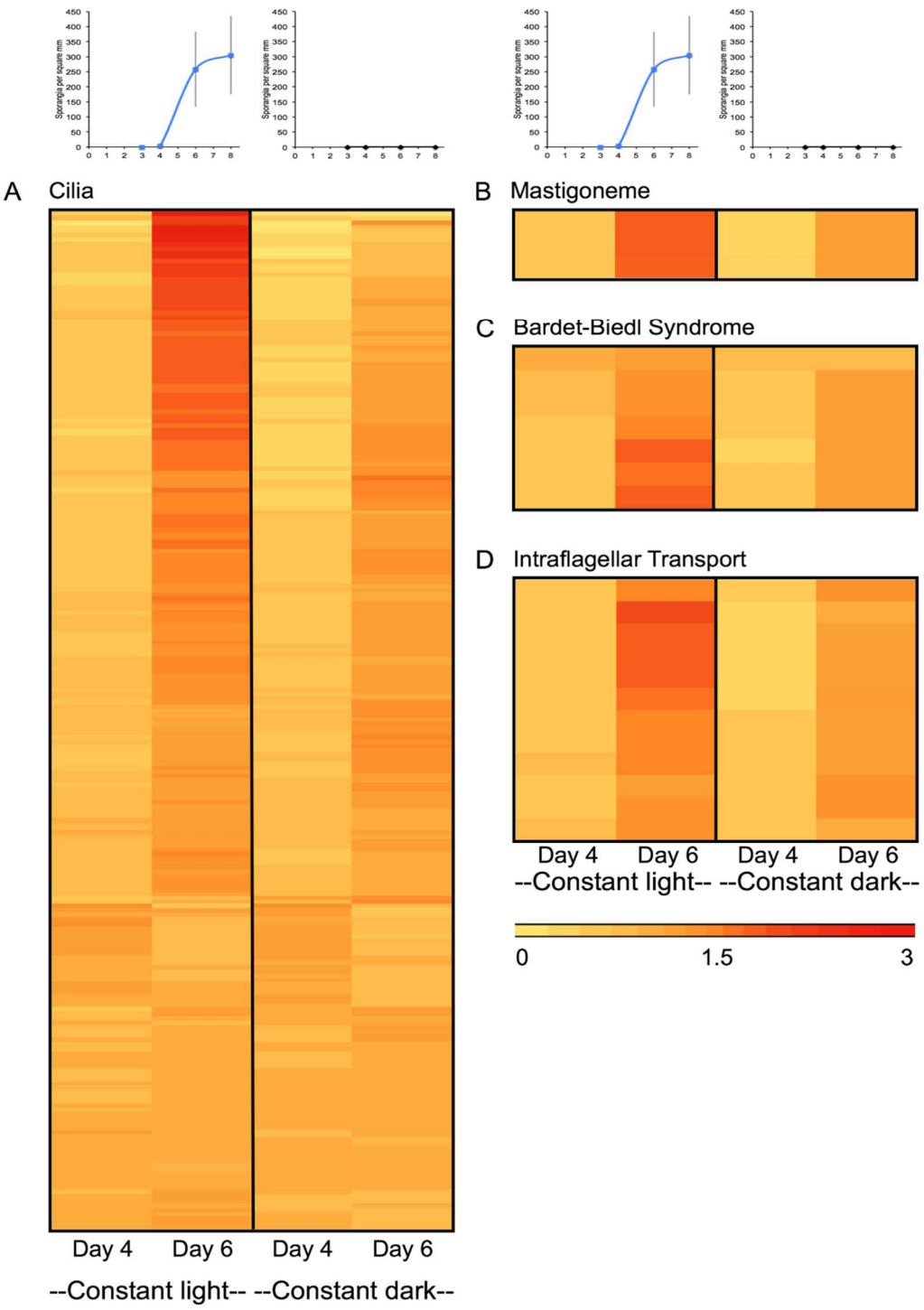

Figure 3.7. Expression of genes in categories A) cilia, B) mastigoneme, C) Bardet-Biedl Syndrome (BBS), and D) intraflagellar transport (IFT) in *P. capsici* under constant light or constant dark conditions. Top panel represents sporulation of each sample.

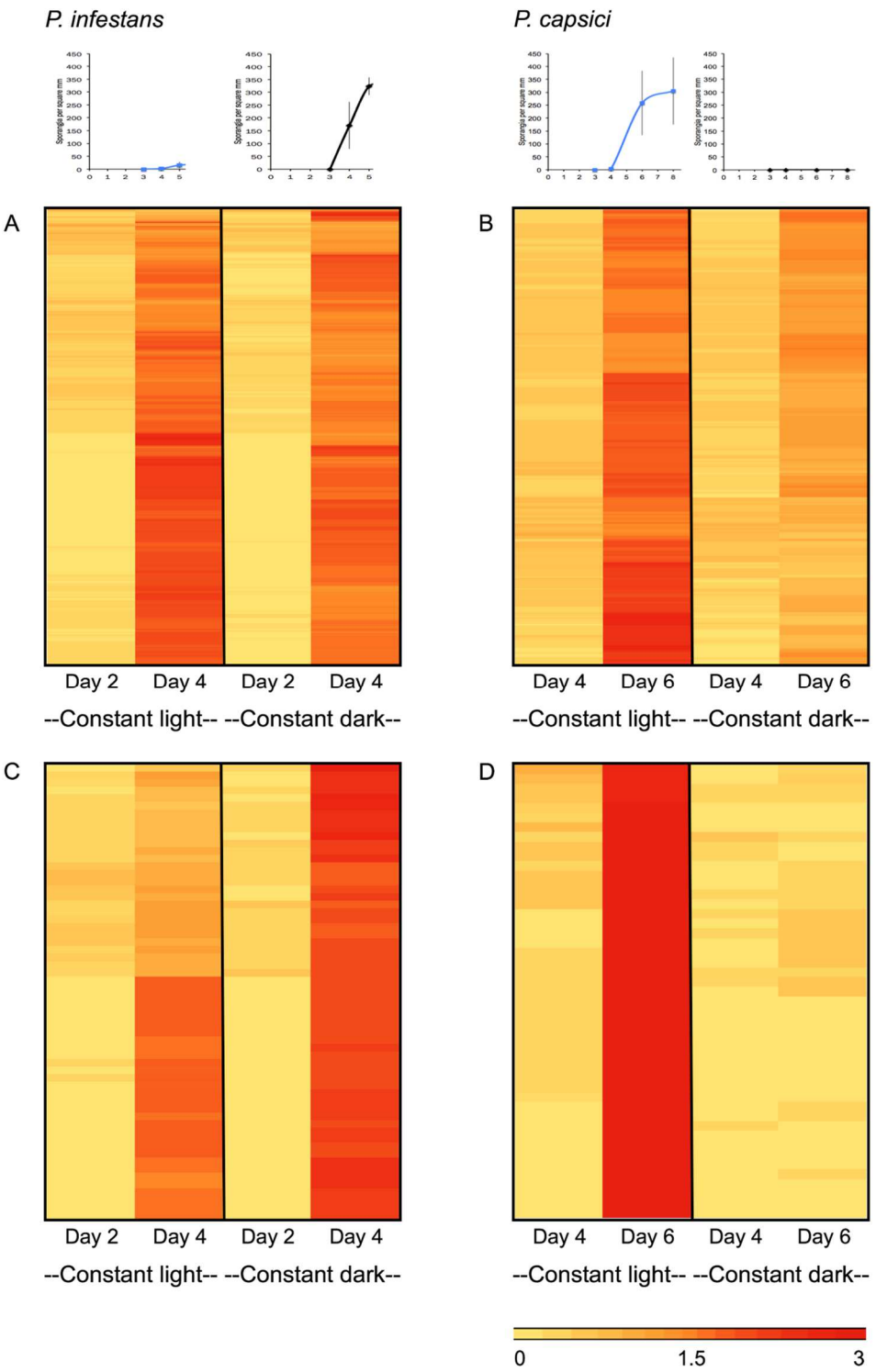

Figure 3.8. Expression of sporulation genes identified from the humidity RNA-seq in A) *P. infestans* and B) *P. capsici*, and a select set of these genes in A) *P. infestans* and B) *P. capsici* under constant light or constant dark conditions.

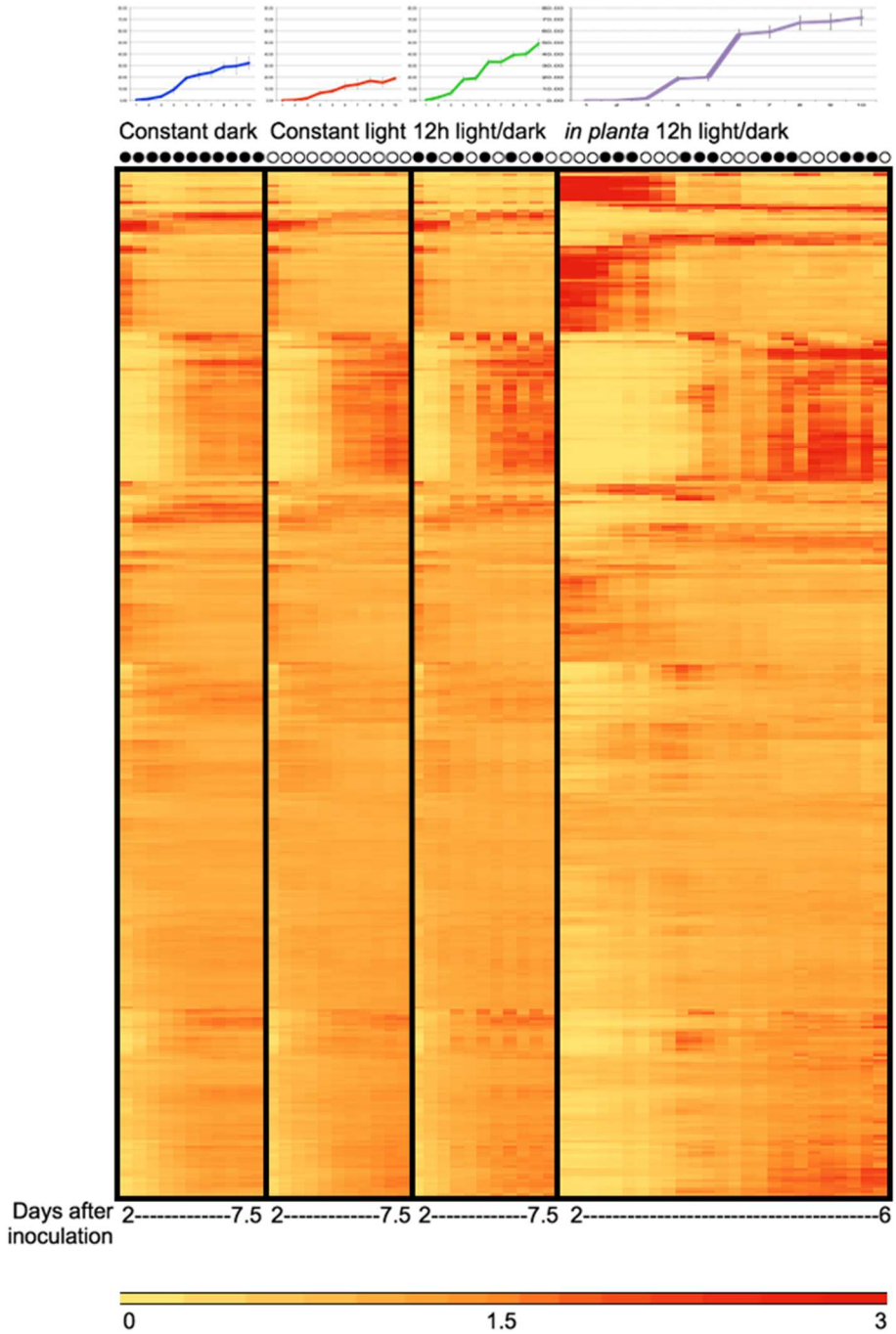

Figure 3.9. Expression of all genes in *P. infestans* under constant light, constant dark, or 12-hour light/dark conditions at high humidity. Black circles represent dark, open circles represent light condition. Top panel represents sporulation of each sample. Media-grown samples were taken at 2 days after inoculation, then day 3, and every 12 hours until day 7.5. *In planta* samples were taken every 4 hours from 2 days after inoculation to day 6.

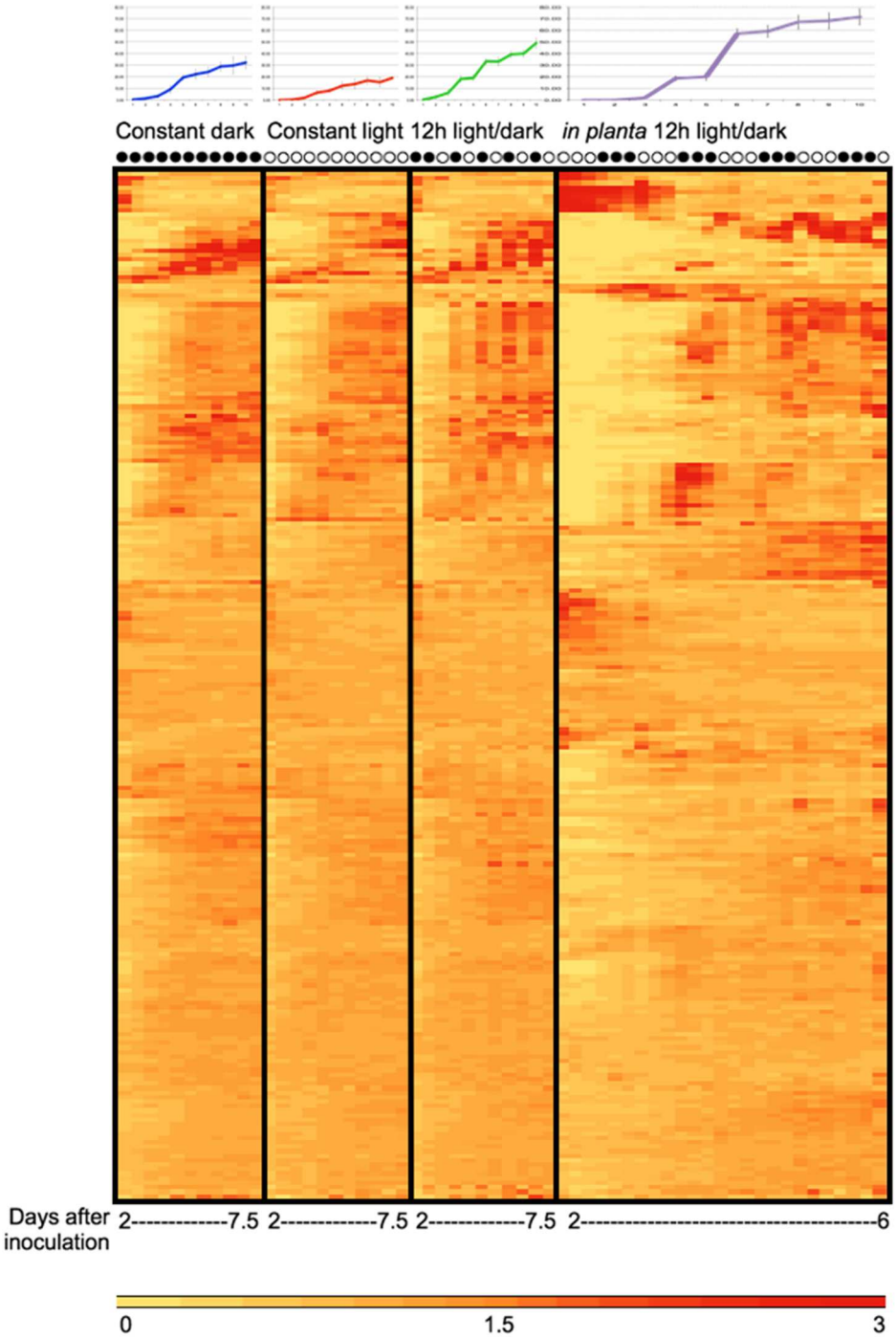

Figure 3.10. Light-related gene expression of transcription factors in *P. infestans*. Black circles represent dark, open circles represent light condition. Top panel represents sporulation of each sample. Media-grown samples were taken at 2 days after inoculation, then day 3, and every 12 hours until day 7.5. *In planta* samples were taken every 4 hours from 2 days after inoculation to day 6.

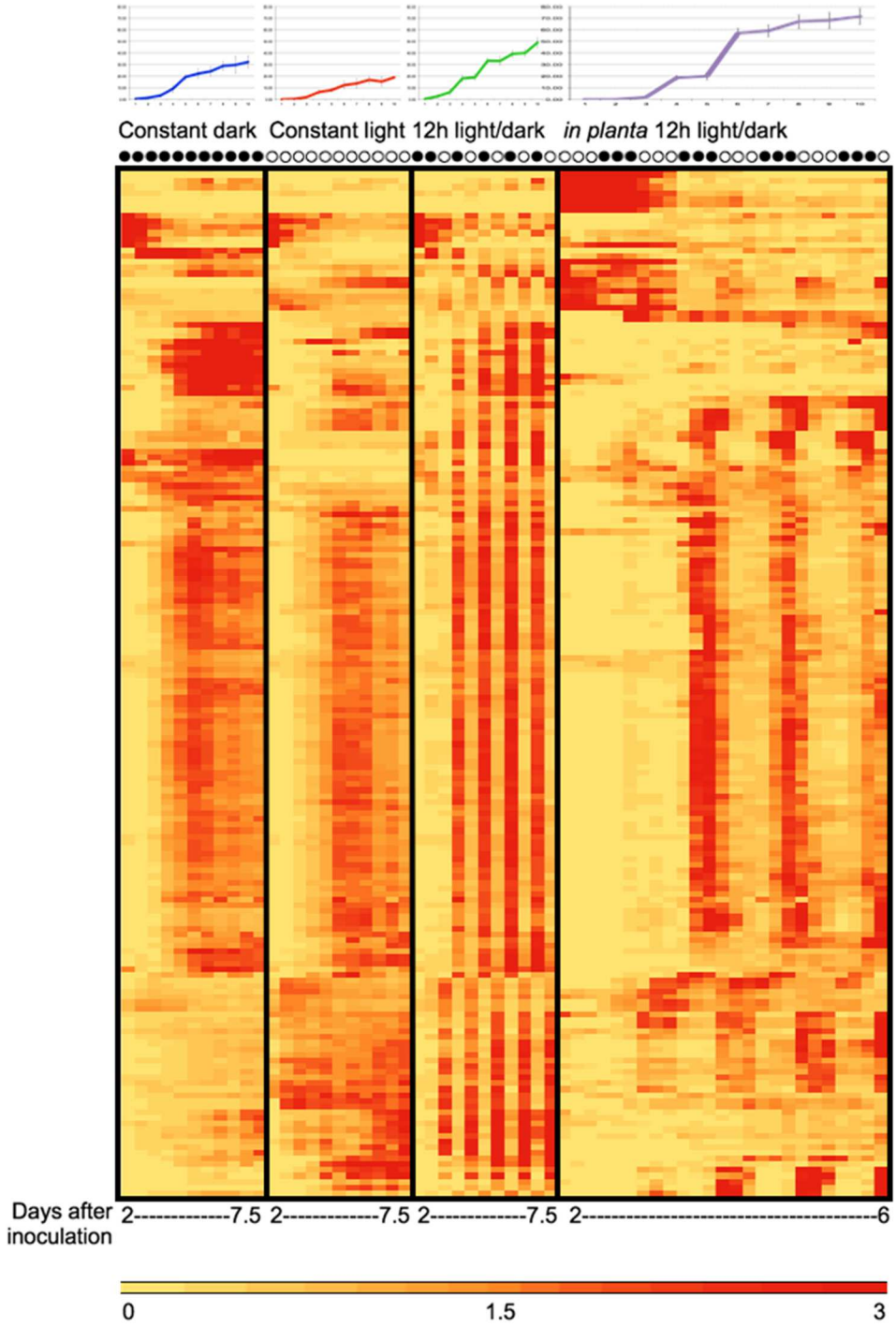

Figure 3.11. Cyclic light/dark-associated gene expression in *P. infestans*. Black circles represent dark, open circles represent light condition. Top panel represents sporulation of each sample. Media-grown samples were taken at 2 days after inoculation, then day 3, and every 12 hours until day 7.5. *In planta* samples were taken every 4 hours from 2 days after inoculation to day 6.

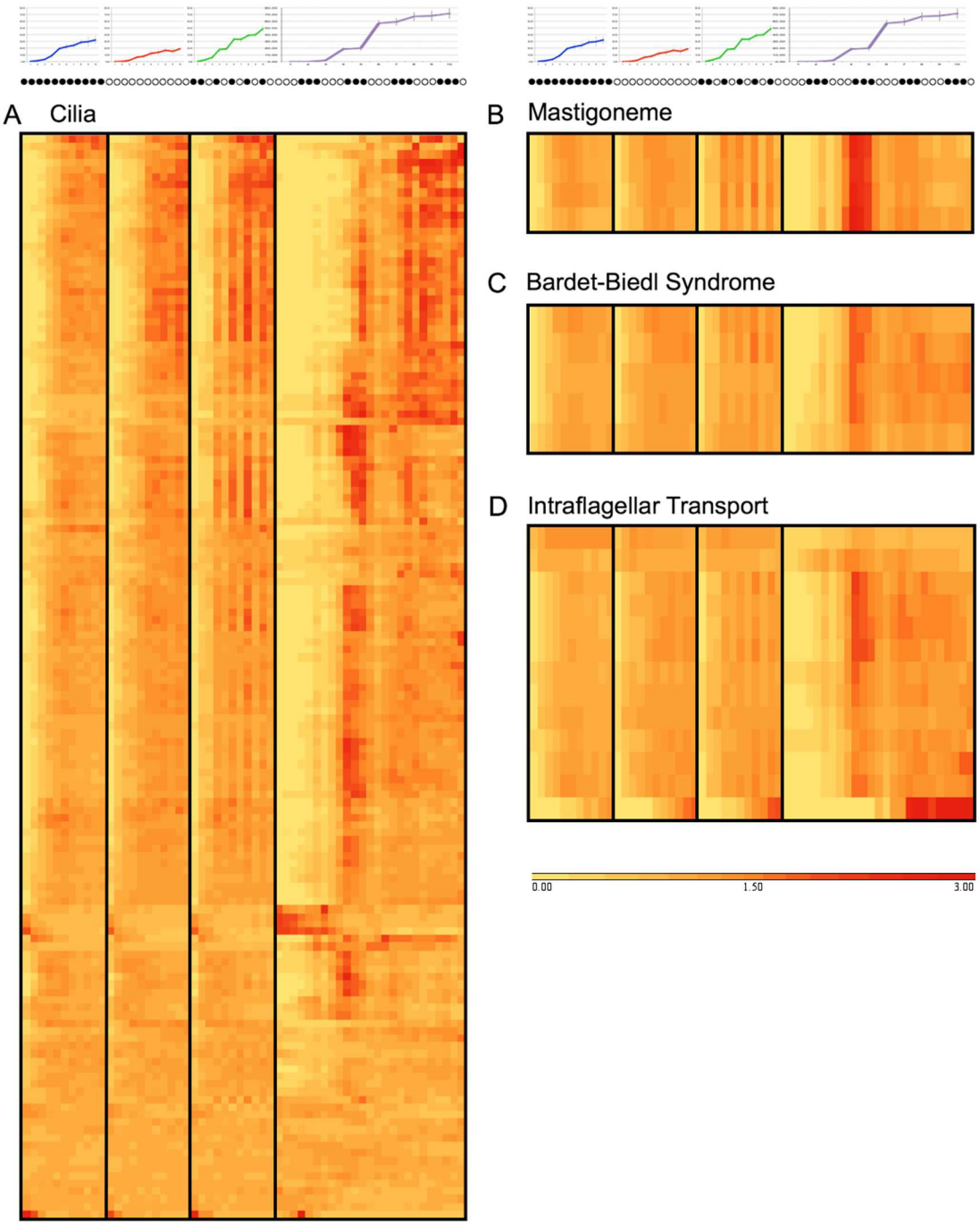

Figure 3.12. Expression of genes in categories A) cilia, B) mastigoneme, C) Bardet-Biedl Syndrome (bbs), and D) intraflagellar transport (IFT) under constant light, constant dark, 12-hour light/dark, and in planta on tomato leaves.

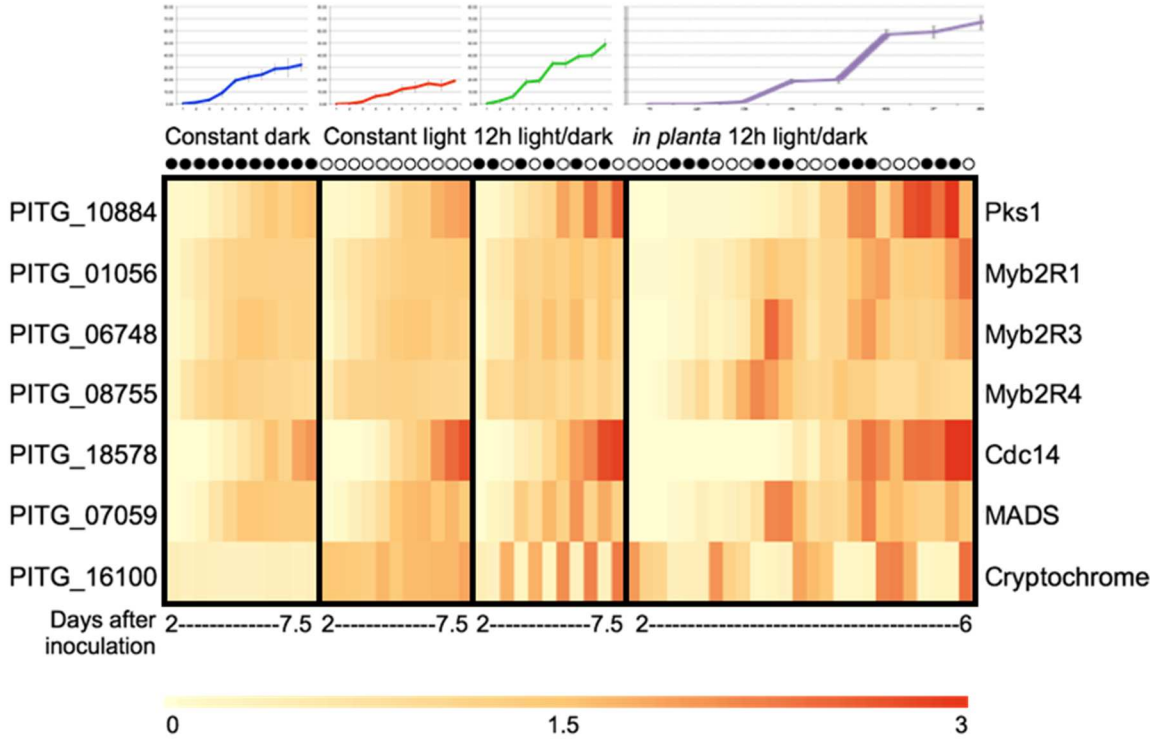

Figure 3.13. Expression of sporulation-related genes in *P. infestans*: Pks1, Myb2R1, Myb2R3, Myb2R4, Cdc14, and MADS, with PITG identification on the left side. Cryptochrome PITG_16100 has light-associated gene expression and was included as a control.

Table 3.1. GO terms of *P. infestans* aging-related genes under low humidity

GO ID	FDR	Term	Ontology
GO:0003774	2.39E-05	motor activity	Molecular function
GO:0004674	4.09E-05	protein serine/threonine kinase activity	Molecular function
GO:0003777	7.03E-04	microtubule motor activity	Molecular function
GO:0007154	1.68E-07	cell communication	Biological process
GO:0003008	7.50E-07	system process	Biological process
GO:0071804	6.57E-06	cellular potassium ion transport	Biological process
GO:0051273	8.17E-05	beta-glucan metabolic process	Biological process
GO:0006813	1.13E-04	potassium ion transport	Biological process
GO:0007165	2.04E-04	signal transduction	Biological process
GO:0032501	2.78E-04	multicellular organismal process	Biological process
GO:0006928	2.84E-04	movement of cell or subcellular component	Biological process
GO:0042391	8.71E-04	regulation of membrane potential	Biological process
GO:0042995	1.12E-15	cell projection	Cellular component
GO:0005929	4.17E-11	cilium	Cellular component
GO:0120038	4.46E-11	plasma membrane bounded cell projection	Cellular component
GO:0005856	1.85E-10	cytoskeleton	Cellular component
GO:0005886	1.41E-09	plasma membrane	Cellular component
GO:0071944	2.18E-08	cell periphery	Cellular component
GO:0009986	6.57E-08	cell surface	Cellular component
GO:0098590	1.09E-06	plasma membrane region	Cellular component
GO:0099080	1.43E-06	supramolecular complex	Cellular component
GO:0015630	2.61E-06	microtubule cytoskeleton	Cellular component
GO:0097458	2.78E-04	neuron part	Cellular component
GO:0005874	3.74E-04	microtubule	Cellular component

Table 3.2. Sporulation-related genes in *P. infestans* constant dark Day 4

Gene ID	Annotation
PITG_10438*	SCP-like extracellular protein
PITG_08442*	Conserved hypothetical protein
PITG_19644*	Carbohydrate-binding protein
PITG_22680*	Conserved hypothetical protein
PITG_12872	Sweet1 sugar transporter, Rag1-activating protein 1
PITG_19642	Endopolygalacturonase
PITG_15644	Acidic endochitinase
PITG_11849	Bifunctional arginine demethylase and lysyl-hydroxylase PSR
PITG_05386	Zinc transporter zupt
PITG_08148	Tyrosinase

*This gene also has FDR<0.05 and >2 fold-change CPM day 4 constant light vs. constant dark

Table 3.3. GO terms of *P. infestans* cyclic light-associated genes

GO ID	FDR	Term	Ontology
GO:0035173	3.09E-04	histone kinase activity	Molecular function
GO:0009411	4.26E-04	response to UV	Biological process
GO:0006546	6.54E-05	glycine catabolic process	Biological process
GO:0048096	1.30E-04	chromatin-mediated maintenance of transcription	Biological process
GO:2000779	9.76E-04	regulation of double-strand break repair	Biological process
GO:0000794	4.01E-03	condensed nuclear chromosome	Cellular component

Table 3.4. GO terms of *P. infestans* cyclic dark-associated genes

GO ID	FDR	Term	Ontology
GO:0004096	2.83E-05	catalase activity	Molecular function
GO:0008422	9.93E-05	beta-glucosidase activity	Molecular function
GO:0016798	2.56E-04	hydrolase activity, glycosyl bonds	Molecular function
GO:0044036	2.22E-08	cell wall macromolecule metabolism	Biological process
GO:0051273	2.87E-08	beta-glucan metabolic process	Biological process
GO:0005976	4.15E-06	polysaccharide metabolic process	Biological process
GO:0044262	1.72E-05	cellular carbohydrate metabolic process	Biological process
GO:0042743	2.05E-04	hydrogen peroxide metabolic process	Biological process
GO:0044277	2.55E-04	cell wall disassembly	Biological process
GO:0071554	3.13E-04	cell wall organization or biogenesis	Biological process
GO:0009986	9.84E-07	cell surface	Cellular component
GO:0009277	1.24E-05	fungal-type cell wall	Cellular component
GO:1990819	7.81E-05	actin fusion focus	Cellular component

Chapter 4: Effect of nutrition on sporulation timing in *Phytophthora infestans*

Introduction

Phytophthora species are non-photosynthetic heterotrophic hemibiotrophs that obtain requisite nutrition from a plant host. Because *Phytophthora* species cannot photosynthesize, when nutrition is exhausted in a host, the microorganism must find a new source of compounds to sustain its growth. For this reason, it has been the paradigm that starvation or a lack of certain nutrients induces sporulation in *Phytophthora*. However, experiments aimed at studying nutrient levels is challenging to conduct *in planta*, as samples would contain both plant and microbe metabolites. An equally worthy hypothesis is that an accumulation of a compound, such as a breakdown product, may be the signal for sporulation.

Hemibiotrophy

Growth by hemibiotrophic plant pathogens, such as *P. infestans*, involves an early biotrophic phase with minimal symptoms of plant damage, then a later phase of necrotrophic growth. During the biotrophic phase, *P. infestans* forms appressoria, primary and secondary hyphae, and specialized structures called haustoria through which proteins and small molecules are exchanged with the plant cells (Abu-Nada et al., 2007). The necrotrophic phase is characterized by further hyphal ramification in the plant tissue, water soaking of plant tissue as a consequence of cell wall degrading enzymes or plant processes, and finally

tissue necrosis (Grenville-Briggs et al., 2005). Sporulation occurs during the later necrotrophic phase. The goal of this study was to gain information about metabolic signals that lead to sporulation in this later phase. Because I am interested in the metabolic signals for *Phytophthora*, I conducted these controlled experiments on artificial media.

Starvation signals in sporulation

It has been shown that sporulation may be triggered in staling media, but the specific compounds that trigger sporulation have not been identified (Cope and Hardham, 1994; Judelson and Blanco, 2005). To help obtain information about metabolic signals during sporulation, I studied the fate of nutrients during growth in media and also which specific compounds would repress sporulation.

Materials and Methods

Strain

P. infestans strain 1306 was grown and maintained on rye-sucrose media at 18°C in the dark.

Metabolomics

Cultures were inoculated by aliquoting 200 µl of a fresh 2×10^5 sporangia/ml water suspension on 85-mm polycarbonate membranes (Sterlitech, Kent, WA) that were fit to the surface of clarified rye media (0.8% agar) in 100-mm plastic Petri dishes, and then gently spread with a glass rod. The spore

suspension was prepared by flooding two to four 5- to 10-day-old cultures with sterile water and gently rubbing the culture surface with a bent glass rod, counting the spores with a hemacytometer, and adjusting the concentration with water.

One experiment was conducted and split into two sets- 1) *P. infestans* hyphae early non-sporulating (day 2) versus sporulating (day 5); and 2) rye-sucrose media uninoculated, day 2 during non-sporulation, and day 5 during active sporulation. For *P. infestans* culture samples, tissue was separated from the polycarbonate membrane for harvest. For media samples, the solid media was pulled out of the petri dish, sliced, and frozen in a 50ml conical tube.

Four biological replicates were run per experiment per time point. Samples were harvested, flash frozen, and lyophilized. Heat maps were generated using Heatmapper (Babicki et al., 2016; heatmapper.ca). Metabolite analysis was conducted by Metabolon, Inc. Samples were processed using four ultra high-performance liquid chromatography/tandem accurate mass spectrometry (UHPLC/MS/MS) methods, and compounds were identified by comparison with a library of 15,000 metabolites using a proprietary analysis pipeline (Metabolon, Inc, Morrisville, NC).

Effect of starvation and supplementation on sporulation

Cultures were inoculated as above, 200 µl of a 2×10^5 sporangia/ml water suspension spread with a glass rod, except that 1.5% agar was used. Cultures

were incubated in the dark in a Percival I-36LLVL environmental control chamber at 18°C in polystyrene crisper boxes. Cultures were grown to sporulation-competence (typically 2-days and 2.5-days after inoculation), and then the polycarbonate membrane was lifted from the agar surface and moved to a new plate. As a control, the membrane was lifted and set back down on the same media; this is described as "not moved," as it was not moved to a new media plate. Membranes were also moved to “fresh rye” (a previously uninoculated plate of rye media), or to “water agar” (water and 1.5% agar only), or to water agar supplemented with 1% casamino acids, 2% sucrose and glucose, 1 mM ammonium sulfate, or individual amino acids at 10 mM, pH 7. Individual amino acids were each made into solution in water, adjusted to pH 7 and filter-sterilized before being added to the water agar to a final concentration of 10 mM. After membranes were moved, ¼ of the culture was excised and checked for sporulation every 4 hours.

Results

Metabolomics

In total, 504 metabolites were identified in either the *P. infestans* hyphae or media. Of these metabolites, 481 were detected in hyphae and 391 were detected in the clarified rye media (Fig. 4.1). The 504 metabolites can be classified into 9 general categories: amino acid metabolism, carbohydrates, lipids, co-factors, nucleotide, peptide, hormone, secondary metabolites, and xenobiotics (Fig. 4.2, Fig 4.3).

Approximately 40% of the lipids present in *Phytophthora* were not present in uninoculated media, and 40% of the cofactors that were present in *Phytophthora* were not present in media (Fig 4.3). The lipids that are not present in media include free fatty acids, glycerolipids, and phospholipids. The lack of lipids in media is not surprising, as lipids are structural and too large to be secreted. The co-factors of cryptochrome/photolyase family proteins (FAD, pterin, FMN) were not found in media, and have the same 65% reduction pattern in the non-sporulating to sporulating *Phytophthora* cultures.

Within the serine family of amino acids, taurocyamine and intermediates in taurocyamine biosynthesis appeared to accumulate during sporulation based on the levels of intermediates and RNA-seq expression of enzymes (Fig. 4.4).

When looking at the 20 amino acids used to make proteins, most are depleted in the media by day 5, with the exception of cysteine and glutamine (Fig. 4.5).

Effect of starvation and individual amino acids on sporulation

When *P. infestans* cultures were grown to sporulation competence on rye-sucrose media, then exposed to different conditions to assess the induction of sporulation, several things were observed. First, it should be explained that sporulation competence means that the culture has the ability to begin sporulation, under suitable conditions. The culture age at which sporulation competence is reached was determined experimentally by me for this experiment

and for the humidity experiment described in Chapter 3. Preliminary results showed that the amount of time to sporulation competence can be influenced by the amount of initial sporangia inoculated (which influences hyphal density), and the environmental conditions during incubation, which influences sporangia germination and hyphal growth rate. Several initial inoculum amounts were tested, and 200 µl of 2×10^5 worked consistently well. Incubation for 2 days after inoculation or 2.5 days after inoculation both worked well, though in trial, 2.5 days was too long. Additionally, 3 days after inoculation was tested many times and found to be borderline- sometimes cultures exhibited sporulation like the 2-day incubated cultures, and other times sporulation signals had already begun, and sporulation would occur regardless of treatment. This is consistent with the RNA-seq results from the humidity experiment in Chapter 3 that showed that several sporulation-related cilia genes increase in expression at day 3 under high humidity (Fig. 3.5A). In summary, sporulation competence means that the hyphae have the ability to start initiate the sporulation program, but have not started to do so yet.

When *P. infestans* cultures were grown to sporulation competence and then moved to water agar, fresh rye, or not moved, the move to water agar induced sporulation (Fig 4.6A). Previous studies have shown that *P. infestans* takes approximately 12-18 hours to develop from vegetative hyphae to mature sporangia (Maltese et al. 1995). Once cultures were moved to water agar, mature sporangia were observed in 12-18 hours. This indicates that the

starvation signal likely induces sporulation. The fresh rye and not moved cultures eventually sporulated after several days, but were not induced, or stimulated, to sporulate, as was seen with the move to water agar. To test which type of starvation may be the trigger for sporulation, I performed a similar experiment in which the sporulation competent cultures were transferred to water agar supplemented with sucrose and glucose, ammonium sulfate, casamino acids, or only glutamine. Cultures that were moved to water agar supplemented with a mixture of sucrose and glucose, or glutamine, sporulated with kinetics similar to that observed for cultures moved to plain water agar (Fig. 4.6B). This indicates that these compounds do not suppress the starvation signal that induces sporulation. Because providing sugars did not suppress sporulation, I hypothesized that nitrogen starvation is likely the trigger for sporulation. Since providing a mixture of amino acids (casamino acids) suppressed the induction while glutamine alone did not, I then tested each amino acid individually.

When each amino acid was tested individually, the results fell into five categories- strongest effect, strong effect, intermediate effect, weak effect, and no effect (Fig. 4.6C). Asparagine had the strongest effect on delaying sporulation; isoleucine, leucine, methionine, and valine had a strong effect; alanine, histidine, and serine had an intermediate effect; arginine, aspartic acid, and glycine had a weak effect; and glutamine, glutamate, proline, phenylalanine, threonine, tryptophan, and tyrosine had no effect (Fig. 4.6C).

Discussion

Metabolomics showed that many changes occur in *P. infestans* hyphae during sporulation, however, correlating the metabolomics data to sporulation was challenging. For taurocyamine biosynthesis, we also used the RNA-seq data and other data from the lab to form the hypothesis that taurocyamine accumulates in the sporangium as an energy store for zoospore motility (Kagda et al., 2018).

From the nutrition experiment, it is clear that starvation induces sporulation. It is possible that accumulation of a breakdown product could also induce sporulation, but no experimental evidence to support that hypothesis is presented here. Because sugars do not suppress the starvation response, availability of nitrogen is more likely the signal than availability of carbon. The addition of ammonium sulfate to the media was toxic to the culture, and therefore did not yield any information. The results of the individual amino acids was surprising, in that the categories do not correlate to previously published results about the utilization of amino acids by *Phytophthora,* or specific shared properties of the groups of amino acids that gave similar phenotypes. More experiments need to be conducted, but the current data indicate that a nitrogen starvation signal triggers sporulation, with differences in the effect of presence of individual amino acids that has yet to be understood.

References

Abu-Nada, Y., Kushalappa, A.C., Marshall, W.D., Al-Mughrabi, K., Murphy, A., 2007. Temporal dynamics of pathogenesis-related metabolites and their plausible pathways of induction in potato leaves following inoculation with *Phytophthora infestans*. European Journal of Plant Pathology 118, 375–391.

Babicki, S., Arndt, D., Marcu, A., Liang, Y., Grant, J.R., Maciejewski, A., Wishart, D.S., 2016. Heatmapper: web-enabled heat mapping for all. Nucleic Acids Research 44, W147–W153.

Cope, M., Hardham, A.R., 1994. Synthesis and assembly of flagellar surface antigens during zoosporogenesis in *Phytophthora cinnamomi*. Protoplasma 180, 158–168.

Grenville-Briggs, L.J., Avrova, A.O., Bruce, C.R., Williams, A., Whisson, S.C., Birch, P.R.J., van West, P., 2005. Elevated amino acid biosynthesis in *Phytophthora infestans* during appressorium formation and potato infection. Fungal Genetics Biology 42, 244–256.

Judelson, H.S., Blanco, F.A., 2005. The spores of Phytophthora: weapons of the plant destroyer. Nature Reviews Microbiology 3, 47–58.

Kagda, M., Vu, A.L., Ah-Fong, A.M.V., Judelson, H.S., 2018. Phosphagen kinase function in flagellated spores of the oomycete *Phytophthora infestans* integrates transcriptional regulation, metabolic dynamics, and protein retargeting. Molecular Microbiology 110, 296–308.

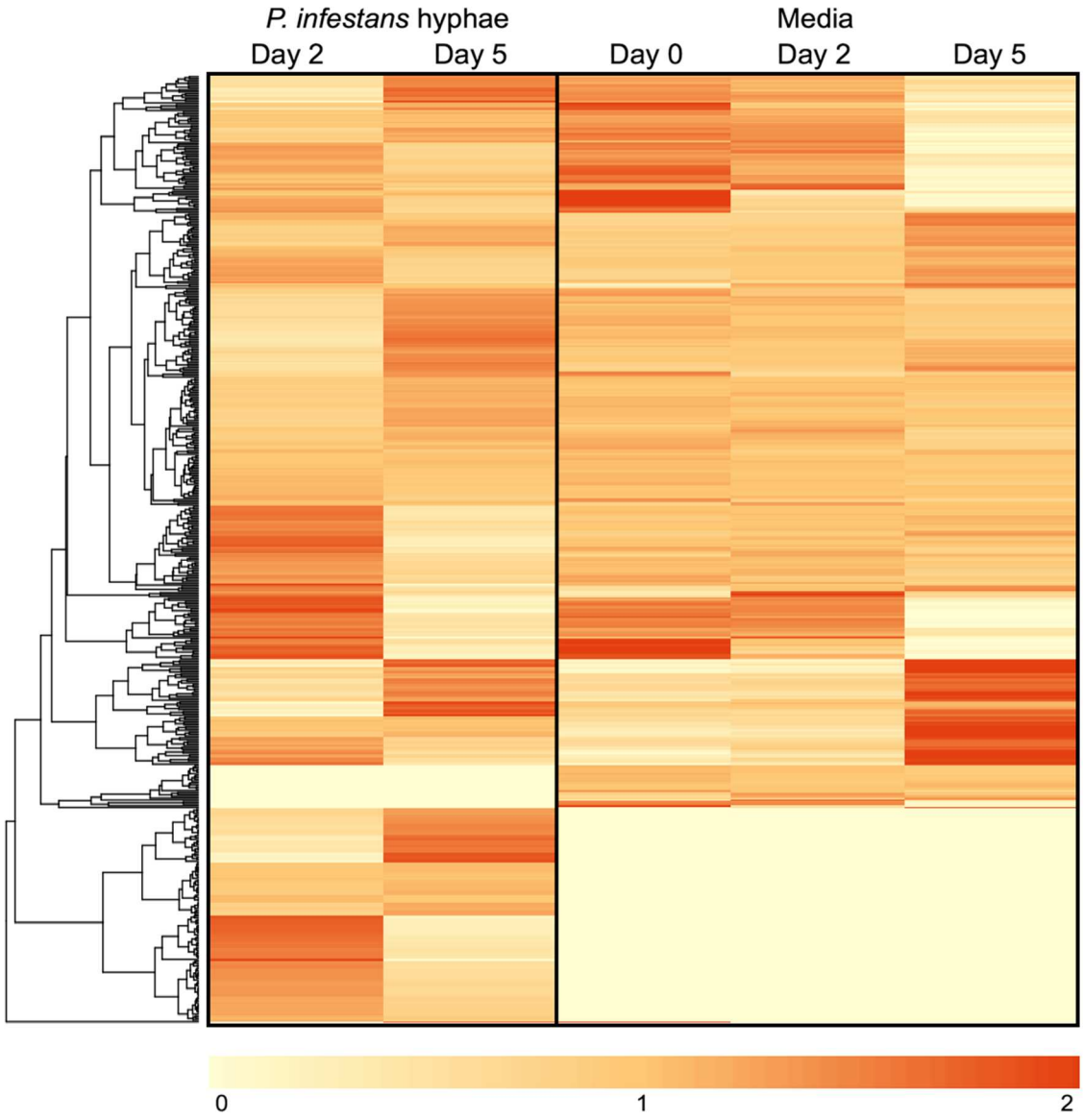

Figure 4.1. Overall results of the 504 metabolites detected in *P. infestans* hyphae or media, by category of compound. Clustering was conducting using average linkage.

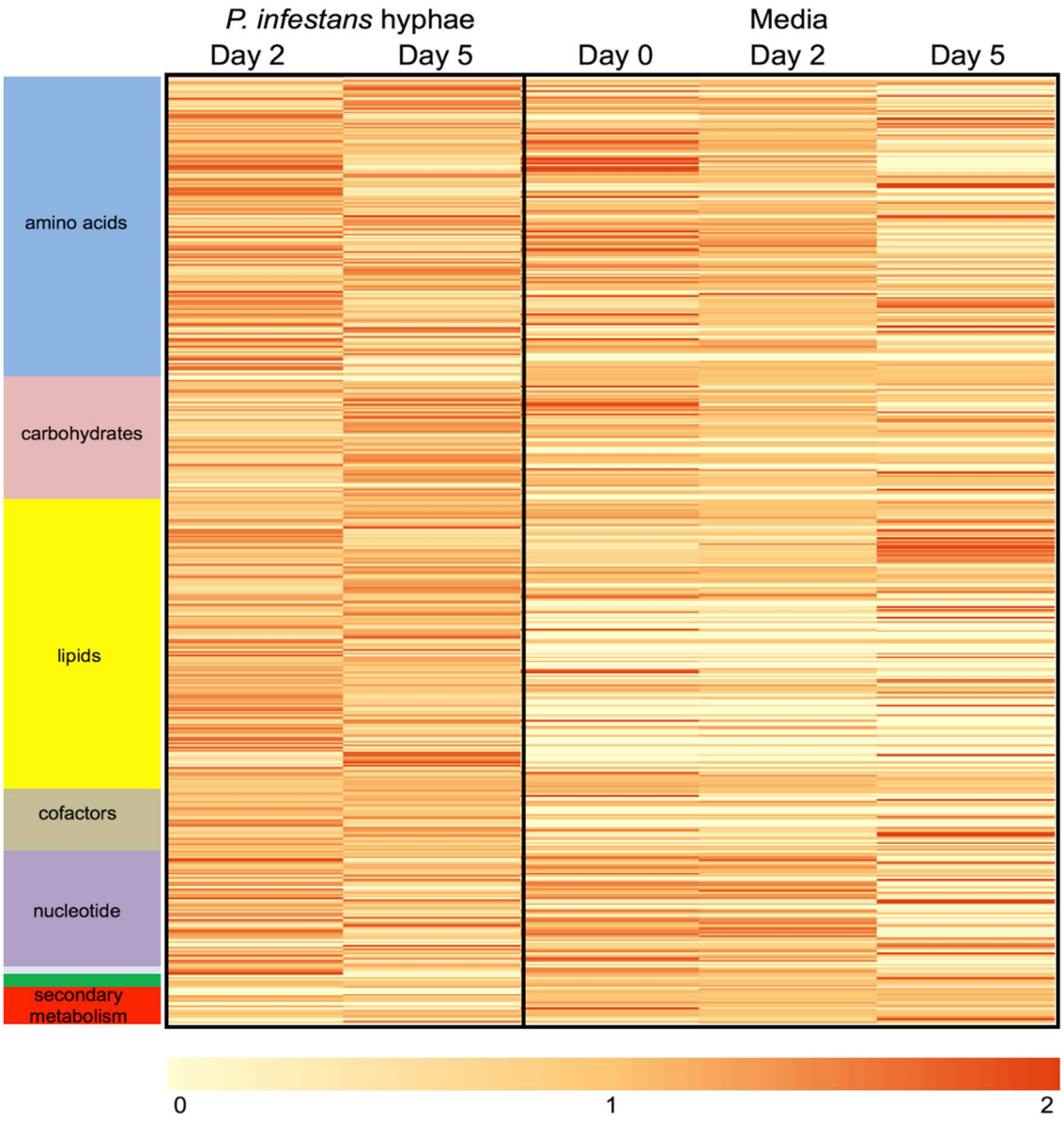

Figure 4.2. Overall results of the 504 metabolites detected in *P. infestans* hyphae or media, by category of compound.

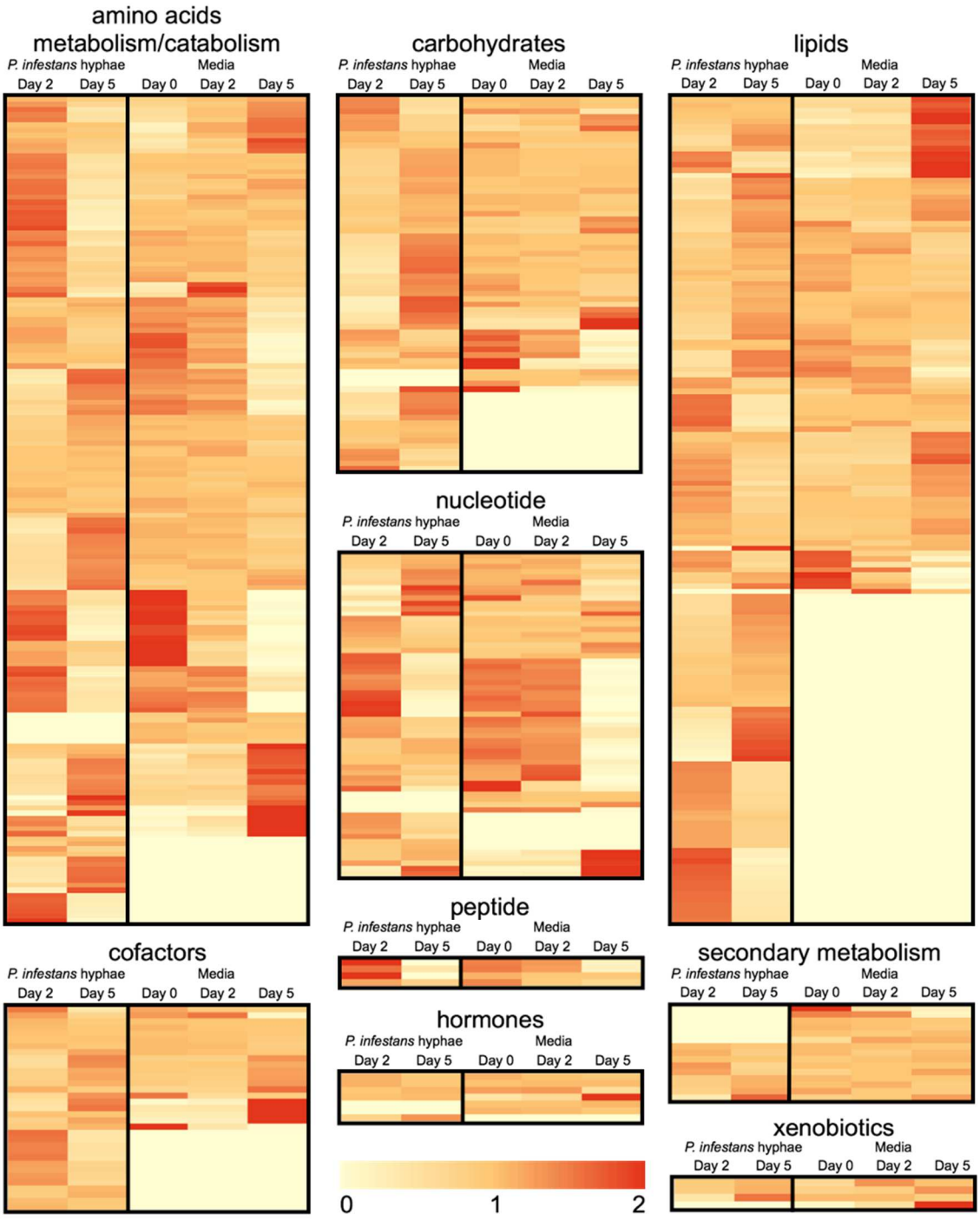

Figure 4.3. Overall results of the 504 metabolites detected in the *P. infestans* hyphae or media by individual category of compound.

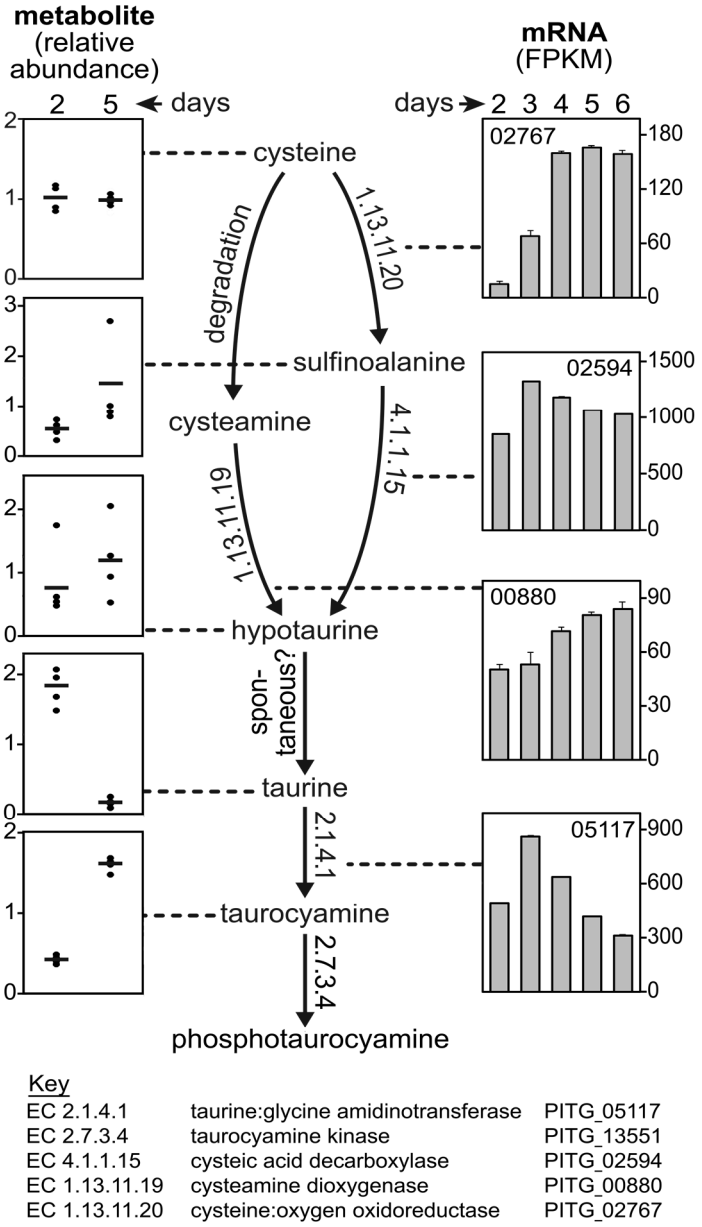

Figure 4.4. Predicted taurocyamine biosynthesis pathway in *P. infestans*. The branched metabolic pathway is shown in the center, with enzymatic steps labeled with Enzyme Commission (EC) numbers. The graphs in the metabolite column indicate relative levels of each compound in 2 day (pre-sporulation) and 5 day (sporulating) cultures, set to mean equals 1.0; horizontal lines represent means of four biological replicates. The graphs in the column labeled 'mRNA FPKM' denote expression of the indicated genes (trimmed of their PITG prefix, e.g. 02767) in cultures from two to six days post-inoculation. A key showing the EC number, enzyme name and *P. infestans* gene name is at the bottom.

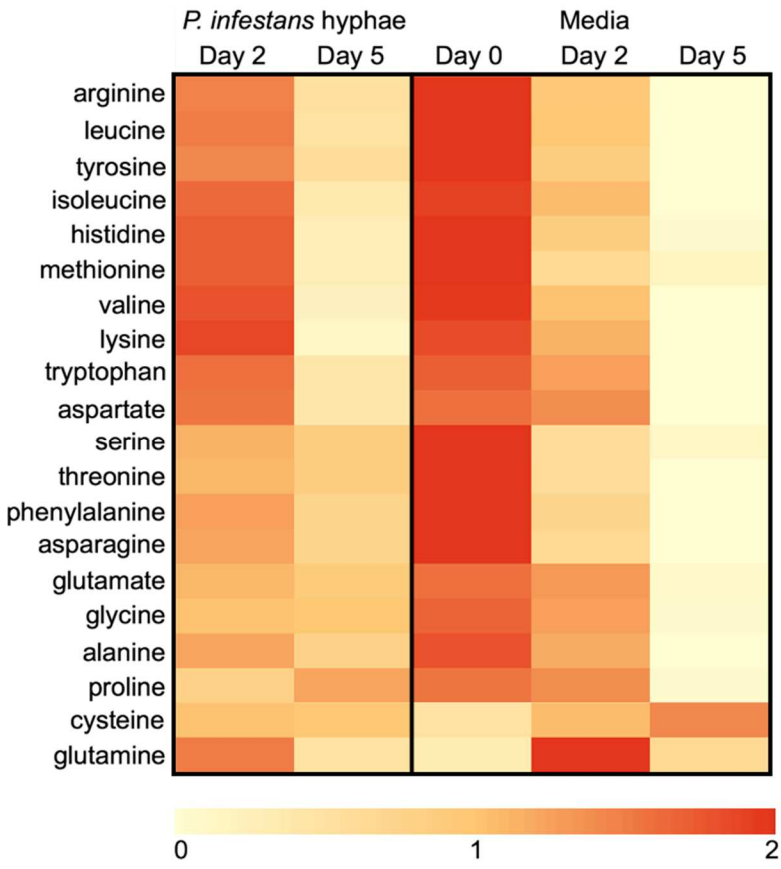

Figure 4.5. Levels of individual amino acids in *P. infestans* hyphae and media before and during sporulation.

A

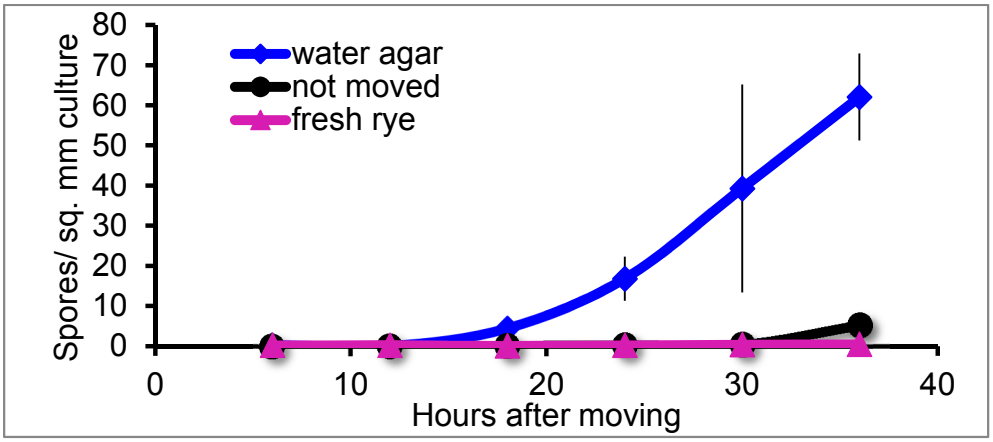

B

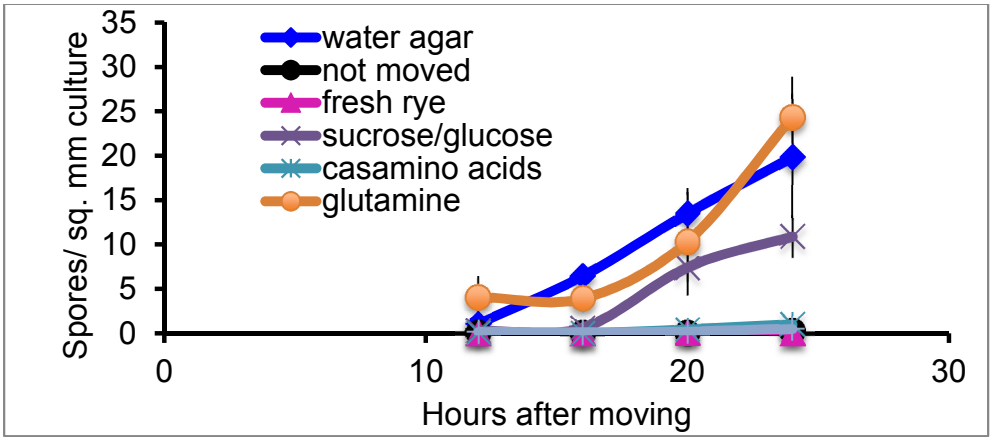

C

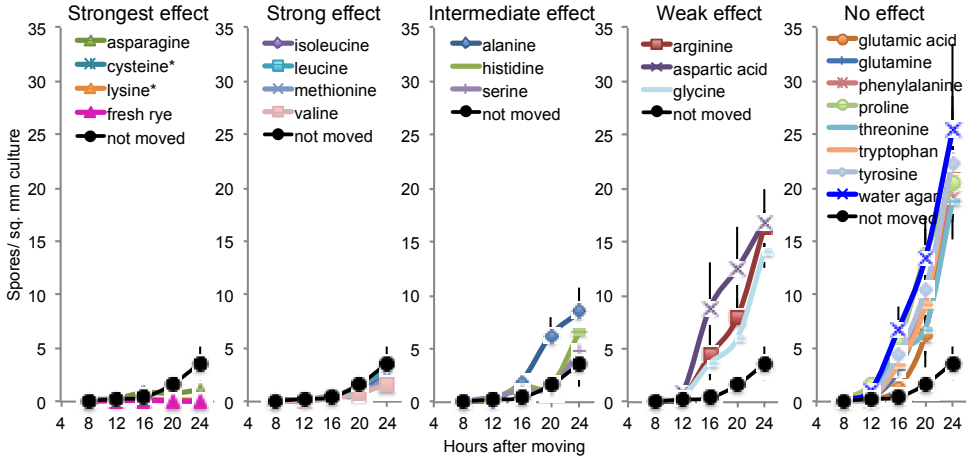

Figure 4.6. Sporulation results when sporulation-competent cultures were moved to A) fresh media, media with no nutrients, or left on the original plate, B) media supplemented with carbon or nitrogen sources, and C) individual amino acids. Asterisk (*) indicates that the condition was toxic to the culture.

Chapter 5: Off-target effects of homology-based gene silencing informs the application of functional genomics tools in *Phytophthora infestans*

Introduction

Tools for functional genomics are important for use in understanding the roles of genes in all organisms, including in *Phytophthora* species. Specifically, gene knockout, knockdown, and overexpression are important methods to understand the role of a gene, particularly in development (Jiang et al., 2013). To use these tools effectively, it is important to understand how the DNA is being transformed and expressed, to understand and account for potential off-target effects. In other systems, it has been shown that transformation can cause chromosomal rearrangements, gene silencing and gene editing may affect off-targets, and regenerated transformants may show somaclonal variation.

Contributing to the success of these strategies is an understanding of the nature of DNA transformation, including its unplanned consequences. Studies across multiple kingdoms have shown that transformation may cause chromosomal rearrangements, gene silencing methods (including RNAi) may affect off-targets, gene editing may modify unintended loci, and regenerants may exhibit somaclonal variation (Doench et al. 2016; Firon et al. 2002; Kaelin 2012; Neelakandan and Wang 2012). An awareness of these complications helps direct the judicious use of functional genomics tools.

Methods for DNA transformation have been developed for several members of the genus *Phytophthora*, which includes many important phytopathogens. These eukaryotic microbes belong to the oomycete clade of the

stramenopile (heterokont) group. Transformation of oomycetes was first achieved with the potato late blight pathogen *P. infestans,* and later extended to the soybean pathogen *P. sojae* and others (Judelson et al. 1991; Judelson et al. 1993a). The most common strategies for introducing plasmid DNA involve treating protoplasts with polyethylene glycol, or electroporating zoospores (Judelson and Ah-Fong 2009). Plasmid DNA usually integrates in tandem arrays at a single locus, based on studies in *P. infestans* (Judelson 1993). Microprojectile bombardment and *Agrobacterium*-based methods for transformation have also been described (Cvitanich and Judelson 2003; Wu et al. 2016).

To date, the functions of about 40 *Phytophthora* genes have been tested through overexpression or silencing studies, including genes encoding effectors and diverse cellular proteins (Bos et al. 2010; rev. in Hardham and Blackman 2018). The latter method, alternatively called DNA-directed RNAi or homology-dependent gene silencing, entails knocking-down mRNA levels of a target gene by expressing sense, antisense, or hairpin sequences from that gene in a stable transformant (Ah-Fong et al. 2008). Despite such advances, transformation remains challenging. Many researchers describe difficulty in obtaining sufficient numbers of transformants, transgene expression can be unstable, and the frequency of effective knockdowns can be low. It is thus common for studies of gene function to be based on a small number of transformants, sometimes as few as one. This is risky since phenotypes may be caused by unexpected

events. About 20% of *P. infestans* transformants exhibit reduced fitness (Judelson et al. 1993b), which, based on studies of other organisms, might result from mutations caused by plasmid integration (Meng et al. 2007). Oomycetes are normally diploid with complex genomes in which gene-dense clusters are surrounded by repetitive DNA (Haas et al. 2009). For example, the 240 Mb genome of *P. infestans* contains about 18,000 genes and 74% high-copy sequences (Haas et al. 2009). Although the integration of plasmids into oomycete chromosomes is believed to involve nonhomologous recombination, no studies have described where plasmids integrate. It is unknown whether plasmid DNA inserts preferentially into gene-dense, gene-sparse, intragenic, or intergenic regions.

Although the mechanism of homology-based silencing has been studied in only a few cases, in *P. infestans* this has been shown to result in small RNA production followed by transcriptional silencing and the formation of repressive chromatin (heterochromatin) at the target site (Ah-Fong et al. 2008; Judelson and Tani 2007; van West et al. 2008). Studies in plants and animals indicate that repressive chromatin can move along a chromosome, although its effect on endogenous genes is limited by barrier insulators or regulated by transcription factors (Elgin and Reuter 2013; Le et al. 2013). In contrast, transgenes or translocated native genes usually lack such protections and thus can become silenced by the *cis*-spreading of heterochromatin (Talbert and Henikoff 2006). It is thus reasonable to consider that heterochromatin may spread beyond the

target of gene silencing in *Phytophthora*, causing a phenotype to be ascribed to the incorrect gene. We previously used the spreading phenomenon to our advantage by knocking-down a cluster of genes in the same metabolic pathway (Abrahamian et al. 2016). However, no study has examined how often silencing spreads in *cis* from a target to an unintended gene in any oomycete. Similarly, whether silencing affects off-targets elsewhere in the genome has remained unexplored.

The goal of this study is to provide data to promote the wise use of transformation in oomycetes, although our findings are also relevant to other systems. We present data from homology-dependent silencing studies of eleven genes to show how often silencing spreads from the intended locus. Genes spaced within 500 nt of the target were frequently co-silenced, but there were exceptions and co-silencing usually did not occur in all transformants. Thus, gene silencing and transformation can be reliable technologies but must be used with prudence.

Materials and Methods

Analyses of flanking genes

To study the spread of silencing, I used the predicted gene models from the annotation of the *P. infestans* reference genome, which was generated by Sanger sequencing of strain T30-4, expressed sequence tag data available in FungiDB, and previously-published RNA-seq data of *P. infestans* strain 1306 (Abrahamian et al., 2016; Haas et al., 2009). Because transformants were made

in *P. infestans* strain 1306, the RNA-seq data was used to verify neighboring genes and gene models in this strain.

Three target genes were selected for analysis: PITG_16100, PITG_01718, and PITG_16104, as described in Chapter 2. Hairpin constructs were cloned into the pSTORA vector and transformed into *P. infestans* strain 1306 by protoplast transformation, and knockdown transformants were identified as described in Chapter 2 (Fig. 2.6).

Expression analysis of the targeted genes and their neighbors was obtained by RT-qPCR as described in Chapter 2, with primers described in Chapter 2.

Results

Frequency of the longitudinal extension of gene silencing

Overall, we examined 38 strains of *P. infestans* from silencing studies of eleven target genes to assess how often transcriptional silencing spread to neighboring loci. This used both newly generated silenced strains and those saved from prior projects. In this chapter, I will describe the analysis of the transformants described in Chapter 2.

Genes that flanked the silencing target were identified and their expression measured by reverse transcription-quantitative PCR (RT-qPCR). The flanking genes were identified using annotations in the *P. infestans* reference assembly (strain T30-4) and comparisons with an assembly of isolate 1306, which was the progenitor of the transformants. The results are presented in Figs.

5.1 and 5.2, where each graph represents a unique transformant. Fig 5.1 shows the genomic position of each gene relative to its neighbors, and the inset shows the position of the hairpin target sequence on each gene.

One case in which the flanking genes were close to the targeted locus is shown in Fig. 5.2A1-5.2A6. These strains were obtained using a hairpin construct based on PITG_16100 (Fig. 5.1A). In this case, each flanking gene was about 400-nt from the targeted gene. In the four transformants in panels 5.2A1 to 5.2A4, both flanking genes were expressed at normal levels. However, the expression of the left neighbor was repressed by about 40% in the two transformants in panels 5.2A5 and 5.2A6. This was observed in two biological replicates.

Similar results were observed in transformants silenced with a hairpin from PITG_01718 (Fig. 5.1B). In both transformants, the knock-down effect did not spread to the right-flanking gene, which was 400-nt from the target of the hairpin. The left-flanking gene was expressed at normal levels in one transformant (Fig. 5.2B1) but was repressed by about 50% in the other (Fig. 5.2B2). The partial knock-down of the left-flanking gene was observed in two biological replicates.

The final example that will be included in this dissertation involves PITG_16104 (Fig. 5.1C), which was silenced using a hairpin from the 5’ end of the gene (Fig. 5.2C1 to 5.2C3) and a hairpin from the 3' end (Fig. 5.2C4). In each of the four transformants, the left-flanking gene exhibited normal expression even though it was only 666-nt from the targeted gene. Since the neighbor to the right,

PITG_16105, was much farther from the target locus (3-kb) it was surprising to see that it was down-regulated by about 50% in each transformant. Interestingly, an analysis of the distribution of RNA-seq reads from isolate 1306 revealed the presence of a non-coding RNA between PITG_16104 and PITG_16105, which is labeled in the figure as ncRNA. This was consistently co-silenced with PITG_16104. Therefore, it seems that a repressive chromatin state was *cis*-propagated through the non-coding RNA locus, which had a mild influence on PITG_16105 transcription.

Discussion

This study focused on the unintended effects of homology-dependent silencing experiments in *P. infestans*. We observed that the expansion of silencing to genes residing less than 500-nt from the target was common, while more distant loci usually escaped co-silencing. However, we observed variation among transformants obtained from the same construct, and even the same transformation reaction.

Protein-coding and non-coding transcription units were both susceptible to the *cis*-spreading phenomenon. This occurred regardless of whether the neighboring gene was at the 5' or 3' end of the target, or if the silencing vector encoded sense sequences or a hairpin designed to generate double-stranded DNA. We therefore recommend that gene silencing studies always include gene expression analyses of flanking genes to ensure that inferences about biological function are reliable and influenced by off-target effects. Since widening of the

silenced zone appeared to be a stochastic event, it should be possible in most studies to identify strains that escape *cis*-silencing through extensive screening.

It is possible that checking for the proximity of the gene of interest to other transcription units may help guide the design of the silencing plasmid. The *cis*-spread of silencing might be reduced by using shorter sequences, or those farther from flanking genes. Smaller constructs might be less effective at triggering silencing, however. A previous study showed that a 21-nt hairpin silenced 2% of transformants, compared to 31% with a 978-nt hairpin from the same gene (Judelson and Tani, 2007). The logic of using larger fragments is that not all 21-mers are equally potent, so longer sequences would allow Dicer to generate pools of 21-mers, of which some may be more effective than others (Luo et al., 2007).

Off-target effects are probably also minimized by the fact that the silencing transgene usually becomes transcriptionally quiescent in stable transformants. However, some researchers have reported achieving transient knock-downs in *P. infestans* using dsRNA, and whether that causes off-target effects remains to be determined (Whisson et al. 2005).

Results from only hairpin constructs were reported in this dissertation chapter. It has been previously shown that hairpin constructs induced silencing three times more often than sense or antisense constructs (Ah-Fong et al., 2008). That conclusion was based on studies of only two genes, but hairpins have also exhibited superior performance in plants (Wesley et al. 2001). It is

possible that degree of expression of the native gene may influence whether hairpin constructs or sense or antisense constructs are more effective, but that question has not been explored. Nevertheless, studies in our laboratory have continued to test both types of constructs. The sense plasmid is often an intermediate in making the hairpin. Therefore, time may be saved by initiating *P. infestans* transformations with a sense construct. However, as discussed in Chapter 2, my studies of the cryptochromes attempting silencing with both hairpin and sense constructs, and only hairpin constructs yielded knockdown strains. A full-length sense plasmid also may yield both silenced and over-expressing transformants.

About two-thirds of *P. infestans* genes reside in gene-dense zones where the median intergenic distance is 435 nt (Roy et al. 2013). This is smaller than that of most eukaryotes, such as *Arabidopsis thaliana* where the median intergenic distance is 1.5 kb (Zhan et al. 2006). Consequently, the expansion of repressive chromatin caused by a gene silencing construct is probably more problematic in *Phytophthora* than most other eukaryotes.

Our understanding of the machinery that causes silencing and its *cis*-spread in oomycetes is limited. Homology-base silencing in *P. infestans* has been linked with the transient expression of small RNAs, which arrests transcription based on nuclear run-on assays (Ah-Fong et al. 2008; Judelson and Tani 2007; Van West et al. 1999). DNAse protection studies and tests of histone modification inhibitors have suggested that silencing heterochromatinizes the

target (Judelson and Tani 2007; van West et al. 2008), although only a few target genes have been studied to date. *P. infestans* encodes the core components for RNA silencing, namely an RNA-dependent RNA polymerase, two Dicers, and five Argonautes (Asman et al. 2016). Studies in model systems have shown that siRNAs bound to Argonaute guide chromatin-modifying enzymes to complementary loci, leading to transcriptional silencing. Work in fission yeast indicated that siRNA-Argonaute complexes are recruited to their targets through interactions with nascent transcripts (Shimada et al. 2016). The *cis*-spread of silencing may thus occur along mRNA molecules. In plants, the signal involved in post-transcriptional silencing was shown to extend 3'→5' and 5'→3' for up to 300 and 1000-nt, respectively (Petersen and Albrechtsen 2005; Vaistij et al. 2002). These distances resemble the zone susceptible to the spread of transcriptional silencing in *P. infestans.* Another mechanism for the *cis*-spread of silencing might involve propagating repressive histone marks. In mammals, histone methyltransferases G9a and GLP forms a complex that binds H3K9me, which allows the enzymes to read their own marks and spread the modification (Shinkai and Tachibana 2011).

Gene editing systems such as CRISPR/Cas9 provide an alternative to gene silencing. This was recently adapted to *P. capsici, P. palmivora* and *P. sojae* but has not yet succeeded with *P. infestans* (Gumtow et al., 2017; Miao et al., 2018; van den Hoogen and Govers, 2018). However, the editing method is not expected to be useful for genes that are essential for growth. In theory, in

such cases gene knockdown is an option since expression is usually not abolished completely. Silencing can also be used to simultaneously suppress members of gene families, which are abundant in oomycetes (Ah-Fong et al., 2017). Artificial microRNA-induced silencing has been attempted in *Phytophthora*, however, this method has not yet been reported as successful. Optimizing both gene editing and gene expression knockdown tools for functional genomics would benefit studies of oomycetes.

References

Abrahamian, M., Ah-Fong, A.M.V., Davis, C., Andreeva, K., Judelson, H.S., 2016. Gene expression and silencing studies in *Phytophthora infestans* reveal infection-specific nutrient transporters and a role for the nitrate reductase pathway in plant pathogenesis. PLOS Pathogens 12, e1006097.

Ah-Fong, A.M.V., Bormann-Chung, C.A., Judelson, H.S., 2008. Optimization of transgene-mediated silencing in *Phytophthora infestans* and its association with small-interfering RNAs. Fungal Genetics and Biology 45, 1197–1205.

Ah-Fong, A.M.V., Shrivastava, J., Judelson, H.S., 2017. Lifestyle, gene gain and loss, and transcriptional remodeling cause divergence in the transcriptomes of *Phytophthora infestans* and *Pythium ultimum* during potato tuber colonization. BMC Genomics 18, 764.

Asman, A. K., Fogelqvist, J., Vetukuri, R. R., and Dixelius, C. 2016. *Phytophthora infestans* Argonaute 1 binds microRNA and small RNAs from effector genes and transposable elements. New Phytologist 211:993-1007.

Gumtow, R., Wu, D., Uchida, J., Tian, M., 2017. A *Phytophthora palmivora* extracellular cystatin-like protease inhibitor targets papain to contribute to virulence on papaya. MPMI 31, 363-373.

Haas, B.J., Kamoun, S., Zody, M.C., Jiang, R.H.Y., Handsaker, R.E., Cano, L.M., Grabherr, M., Kodira, C.D., Raffaele, S., Torto-Alalibo, T., Bozkurt, T.O., Ah-Fong, A.M.V., Alvarado, L., Anderson, V.L., Armstrong, M.R., Avrova, A., Baxter, L., Beynon, J., Boevink, P.C., Bollmann, S.R., Bos, J.I.B., Bulone, V., Cai, G., Cakir, C., Carrington, J.C., Chawner, M., Conti, L., Costanzo, S., Ewan, R., Fahlgren, N., Fischbach, M.A., Fugelstad, J., Gilroy, E.M., Gnerre, S., Green, P.J., Grenville-Briggs, L.J., Griffith, J., Grünwald, N.J., Horn, K., Horner, N.R., Hu, C.-H., Huitema, E., Jeong, D.-H., Jones, A.M.E., Jones, J.D.G., Jones, R.W., Karlsson, E.K., Kunjeti, S.G., Lamour, K., Liu, Z., Ma, L., Maclean, D., Chibucos, M.C., McDonald, H., McWalters, J., Meijer, H.J.G., Morgan, W., Morris, P.F., Munro, C.A., O'Neill, K., Ospina-Giraldo, M., Pinzón, A., Pritchard, L., Ramsahoye, B., Ren, Q., Restrepo, S., Roy, S., Sadanandom, A., Savidor, A., Schornack, S., Schwartz, D.C., Schumann, U.D., Schwessinger, B., Seyer, L., Sharpe, T., Silvar, C., Song, J., Studholme, D.J., Sykes, S., Thines, M., van de Vondervoort, P.J.I., Phuntumart, V., Wawra, S., Weide, R., Win, J., Young, C., Zhou, S., Fry, W., Meyers, B.C., van West, P., Ristaino, J., Govers, F., Birch, P.R.J., Whisson, S.C., Judelson, H.S., Nusbaum, C., 2009.

Genome sequence and analysis of the Irish potato famine pathogen *Phytophthora infestans*. Nature 461, 393–398.

Jiang, D., Zhu, W., Wang, Y., Sun, C., Zhang, K.-Q., Yang, J., 2013. Molecular tools for functional genomics in filamentous fungi: recent advances and new strategies. Biotechnology Advances 31, 1562–1574.

Judelson, H.S., Tani, S., 2007. Transgene-induced silencing of the zoosporogenesis-specific NIFC gene cluster of *Phytophthora infestans* involves chromatin alterations. Eukaryotic Cell 6, 1200–1209.

Luo, Q., Kang, Q., Song, W.-X., Luu, H.H., Luo, X., An, N., Luo, J., Deng, Z.-L., Jiang, W., Yin, H., Chen, J., Sharff, K.A., Tang, N., Bennett, E., Haydon, R.C., He, T.-C., 2007. Selection and validation of optimal siRNA target sites for RNAi-mediated gene silencing. Gene 395, 160–169.

Miao, J., Chi, Y., Lin, D., Tyler, B., Liu, X.L., 2018. Mutations in ORP1 conferring oxathiapiprolin resistance confirmed by genome editing using CRISPR/Cas9 in *Phytophthora capsici* and *P. sojae*. Phytopathology 108, 1412–1419.

Petersen, B. O., and Albrechtsen, M. 2005. Evidence implying only unprimed rdrp activity during transitive gene silencing in plants. Plant Molecular Biology 58, 575–583.

Roy, S., Kagda, M., and Judelson, H. S. 2013. Genome-wide prediction and functional validation of promoter motifs regulating gene expression in spore and infection stages of *Phytophthora infestans*. PLoS Pathog. 9:e1003182.

Shinkai, Y., and Tachibana, M. 2011. H3k9 methyltransferase G9a and the related molecule GLP. Genes and Development 25, 781–788.

Shimada, Y., Mohn, F., and Buhler, M. 2016. The RNA-induced transcriptional silencing complex targets chromatin exclusively via interacting with nascent transcripts. Genes and Development 30, 2571–2580.

Vaistij, F. E., Jones, L., and Baulcombe, D. C. 2002. Spreading of RNA targeting and DNA methylation in RNA silencing requires transcription of the target gene and a putative rna-dependent RNA polymerase. Plant Cell 14, 857–867.

van den Hoogen, J., Govers, F., 2018. Attempts to implement CRISPR/Cas9 for genome editing in the oomycete *Phytophthora infestans*. bioRxiv 274829.

van West, P., Kamoun, S., Van 't Klooster, J. W., and Govers, F. 1999. Internuclear gene silencing in *Phytophthora infestans*. Molecular Cell 3, 339–348.

van West, P., Shepherd, S. J., Walker, C. A., Li, S., Appiah, A. A., Grenville-Briggs, L. J., Govers, F., and Gow, N. A. 2008. Internuclear gene silencing in *Phytophthora infestans* is established through chromatin remodelling. Microbiology 154, 1482–1490.

Wesley, S. V., Helliwell, C. A., Smith, N. A., Wang, M. B., Rouse, D. T., Liu, Q., Gooding, P. S., Singh, S. P., Abbott, D., Stoutjesdijk, P. A., Robinson, S. P., Gleave, A. P., Green, A. G., and Waterhouse, P. M. 2001. Construct design for efficient, effective and high-throughput gene silencing in plants. Plant Journal 27, 581–590.

Whisson, S. C., Avrova, A. O., van West, P., and Jones, J. T. 2005. A method for double-stranded RNA-mediated transient gene silencing in *Phytophthora infestans*. Molecular Plant Pathology 6, 153–163.

Zhan, S., Horrocks, J., and Lukens, L. N. 2006. Islands of co-expressed neighboring genes in *Arabidopsis thaliana* suggest higher-order chromosome domains. Plant Journal 45, 3347–3357.

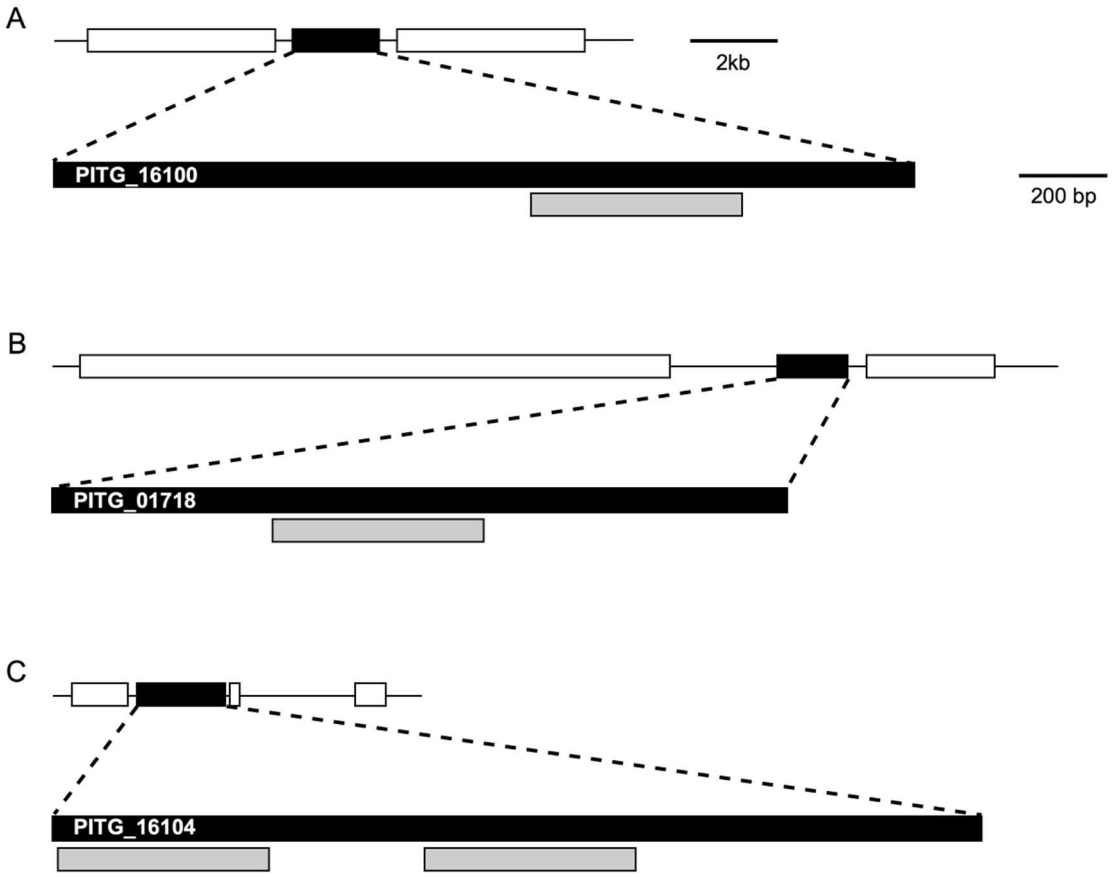

Figure 5.1. Genomic position of target genes (black) and neighboring genes (white) for A) PITG_16100, B) PITG_01718, and C) PITG_16104. Transgene construct targets are represented in gray.

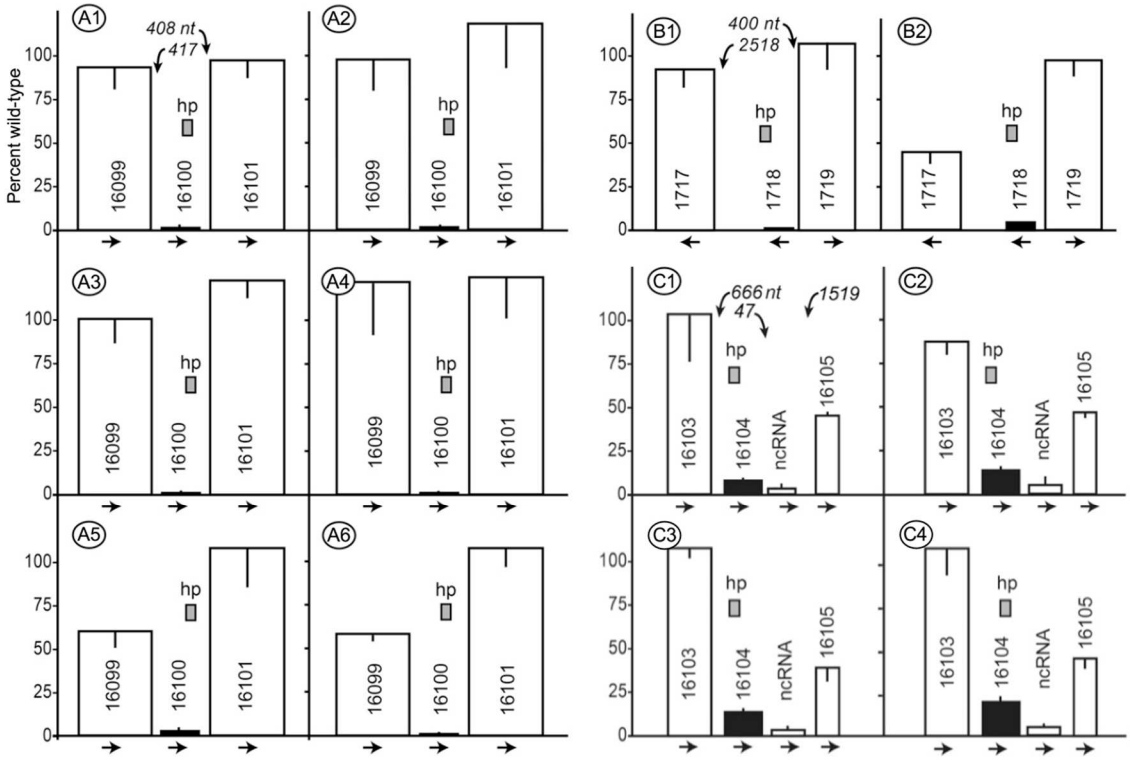

Figure 5.2. Expression levels of genes flanking the silenced target. Indicated in each panel are the genes targeted for silencing (black bars) and the closest genes that flank the target (white bars). The y-axis indicates the mRNA level of each gene relative to wild type. The x-axis is drawn to scale and portrays the size of each gene and the distance to its neighbors. Distances to flanking genes are denoted in italics. Each gene is labeled with its database number (trimmed of the PITG prefix) and an arrow that indicates the orientation of transcription. The gray bars indicate the sequences used in the silencing vector are hairpin (hp) constructs.

Chapter 6: Conclusions

Phytophthora species are among the most destructive plant pathogens worldwide. Part of what makes these organisms such successful pathogens is the ability to sense and respond to environmental conditions to optimize dispersal, growth, and survival. Over time, species in this genus have adapted to various climates and specific niches.

Within this genus of approximately 100 individual species, species range from narrow to broad host range, attack different parts of the plant, vary in soilborne survival, and differ in preferred geographic locations. Some species have adapted to long-term survival in soil, such as *P. capsici*, while other species such as *P. infestans*, have lost the chlamydospore resting structure and rarely exist long-term in soil (Danies et al., 2014; French-Monar et al., 2007). Additionally, some *Phytophthora* species, such as *P. infestans*, have a center of origin in a sub-humid temperate climates with distinct rainy and dry seasons (Toluca Valley, Mexico), while other species, such as *P. colocasiae*, have a center of origin in a humid sub-tropical climate with a thick humid fog that lasts for at least two full months per year (Hainan, China) (Beck et al., 2018; Goss et al., 2014; Zhang et al., 1994).

Timing of spore production in various species in this genus has evolved for the specific niches and climates that these species occupy. In the field, *P. infestans* sporulates in the pre-dawn dark when humidity is high. Sporulating when humidity is high allows for wind dispersal without desiccation. *P. capsici,* in

contrast, sporulates in high light, usually around mid-day to early afternoon, when humidity is low. However, *P. capsici* requires water for caducity, or detachment of the sporangium from the sporangiophore, and therefore does not expose the sporangium to desiccation by drying during dispersal.

Light and photoreception

Previous to this study, very little research had been conducted to understand the molecular basis of photoreception in *Phytophthora* species. Genomes of sequenced *Phytophthora* species contain only cryptochrome photoreceptors.

It is notable that oomycete genomes lack LOV domain-containing photoreceptors. LOV domains are thought to be ancient proteins, with LOV-histidine kinase proteins estimated as primordial LOV proteins (Krauss et al., 2009). LOV domains are still found in all kingdoms of life; however, LOV domains are currently only found in stramenopiles with active photosynthesis. Specifically, photosynthetic stramenopiles, such as xanthophyte *Vaucheria frigida* and diatom *Phaeodactylum tricornutum,* have bZIP transcription factor blue light receptors known as aureochromes (Costa et al., 2013; Takahashi et al., 2007). Whether *Phytophthora* evolved from a photosynthetic ancestor, or gained and lost photosynthesis during evolution, or evolved before the acquisition of a photosynthetic endosymbiont in the stramenopiles and has never included

photosynthesis in its evolutionary history remains a contested question in biology (Richards et al., 2011; Seidl et al., 2012; Tyler et al., 2006; Wang et al., 2017). Although LOV domains and the acquisition of photosynthesis are not necessarily linked (i.e. fungi have LOV domains and no photosynthesis), my hypothesis is that in the evolution of stramenopiles, LOV domains were acquired from the same endosymbiont that photosynthesis was acquired from. This theory does not speculate as to the evolutionary history of *Phytophthora*, simply that the lack of LOV domains is evolutionarily related to the lack of photosynthesis.

It is possible that *Phytophthora* species encode novel photoreceptors with non-canonical chromophore-binding domains and possibly even novel chromophores. However, it is more likely that the cryptochromes sense blue and red light in *Phytophthora*. Primary blue light reception by a cryptochrome is observed in plants, stramenopiles, and many other organisms, and is likely what is occurring in *Phytophthora*.

Because cryptochromes are the only light receptors that can be found in *Phytophthora*, and sporulation in *Phytophthora* is influenced by light, it was therefore hypothesized that *Phytophthora* cryptochromes play a role in sporulation. *P. infestans* has three putative cryptochromes, and although I was not able to obtain reliable knockout or knockdown transformants for one of these genes (PITG_16104), and knockout of one of these genes did not appear to have an effect on sporulation (PITG_16100), knockout of PITG_01718 led to disruption

in sporulation: showing a severe decrease or delay in sporulation as compared to wild type (Fig. 2.7).

P. infestans encodes three predicted cryptochromes, while *P. capsici* encodes two predicted cryptochromes (Fig. 2.3). PITG_01718 is a predicted cryptochrome that lacks the N-terminal extension before the photolyase homology domain that is present in the other *Phytophthora infestans* cryptochromes, making it smaller than the other *P. infestans* cryptochromes (Fig. 2.4). PITG_01718 has orthologs in other *Phytophthora* species, but not all *Phytophthora* genomes encode an ortholog to this protein (Fig. 2.3). The other two *P. infestans* cryptochromes, PITG_16100 and PITG_16104, have predicted orthologs in all of the examined *Phytophthora* genomes (Fig 2.3). PITG_01718 has an ortholog in the evolutionarily-related species *P. parasitica*, and all of the downy mildews that were examined, but is lacking in the genomes of soil-adapted *P. capsici* and *P. cinnamomi*. *Peronospora belbahrii*, like *P. infestans*, is predicted to contain 3 cryptochromes; with one ortholog per gene in *P. infestans.* *Peronospora belbahrii*, a foliar downy mildew pathogen, also has sporulation that responds to red light and blue light (Cohen et al., 2013; Thines et al., 2019). *Peronospora belbahrii* also has sporulation that is repressed by constant white light, and specifically can develop sporangiophores with ballooned tips, but is inhibited from a later stage of production of the mature sporangium, which was shown with visualization by microscopy (Cohen et al., 2013).

Another conclusion from the first part of this dissertation work is that *P. infestans* sporulation is red light responsive, while *P. capsici* sporulation is not red light responsive. I hypothesize that this red light sensing is an adaptation to a foliar lifestyle and involves PITG_01718. This gene could perhaps sense both blue and red light. Because the repression of sporulation by constant light is observed in *P. infestans* and downy mildews, I hypothesize that PITG_01718 may be involved in this regulation, and may too be an adaptation to foliar lifestyle (Fig. 6.1).

PITG_01718 can be silenced and overexpressed. The silenced transformant showed a developmental delay, and sporulation repression or delay. However, because only one silenced transformant was obtained, drawing strong conclusions is challenging. Two knockdown transformants were obtained, but were possible heterokaryons and were somewhat weak knockdowns over time after single nuclear purification, and did not have stable cultural phenotypes. Several overexpression transformants were obtained, but phenotype is still ambiguous. PITG_01718 mRNA is constitutively expressed, regardless of light condition or developmental stage, so it is likely regulated post-translationally. Identifying and understanding PITG_01718 regulation and interaction partners will provide insight on how this protein functions in sporulation regulation.

Light

Light has two distinct roles in sporulation: an early stimulation signal and a later repression signal (Fig. 6.1). In *P. infestans*, both signals can be active in the same culture- meaning, 12 hours of light can turn on early sporulation genes that are turned on pre-sporangiophore initial stage such as MADS, but constant light can also stop the final maturation of the sporangium after the production of the sporangiophore, likely after the ballooning of the tip of the sporangiophore (as has been demonstrated in downy mildews) with early sporulation genes such as MADS fully turned on the same in both constant light and constant dark cultures, with slightly higher expression in the non-sporulating constant light condition (Fig. 3.13) (Cohen et al., 2013). I propose that the two signals are related to the length of light exposure and involve different cryptochromes. PITG_16104 gene expression is slightly light responsive with 60 minutes of light exposure and 48 hours of light exposure, but more than 48 hours of light exposure results in expression similar to expression in darkness. For this reason, I hypothesize that PITG_16104 responds to light exposure of less than 48 hours, but acclimatizes in longer light exposure, and is upstream of early sporulation genes that show gene expression changes with light exposure less than 48 hours, such as MADS (Fig. 6.1). As mentioned above, I hypothesize that the long-term light exposure response is mediated by PITG_01718, downstream of early and intermediate sporulation genes such as MADS and Pks1 (Fig. 6.1).

Humidity

Humidity is a strong regulator of sporulation. Based on RNA-seq analysis of known sporulation genes, specifically sets of cilia-related genes, humidity represses sporulation before the early sporulation genes are turned on, including MADS and Cdc14, which have both been shown to be turned on before or during the sporangiophore initial stage. Therefore, I conclude that humidity regulates sporulation pre-sporangiophore (Fig. 6.1).

Nutrition

Starvation induces sporulation, specifically nitrogen starvation. This had been assumed, but through media experiments using a polycarbonate membrane to keep *P. infestans* cultures separate from the substrate, this phenomenon was confirmed experimentally in this dissertation work. When sporulation-competent *P. infestans* cultures are moved from rich rye media to nutrient-deficient water agar, sporulation is induced and spores are observed within 12-18 hours. Based on the observation that sporangia take 12-18 hours to be formed from vegetative hyphae, this is likely a strong induction signal that immediately induces sporulation, starting with the initial (Maltese et al., 1995). Moving sporulation-competent cultures to carbon-rich media such as sucrose- and glucose-supplemented water agar, did not change the starvation-induced sporulation (Fig. 4.6B). This indicates that carbon or simple sugar availability is

unlikely involved in the starvation signal. This led to the hypothesis that nitrogen availability may be involved in the starvation signal.

Casamino acids, a mix of all of the essential amino acids (except tryptophan) and small peptides that are produced from acid hydrolysis of casein, is common addition to microbial culture media, as it provides a completely hydrolyzed protein nitrogen source. When sporulation-competent cultures were moved to casamino acids-supplemented water agar, sporulation was not induced, indicating that the starvation signal is likely the lack of something that is provided by the casamino acids. Each of the twenty protein-building amino acids was then tested individually, and different degrees of sporulation stimulation were observed (Fig. 4.6C). Ammonium nitrate was also tested, but appeared toxic and arrested growth. Cysteine and lysine also appeared toxic and arrested growth. Asparagine consistently repressed the starvation-induced sporulation the strongest. Isoleucine, leucine, methionine, and valine had a strong repression of the starvation-induced sporulation. Alanine, histidine, and serine had an intermediate effect; and arginine, aspartic acid, and glycine had a weak effect. Addition of glutamic acid, glutamine, phenylalanine, proline, threonine, tryptophan, or tyrosine to water agar did not repress the sporulation stimulation, with sporulation similar to that on water agar. Analysis of the properties and pathways of these groups did not reveal any obvious similarities between the groups that would explain the phenotypes observed.

This data leads to the conclusion that nitrogen limitation induces sporulation, and this signal can induce sporulation immediately, with spores observed 12-18 hours after the starvation signal is triggered, which is the same amount of time that has been observed for naturally formed sporangia from vegetative hyphae (Fig. 6.1).

Overall conclusions that feed into the *Phytophthora* sporulation model

- PITG_01718 is required for normal sporulation in *P. infestans*, but does not have orthologs in all *Phytophthora* species
- 12-hour light regulates sporulation genes differently than constant light in *P. infestans*
- Different cryptochromes are likely involved in different stages of sporulation regulation in *P. infestans*
- Nitrogen starvation strongly induces sporulation, with spores observed 12-18 hours after the starvation signal is sent
- Humidity is a strong regulator of sporulation and is required for expression of early pore-sporangiophore sporulation genes

Future directions

There is still much to be understood about photoreception and the way in which light controls sporulation. Specifically, identifying interactor proteins and transcription factors involved in the regulation of sporulation by light should be

priorities in future research. It should also be explored how or if the cryptochromes interact with or regulate each other in *Phytophthora*.

We have found that in *P. infestans*, humidity is the strongest regulator of sporulation in *Phytophthora*. However, it remains undetermined how the humidity and nutritional signals interact. Running the nutrition deficiency/starvation experiment in the low humidity compressed air chamber would be a way to ask that question. Additionally, running the humidity experiment with *P. capsici* instead of *P. infestans* under differential light conditions would also ascertain how these signals interact. Because *P. capsici* is not windborne and requires water for detachment of the sporangium from the sporangiophore, the interaction of humidity with the other environmental conditions, particularly light, may differ from that in *P. infestans*.

References:

Beck, H.E., Zimmermann, N.E., McVicar, T.R., Vergopolan, N., Berg, A., Wood, E.F., 2018. Present and future Köppen-Geiger climate classification maps at 1-km resolution. Scientific Data 5, 1–12.

Cohen, Y., Vaknin, M., Ben-Naim, Y., Rubin, A.E., 2013. Light suppresses sporulation and epidemics of *Peronospora belbahrii*. PLoS ONE 8, e81282.

Costa, B.S., Sachse, M., Jungandreas, A., Bartulos, C.R., Gruber, A., Jakob, T., Kroth, P.G., Wilhelm, C., 2013. Aureochrome 1a is involved in the photoacclimation of the diatom *Phaeodactylum tricornutum*. PLOS ONE 8, e74451.

Danies, G., Myers, K., Mideros, M.F., Restrepo, S., Martin, F.N., Cooke, D.E.L., Smart, C.D., Ristaino, J.B., Seaman, A.J., Gugino, B.K., Grünwald, N.J., Fry, W.E., 2014. An ephemeral sexual population of *Phytophthora infestans* in the northeastern United States and Canada. PLoS ONE 9, e116354.

French-Monar, R.D., Jones, J.B., Ozores-Hampton, M., Roberts, P.D., 2007. Survival of inoculum of *Phytophthora capsici* in soil through time under different soil treatments. Plant Disease 91, 593–598.

Goss, E.M., Tabima, J.F., Cooke, D.E.L., Restrepo, S., Fry, W.E., Forbes, G.A., Fieland, V.J., Cardenas, M., Grünwald, N.J., 2014. The Irish potato famine pathogen *Phytophthora infestans* originated in central Mexico rather than the Andes. PNAS 111, 8791–8796.

Krauss, U., Minh, B.Q., Losi, A., Gärtner, W., Eggert, T., Haeseler, A. von, Jaeger, K.-E., 2009. Distribution and phylogeny of Light-Oxygen-Voltage-blue-light-signaling proteins in the three kingdoms of life. Journal of Bacteriology 191, 7234–7242.

Maltese, C.E., Conigliaro, G., Shaw, D.S., 1995. The development of sporangia of *Phytophthora infestans*. Mycological Research 99, 1175–1181.

Richards, T.A., Soanes, D.M., Jones, M.D.M., Vasieva, O., Leonard, G., Paszkiewicz, K., Foster, P.G., Hall, N., Talbot, N.J., 2011. Horizontal gene transfer facilitated the evolution of plant parasitic mechanisms in the oomycetes. PNAS 108, 15258–15263.

Seidl, M.F., Ackerveken, G.V. den, Govers, F., Snel, B., 2012. Reconstruction of oomycete genome evolution identifies differences in evolutionary trajectories leading to present-day large gene families. Genome Biology and Evolution 4, 199–211.

Takahashi, F., Yamagata, D., Ishikawa, M., Fukamatsu, Y., Ogura, Y., Kasahara, M., Kiyosue, T., Kikuyama, M., Wada, M., Kataoka, H., 2007. AUREOCHROME, a photoreceptor required for photomorphogenesis in stramenopiles. PNAS 104, 19625–19630.

Thines, M., Sharma, R., Rodenburg, S.Y.A., Gogleva, A., Judelson, H.S., Xia, X., Hoogen, J. van den, Kitner, M., Klein, J., Neilen, M., Ridder, D. de, Seidl, M.F., Ackerveken, G.V. den, Govers, F., Schornack, S., Studholme, D.J., 2019. The genome of *Peronospora belbahrii* reveals high heterozygosity, a low number of canonical effectors and CT-rich promoters. bioRxiv 721027.

Tyler, B.M., Tripathy, S., Zhang, X., Dehal, P., Jiang, R.H.Y., Aerts, A., Arredondo, F.D., Baxter, L., Bensasson, D., Beynon, J.L., Chapman, J., Damasceno, C.M.B., Dorrance, A.E., Dou, D., Dickerman, A.W., Dubchak, I.L., Garbelotto, M., Gijzen, M., Gordon, S.G., Govers, F., Grunwald, N.J., Huang, W., Ivors, K.L., Jones, R.W., Kamoun, S., Krampis, K., Lamour, K.H., Lee, M.-K., McDonald, W.H., Medina, M., Meijer, H.J.G., Nordberg, E.K., Maclean, D.J., Ospina-Giraldo, M.D., Morris, P.F., Phuntumart, V., Putnam, N.H., Rash, S., Rose, J.K.C., Sakihama, Y., Salamov, A.A., Savidor, A., Scheuring, C.F., Smith, B.M., Sobral, B.W.S., Terry, A., Torto-Alalibo, T.A., Win, J., Xu, Z., Zhang, H., Grigoriev, I.V., Rokhsar, D.S., Boore, J.L., 2006. Phytophthora genome sequences uncover evolutionary origins and mechanisms of pathogenesis. Science 313, 1261–1266.

Wang, Q., Sun, H., Huang, J., 2017. Re-analyses of “algal” genes suggest a complex evolutionary history of oomycetes. Frontiers in Plant Science 8.

Zhang, K.M., Zheng, F.C., Li, Y.D., Ann, P.J., Ko, W.H., 1994. Isolates of *Phytophthora colocasiae* from Hainan Island in China: evidence suggesting an Asian origin of this species. Mycologia 86, 108–112.

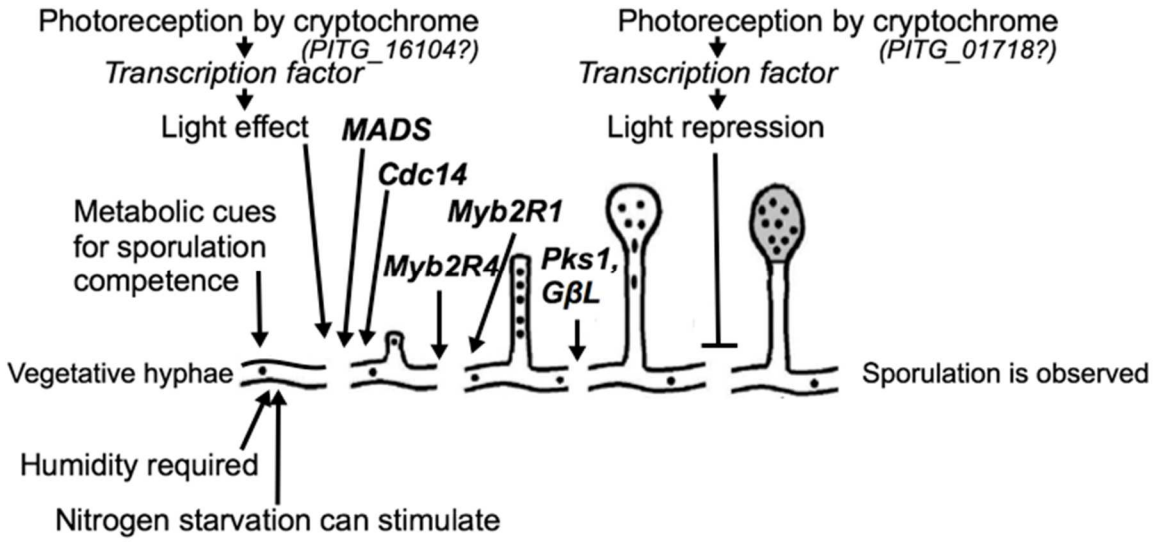

Figure 6.1. Model of environmental control of sporulation in *P. infestans.*